SYNTHESIS, CHARACTERIZATION AND EVALUATION OF FLUOROCARBON-CONTAINING RHODIUM COMPLEXES FOR BIPHASIC HYDROFORMYLATION REACTIONS

Latisa Maqeda

UNIVERSITY OF CAPE TOWN

2014

Synthesis, Characterization and Evaluation of Fluorocarbon-containing Rhodium Complexes for Biphasic Hydroformylation Reactions

Latisa Maqeda

A thesis submitted in fulfilment of the requirement for the degree

Masters in Chemistry

Department of Chemistry

University of the Cape Town

Supervisor: Associate Professor Gregory S. Smith

August 2014

DECLARATION

I declare that "**Synthesis, Characterization and Evaluation of Fluorocarbon-containing Organometallic Complexes for Biphasic Catalysis**" is my own work and to the best of my knowledge has never been reported or submitted for any degree or examination in any university. All sources of information used are cited, acknowledged and completely referenced at the end of each chapter.

…… ……/……/……..

Latisa Maqeda Date

ACKNOWLEDGMENTS

I would like to thank the following individuals, without their contribution this thesis would not be possible:

I would like to thank God who made it possible for me to carry out this work.

My one and only supervisor, Associate Professor Gregory Smith, for all the support, the encouragement and guidance he provided throughout the entire project. A special thanks to the organometallic research group for their support and help in the laboratory. In particular, I would like to thank Dr Banothile Makhubela for her continuous support throughout the research project and also for proof reading my thesis. Also I would like to say thank you to Dr Tameryn Stringer for proof reading this thesis.

Special thanks to Mr Pete Roberts for recording of NMR spectra, Mr Piero Benincasa for elemental analysis and EI-MS. Also, Dr Hong Su for the single crystal X-ray structure determinations. I would also like to thank Dr. Marietjie Stander (University of Stellenbosch) for the ESI-MS.

Lastly, I would like to thank my family especially my dad, mom and my sisters Zimvo and Zezethu for all their endless support and encouragement. A very special thanks to my boyfriend Akhona for always being there for me and for the support he provided. Also I would like to thank my friends especially Leah, Shepherd, Valerie and Nadia for comforting me through the hard times I encountered during my research.

I would like to give thanks to the National Research Fund (NRF) and C* Change for their financial support throughout this project.

ABSTRACT

The synthesis and characterization of fluorocarbon-containing salicylaldimine and iminophosphine ligands and their Rh(I) complexes is described. These ligands were obtained *via* a Schiff base condensation reaction between 2-diphenylphosphinobenzaldehyde and salicylaldehyde with the appropriate amines. The ligands were subsequently used to synthesize various Rh(I) complexes of the type [Rh(P^N)Cl(CO)] and [Rh(N^O)COD] from metal precursors $[RhCl(CO)_2]_2$ and $[RhCl(COD)]_2$, respectively. The complexes were isolated as air stable solids.

The synthesized ligands and complexes were characterized using different analytical and spectroscopic techniques including (^1H, $^{13}C\{^1H\}$, $^{31}P\{^1H\}$ and $^{19}F\{^1H\}$ NMR spectroscopy), FT-IR spectroscopy, mass spectrometry (ESI and EI), elemental analysis. In addition, single crystal X-ray diffraction was also used for characterization.

The hydroformylation of 1-octene using the synthesized Rh(I) based complexes under fluorous biphasic conditions in the presence and absence of toluene is described. The hydroformylation results showed that the iminophosphine and salicylaldimine-based catalyst precursors are active and selective under mild conditions, converting 1-octene to mostly aldehydes and a small amount of *iso*-octenes. The aldehydes formed were branched aldehydes and linear aldehydes. On omitting toluene from the reaction, better linear to branched ratios were obtained. The best results obtained using the established optimum reaction conditions were compared to available commercial systems for hydroformylation of propene and with those reported in literature under fluorous biphasic conditions.

One of salicylaldimine and iminophosphine-based complexes were used in recycling studies, and due to leaching of the catalyst into the organic phase (toluene), the catalyst showed poor conversions after the second run. However, when recycling studies were performed in neat reactions (using only a fluorous solvent), high conversions were retained after the second run.

LIST OF ABBREVIATIONS

Å	Angstroms
acac	Acetyl acetonate
ca	Approximately
Ar	Aromatic
br	Broad
^{13}C NMR	Carbon-13 nuclear magnetic resonance
Calc.	Calculated
$CDCl_3$	Deuterated Chloroform
δ	Chemical shift/ Delta
COD	1,5-Cyclooctadiene
COSY	Correlation spectroscopy
°C	Degrees celsius
d	Doublet
dd	Doublet of doublets
DCM	Dichloromethane
EA	Elemental analysis
EI-MS	Electron impact mass spectrometry
ESI-MS	Electrospray ionization mass spectrometry
Eqv.	Equivalent
EtOH	Ethanol

^{19}F NMR	Fluorine nuclear magnetic resonance
FT-IR	Fourier transform infrared spectroscopy
GC	Gas chromatography
g	Gram(s)
^{1}H NMR	Proton nuclear magnetic resonance
HSQC	Heteronuclear single quantum correlation
Hz	Hertz
ICP-MS	Inductively coupled plasma mass spectrometry
IR	Infrared
J	Coupling constant
m	Multiplet
MeOH	Methanol
MHz	Megahertz
mL	Millilitre
mol	Mole(s)
mmol	Millimole(s)
MS	Mass spectrometry
m/z	Mass to charge ratio
NMR	Nuclear magnetic resonance
1-D	One dimensional
^{31}P NMR	Phosphorus nuclear magnetic resonance

ppm	Parts per million
PMCH	Perfluoromethylcyclohexane
RT	Room temperature
s	Singlet
t	Triplet
2-D	Two dimensional
THF	Tetrahydrafuran
cm^{-1}	Wavenumbers

CONFERENCE CONTRIBUTION

November 2013 – Poster Presentation

Synthesis, Characterization and Evaluation of Fluorocarbon-containing Organometallic Complexes for Biphasic Catalysis. Catalysis Society of South Africa (CATSA) conference, Kwazulu-Natal, South Africa.

TABLE OF CONTENTS

A Review on Catalysis and Biphasic Catalysis

1.1 Catalysis

Developing new products, processes and services that attain all the benefits of sustainable development is the biggest challenge that chemists and others face.[1a] New approaches that minimize the input of materials and energy to a process and consequently utilize and maximizes efficiency is required.[1a] Dispersal of harmful chemicals in the environment must be decreased if possible eliminated and the use of renewable and recyclable products increased.[1a] This is achieved by making greener products and processes that are environmentally friendly and economically attractive and allows the industry to meet the societal needs.[1a]

Green chemistry has been identified as a new approach to scientifically based environmental protection and as an economically beneficial approach. It can be defined as the design of chemical products and processes that minimize or eradicate the use and generation of hazardous substances in the design, manufacture, and application of chemical products.[1b-7] Green chemistry uses a set of twelve principles (**Figure 1.1**) that decreases the generation of hazardous substances in the manufacturing, designing and the application of chemical products.[4b, 4c]

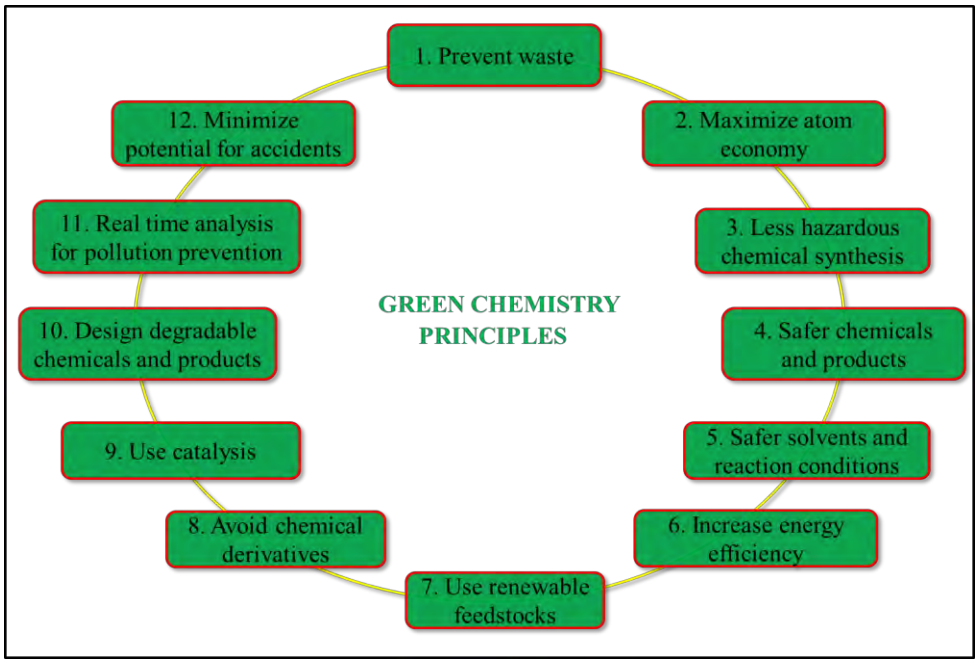

Figure 1.1: 12 Principles of Green chemistry.[4b, 4c]

Catalysis is identified as one of the most important areas for implementing the twelve principles of green chemistry (**Figure 1.1**).[2-4a] It is also known as the "foundational pillar" of green chemistry[1b, 3b] and one of the dominant technologies that plays an important role in the chemical industry and in providing environmental protection.[1a, 8-9a] It is employed because of its ability to stimulate reactions by accumulating one molecular fragment to another, with combination of most or all atoms in both fragments in the final product.[1a] Catalysis offers a number of advantages which include lower energy requirements, increased selectivity, reduced processing and separation agents, the use of less toxic materials and catalytic amounts as opposed to stoichiometric amounts.[1b-3a] The design of a catalyst attempts to enhance factors such as turnover number, stability, solubility and easy catalyst separation from the products.[1b-3a] The choice of metal and ligand design can provide substantial improvements in energy consumption, selectivity and solvent utilization.[1b-3a, 9b]

Catalysis is applied in more than 90 % of the industrial processes.[1b, 10] The chemical industry makes use of catalysis in areas such as pharmaceuticals, petroleum refining and food processing to name a few.[10]

Research interest in catalysis by transition metal complexes has increased since the 1940's.[11a] This is mainly because of the progressive catalytic properties of a number of transition metals and how these properties can be altered when coordinated with suitable ligands to form coordination complexes.[11a] Some of the early discoveries in transition metal catalysis involved platinum in the Ostwald Process in the 1880's and the Contact Process in 1831.[11b]

Subsequently, catalysis research has grown to be one of the most important field in a number of areas such as chemical engineering, material science and organometallic chemistry.[1, 10, 12a] Catalytic synthesis can be conducted using heterogeneous or homogenous organometallic complexes.[12b]

1.2 Homogeneous and Heterogeneous Catalysis

Heterogeneous catalysts are normally metal or metal oxides on a solid support such as silica and alumina.[13] They are stable at high pressures and can be used at high temperatures unlike homogeneous catalysts. They are in a different phase from the substrate and products; this means

that only the surface is accessible for the reaction.[13a, 13b] Heterogeneous catalysis specifically addresses one of the green chemistry goals by providing easy separation of the catalyst from products, thus eliminating the necessity for separation through extraction or distillation.[1b] However, heterogeneous catalysts have poor selectivity, there is leaching of the metal into the products and there is a problem of irreproducibility.[11a]

Homogeneous catalysts are usually dissolved in the same reaction media as the substrate and products and comprise of organometallic complexes which contain a metal center surrounded by organic ligands.[13a, 14-15] Homogeneity is an advantage because all the catalytic sites are accessible for the reaction unlike heterogeneous catalysts. One of the drawbacks with homogeneous catalysts is that they cannot be applied efficiently in industry because of the major problem of separating the catalyst from the products or reaction solvents.[12b-15] The separation problem arises because most of the used separation methods like distillation requires high temperatures except if the product is volatile.[15b] Homogeneous catalyst commonly decompose below 150 °C because most of them are thermally sensitive.[15b] Chromatography is the other conventional process that result in the loss of a catalyst. Most industrial homogeneous processes either include products that are volatile or they do not include organic ligands that are thermally sensitive.[15b] Advantages and disadvantages of heterogeneous and homogeneous catalysts are shown in **Table 1.1**.

Table 1.1: Comparison of homogeneous versus heterogeneous catalysts.[13a]

	Heterogeneous	Homogeneous
Catalyst form	Solid, metals or metal oxides	Soluble metal complexes
Selectivity	Low	Can be tuned
Stability	Stable to high temperature	Often decompose <100°C
Solvent	Usually not required	Usually required
Recyclability	Simple	Very difficuly and expensive
Mode of use	Fixed bed or slurry	Dissolved in a reaction medium
Special reactions	Haber process, exhaust clean up, etc.	Hydroformylation of alkenes, Methanol carbonylation, etc.

The recovery of highly selective homogeneous catalysts is crucial in industrial processes.[12b, 15] Thus strategies to minimize waste streams and techniques to potentially recycle catalysts have been developed. Multiphasic systems and solid-supported homogeneous catalysts are some of the techniques that have been developed for this purpose.[12b, 13b, 15]

1.3 Separation Techniques

To improve the recovery of homogeneous catalysts a number of approaches have been established. These approaches can be widely grouped into two types. The first type is frequently referred to as "heterogenizing homogeneous catalysts".[15b] In this process, the catalyst is attached to a particular insoluble or soluble support, and filtration is used for the separation. The second type encompasses the design of a catalyst in such a way that it is soluble in some solvent, and it is immiscible with the reaction products in certain conditions.[15b] The reactions involve two phases and are generally referred to as biphasic systems.[3b, 15b, 16a] The catalyst is dissolved in one phase and the product/reactants in the second phase and decantation is used as the separation technique.[15] Biphasic systems involve alternative solvents as reaction medium replacing hazardous organic solvents. These may include ionic liquids, supercritical media (supercritical CO_2), water and perfluorinated solvents.[15b]

1.3.1 Insoluble and Soluble Supports

1.3.1.1 Insoluble Supports

Homogeneous catalysts can be attached to insoluble supports such as organic supports (e.g polystyrene) and inorganic supports (e.g silica and alumina).[13a, 15b, 17-18] This process is "heterogenizing the homogeneous catalyst".[13a, 15b] Polystyrene (**Figure 1.2a**) has been widely used as an organic solid support mainly because it's cheap and readily available commercially.[13a, 19a] However in industry, for fixed bed reactors, the polystyrene polymer blocks the inter-bed channels resulting in a reduced flow through the reactor.[13a] Nonetheless, polystyrene is a good support for laboratory scale reactors. Polystyrene-supported catalysts have been used in a range of reactions such as, hydroformylation, Suzuki cross-coupling, hydrogenation, oligomerisation, metathesis, hydrosilation, and Heck arylation.[19, 20a]

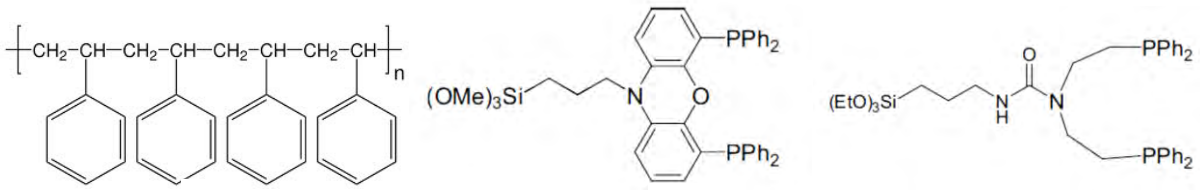

a **b** **c**

Figure 1.2: Structures of supported-ligands used for immobilizing metal catalysts.[20]

Inorganic supports such as silica have been linked to the catalyst through covalent bonding.[13a, 20a] To obtain silica immobilized catalyst, one of the strategies used is covalently bonding alkoxysilane functionalized ligands to a silica material *via* a condensation step.[13a, 20a] The covalent bonding between the homogenous catalyst and the inorganic oxide means that the catalyst can resist the harsh conditions during catalytic reaction.[13a, 15b] The main problem in this approach is that there is breakage of bonds between the ligand and the metal and also they are reformed during the catalytic reaction.[13a, 16a] As a result, the catalyst leaches because it detaches from the support, consequently it loses its activity in subsequent runs.[15b]

To reduce leaching of the catalyst, the catalyst may be attached to the pores of zeolites (ship-in-a bottle catalysts) and leaching from the pores is prevented by the size of the catalyst.[13a, 16a, 18 , 20b] Another approach to prevent the leaching of the catalyst pioneered by Panster,[20c] was to attach the hydroformylation catalyst to a sol-gel solution. [16a, 20] Ligands **b** and **c** in **Figure 1.2** were obtained using the sol-gel method.[20]

Ligand **b** in **Figure 1.2** was formed by incorporating a ligand from the xanthphos family of ligands to a sol-gel solution.[15b] This ligand was then attached to a rhodium centre. This catalyst has been used in a number of hydroformylation reactions using a variety of reaction conditions and there was little or no leaching of the catalyst.[15b] The selectivity for the linear product was very high because the ligand bound to the rhodium metal belongs to the xantphos family which are known for very high selectivities.[15b, 16a, 18]

1.3.1.2 Soluble supports

In this approach, the supports used may be soluble in the reaction medium. This is an advantage since all catalytic sites are available for the reaction.[15b] The supports can be soluble polymers or dendrimers and ultrafiltration is used to separate the catalyst from the products after the

reaction.[21] An example of a soluble polymer was formed from the exchange of anions of ligand **a** and **b** in **Figure 1.3** to form a polyelectrolyte.[15b] This polyelectrolyte was used as a catalyst in the hydroformylation of 1-octene and the catalyst was recovered by ultrafiltration.[15b] The catalyst showed good reaction rates and 93% of the catalyst could be recycled.[15b]

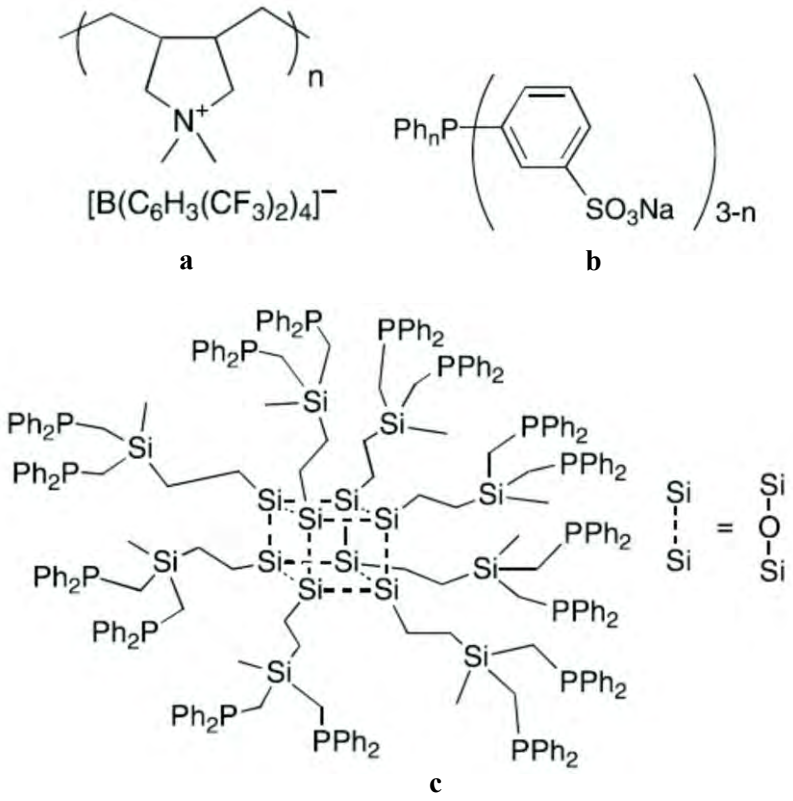

Figure 1.3: Examples of soluble catalyst supports.

Homogeneous catalysts can also be anchored to dendrimers.[15b, 21] Dendrimers are tree-like polymers and have a well-defined geometry of binding sites on the surface and may exhibit multidentate coordination.[15b, 22-24a] This is an advantage because the selectivity of the linear product may be high as a result.[15b, 16a, 24a] Also they can show very high selectivities towards desired products than their mononuclear analogues.[15b] For example, **Figure 1.3** shows dendrimer **c** that contains sixteen PPh_2 groups on its periphery, which showed better linear: branch ratios (13.9:1) in 1-octene hydroformylation reaction than small-molecule analogue (3.8:1).[15b, 24b]

1.3.2 Biphasic Systems

Liquid-liquid biphasic systems have been developed to overcome the problem of separating a catalyst from the product while retaining the benefits of the homogeneous catalyst.[24c] Biphasic systems involve two immiscible liquid phases in one reactor. One phase (organic phase) contains the substrate/products and the second phase (water/fluorous) contains the dissolved catalyst.[8a, 24c] The products are separated from the catalyst phase by decantation, and this allows the catalyst to be recycled without the loss of activity.[8a, 24c] Biphasic systems may involve ionic liquids, supercritical fluids, aqueous and fluorous solvents.[24c]

1.3.2.1 Ionic Liquids

Ionic liquids are salts that are composed of ions and are liquids at ambient temperature.[15b, 25-32] They have very low vapour and they can dissolve in organic solvents depending on their design. Ionic liquids at ambient temperature are organic cations and some of the examples are shown in **Figure 1.4**.[15b, 25-32]

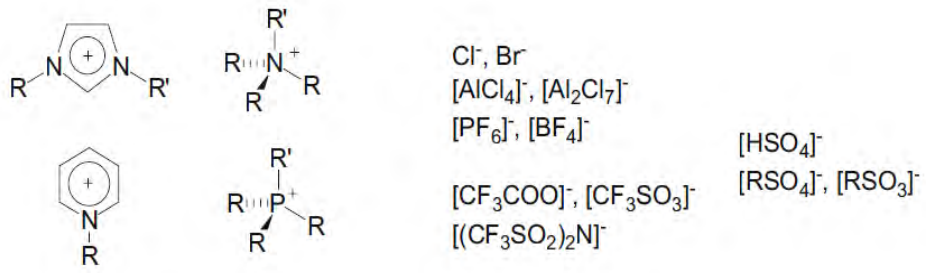

Figure 1.4: Examples of Ionic Liquids (ILs).[25, 26, 28, 30-31]

Ionic liquids at room temperature have various chemical-physical properties which make them suitable for performing green catalytic reactions.[13a, 29] They are non-volatile, have low viscosity, higher density than most organic solvents, and they are liquids over a variety of temperatures.[15b, 29-30] Polarity, hydrophobicity and or hydrophilicity can be achieved when suitable cations and anions are combined.[28] Thus, solubility of ionic liquids can be adjusted, and this is an advantage for liquid-liquid biphasic catalysis.[13a] For example, if an ionic liquid can dissolve a catalyst, partially dissolve the reaction substrates and show poor solubility towards products, the catalyst

can then be immobilized in the ionic liquid which can allow easy separation of products from catalyst in homogeneous system.[13a]

This was seen in the first hydroformylation reaction performed in an ionic liquid which was the hydroformylation of 1-pentene using rhodium pre-catalyst with a sulfonated phosphine ligand **b** in **Figure 1.3**.[15b,28] However the conversions were very low possibly because of the high sodium salt lattice energies caused the complexes to be insoluble in ionic liquids.[15b] Most recently, high activity and regioselectivity has been shown in rhodium-catalyzed hydroformylation of 1-octene using xantphos-type ligands in ionic liquids.[15b] Improvement on catalyst separation can be achieved using supercritical carbon dioxide ($ScCO_2$) as a second phase, whereby the catalyst is retained in the ionic liquid phase and the product is removed from the $ScCO_2$.[28]

1.3.2.2 Supercritical fluids

Supercritical fluids are gases that are pressurised, heated above their critical pressure and temperature and their density is higher or close to their critical density.[16a, 26a, 28-29, 32-33] The most commonly used supercritical fluid is supercritical carbon dioxide ($ScCO_2$). They are non-polar and their densities are similar with the organic liquids, this allows them to dissolve a variety of non-polar organic substrates. For example fluoropolymers dissolve only in chlorofluorocarbons and in $ScCO_2$. This is an advantage to green chemistry since $ScCO_2$ can replace environmentally hazardous halogenated solvents.[22, 36] $ScCO_2$ has been used as a reaction medium in the hydroformylation of propylene using unmodified cobalt carbonyl catalyst.[16b] Most research is based on dissolving rhodium-based triphenylphosphine complexes in $ScCO_2$. Achievements have been made by attaching groups such as fluorous tails to the phenyl groups of the triphenylphosphine (**Figure 1.5**).[15b, 16a]

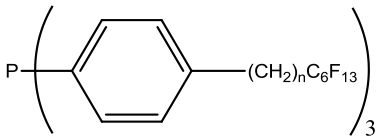

Figure 1.5: Perfluorinated ligand used to enhance solubility of catalysts in $ScCO_2$.[15b]

The use of $ScCO_2$ permits easy separation of solvent from products and catalyst; however it does not address the separation problem of the catalyst from products. A number of approaches have been identified to solve this problem, these include immobilizing the catalyst to an ionic liquid.[26a, 31, 32, 34-36] In this approach the catalyst is retained in the ionic liquid while the product is removed from the supercritical carbon dioxide and thus catalyst and ionic liquid can be recycled.[26, 28, 34-36] In this addition, the products are separated from the catalyst with very low leaching (<<ppm).[26a] These systems have been applied to a variety of homogeneously catalyzed reaction. These include rhodium-based hydroformylation, oxidation and hydrogenation. Supercritical fluid-ionic liquid systems not only solve the problem of solubilizing a catalyst in a CO_2 system, but also solve the problem of removing the products from ionic liquids.[26a] Another alternative approach for separation of the metal catalyst from products is aqueous biphasic system.

1.3.2.3 Aqueous Biphasic Systems

An aqueous biphasic system is a two-phase system (water layer and organic layer), whereby water is used as a solvent in which the catalyst resides (**Figure 1.6**). Water is used because of its many attractive advantages. Water is abundant and readily available; it is not expensive, non-toxic, non-hazardous and it is environmentally friendly.[3b, 12b, 13a, 16, 26a, 28-29, 37-43] Using water as a solvent applies one of the principles of green chemistry since it is a non-toxic solvent and the separation becomes easy when using water because it is immiscible in organic solvents as they are hydrophobic. This makes it suitable for biphasic catalysis.[12b, 26a, 37-38] Aqueous biphasic systems are the most applied and studied systems. They have been used in a number of reactions which include hydroformylation, carbonylation, alkene metathesis and hydrogenation.[3b, 38]

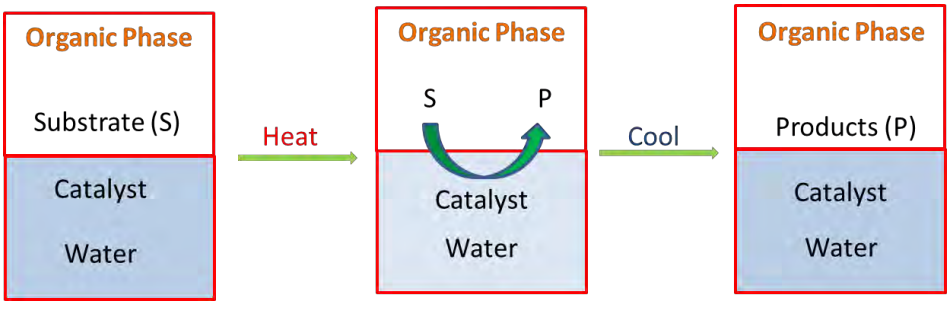

Figure 1.6: Illustration of aqueous biphasic catalysis. S: substrate and P: product.

The catalyst used in aqueous biphasic catalysis has to be soluble in water. This is attained by attaching hydrophilic (water-soluble) moieties in the ligands or by using a water soluble metal precursor.[37] A number of water-soluble ligands have been designed for aqueous biphasic catalysis, for example sulfonated phosphines such as triphenylphospine mono-sulfonated sodium salt (TPPMS) and triphenylphospine tris-sulfonated sodium salt (TPPTS) as indicated in **Figure 1.7**. [3b, 12b, 16, 26a, 28, 37-41] An aqueous biphasic system involving a Rh catalyst is employed in the hydroformylation of propene to butyraldehyde in industry. This process was formerly known as the Ruhrchemie/Rhône-Poulenc process and is currently the Oxea Process. [3b, 13a, 16, 26, 37] On a 600 000 metric ton scale this process is highly efficient, with a catalyst that indicates high activity and selectivity for the desired linear aldehyde product.

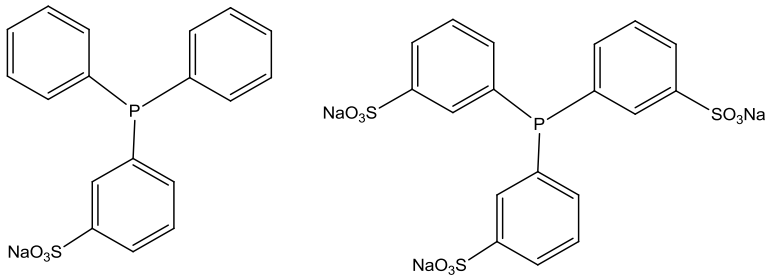

a) TPPMS b) TPPTS

Figure 1.7: Water-soluble ligands : a) Trphenylphosphine mono-sulfonated sodium salt (TPPMS), b) Triphenylphosphine tris-sulfonated sodium salt (TPPTS).

The Oxea Process has economic and environmental benefits such as, easy and complete recovery of the catalyst and also the use of water reduces the costs of using expensive separation processes. [3b, 12b, 26a, 37-41] The major drawback of aqueous biphasic systems is that they are not effective with higher olefins (> C_5) because of their low solubility in water. The decreasing solubility of alkenes with increasing number of carbons in the starting olefins and the products is illustrated in **Figure 1.8**.[26b] This shows that from C_8 onwards, solubility in water is not possible.

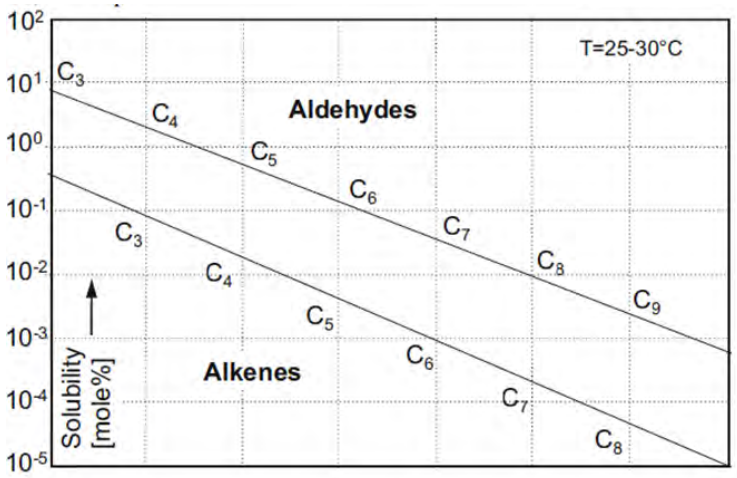

Figure 1.8: The solubility of alkenes in water.[26b]

A number of techniques have been employed to overcome this problem. For example, different biphasic system can be employed such as a fluorous biphasic system, ionic liquid or supercritical fluids.[3b, 16, 26a, 28, 37-41] This research project focuses on investigating the efficacy of fluorous biphasic systems for the hydroformylation of higher olefins, such as 1-octene.

1.3.2.4 Fluorous Biphasic Systems

Fluorous-organic biphasic systems were introduced by Horvath and Rabai to solve the problem of solubility experienced in the aqueous biphasic systems.[44c-d] Fluorous biphasic systems consist of two phases, one phase is an organic phase containing an organic solvent such as, acetone, toluene or tetrahydrofuran (THF), and the second phase is a fluorous phase containing fluorinated solvents such as perfluoroalkanes, perfluorotrialkyl amines or perfluorodialkyl ethers and the catalyst.[1b, 3b, 44-67] This is illustrated in **Figure 1.9**.

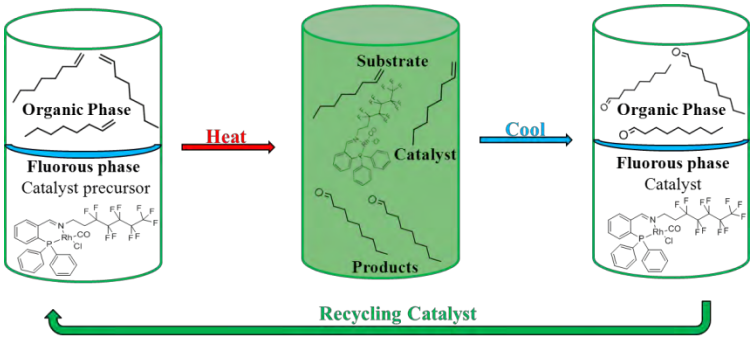

Figure 1.9: Fluorous biphasic catalysis illustrated for the hydroformylation of 1-octene.

The organic and the fluorous phase are immiscible at room temperature and become miscible at raised temperatures. This is an advantage because biphasic catalysis can be achieved, and at high temperatures monophasic catalysis can be performed with rapid separation of the catalyst from the products at lower temperatures.[1b, 3b, 44, 46, 51, 61, 63] One major advantage of the fluorous systems over aqueous systems is that on heating a single phase is formed and the catalyst and the substrate are in intimate contact with each other.[63]

A requirement for fluorous biphasic system is that the catalyst must be designed in such a way that it is soluble in fluorous solvents. This is achieved by attaching fluorocarbon moieties to the ligands (**Figure 1.10**). These are also known as fluorous ponytails.[3b, 44, 46, 51, 61, 63] Since the fluorine atom has electron-withdrawing properties, the electronic properties and the activity of the catalyst and fluorous reagents can be changed significantly on attaching the fluorous ponytails.[1b, 3b, 44-67] For example ponytails will reduce the electron density on phosphorous and consequently decrease the activity of the catalyst. To overcome this problem, the insertion of an insulating group such as hydrocarbons (organic spacer) between the fluorous ponytail and the coordinating atom (e.g phosphorous) may be required in order reduce the electron-withdrawing effects.[1b, 3b, 44-67]

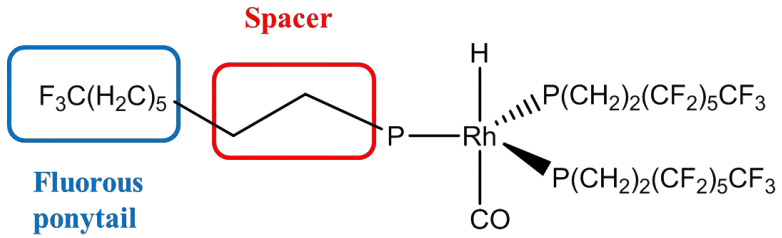

Figure 1.10: Illustration of fluorous catalyst.

Fluorous solvents

Perfluorocarbon solvents have a wide range of properties which makes them suitable for applications in the biotech, medicine, oil and gas as well as electronics industries.[44] Perfluoroalkanes, perfluorotrialkyl amines and perfluorodialkyl ethers are the only used fluorous solvents. Examples of commercially available fluorous solvents are indicated in **Figure 1.11**.[3b, 46]

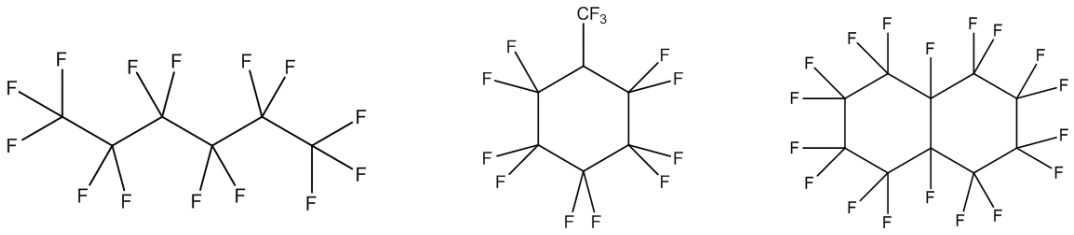

Figure 1.11: Examples of fluorous solvents.

Fluorous solvents are hydrophobic, non-toxic, have high oxygen solubility, are inert, highly thermally stable, non-flammable and have an efficient heat capacity.[44] The characteristics of fluorous solvents are due to the high stability of the carbon-fluorine (C-F).[44] These solvents are inert to atmosphere.[44]

Fluorous Soluble Catalysts

For fluorous biphasic catalysis, organometallic catalysts have to be designed in such a way that they are soluble in fluorous solvents (**Figure 1.11**). To avoid significant leaching of fluorous reagents and catalysts, the partition coeffients of fluorous intermediates involved must be modified for fluorous phase affinity.[44-67] This is achieved by attaching "fluorophilic" ligands into the (organometallic) pre-catalyst. Fluorous ponytails should be attached in the ligands in an appropriate number, length or shape in order to give them a high fluorous preference. Studies on solubility have shown that only ligands which contain three or more fluorous ponytails are soluble in perfluorocarbon solvents.[1b, 52]

A number of transition metal-containing fluorous catalysts have been prepared and several of them are based on fluorous phosphine ligands (fluorophilic ligands). The fluorous soluble ligands are prepared from a number of fluorous building blocks (**Figure 1.12**) using conventional synthetic routes.[46]

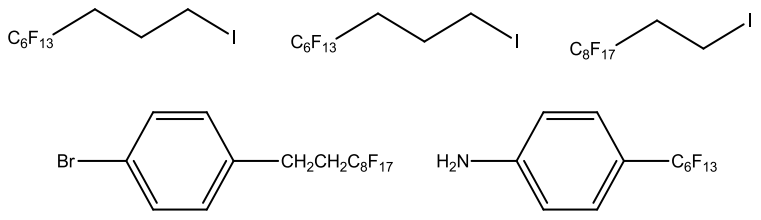

Figure 1.12: Commercially available fluorous building blocks.[46]

These are typically fluorous alcohols, halides and amines and they all contain hydrocarbon spacers (e.g. C_3H_6).

Phosphine (III) ligands are the most widely used ligands to prepare fluorocarbon-containing organometallic catalysts. They are grouped in three classes, namely i) trialkylphosphines, ii) triarylphosphites iii) triarylphosphines.[61] Examples of fluorinated phosphorous ligands (triarylphosphines and triarylphosphites) are shown in **Figure 1.13**.[47, 61]

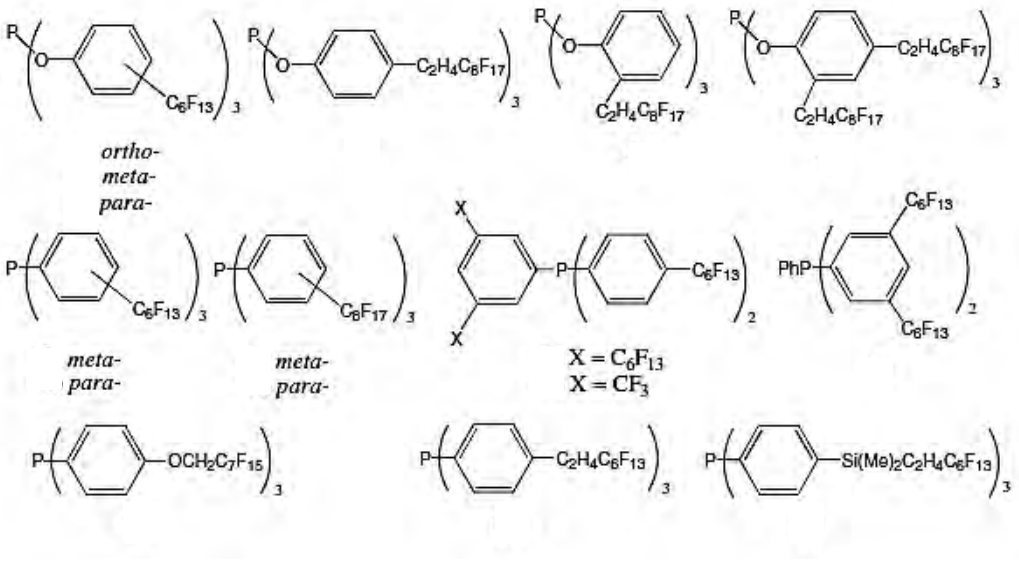

Figure 1.13: Examples of perfluoroalkyl-substituted phosphorous(III) ligands.[47, 61]

General synthetic routes for the preparation of various phosphorus(III) ligands containing perfluorocarbon groups (**Figure 1.13**) have been reported.[47, 51-58] Nitrogen ligands are also used to prepare perfluorocarbon-containing organometallic catalysts and their synthetic routes have been reported by Horvath and co-workers[44, 59-60] and have been used in fluorous catalysis.

Fluorous biphasic catalysis has been applied to a number of homogeneous catalytic reactions such as, hydroformylation, hydrogenation, hydroboration, alkane and alkene functionalization.[48] This research project focuses on the hydroformylation of higher olefins in fluorous biphasic systems.

1.4 Hydroformylation

Hydroformylation also known as "oxo synthesis" was discovered by a German chemist Otto Roelen in 1938. Roelen was investigating the origin of oxygenated products seen in cobalt-

catalyzed Fischer-Tropsch synthesis.[9b, 13b, 15a, 16, 68-73] Today, hydroformylation is the world's foremost industrial homogeneously catalysed reaction which produces more than six million tonnes of aldehydes per annum.[9b, 15a, 16, 68-72] In the hydroformylation reaction, aldehydes are formed by reacting alkenes with carbon monoxide (CO) and hydrogen (H_2) in the presents of a transition metal catalyst. The aldehydes formed can be either branched (*iso*) or linear (normal). For example in **Equation 1.1**, propene reacts with CO/H_2 in the presents of a catalyst to form a branched aldehyde (*iso*-butanal) and a linear aldehyde (butanal).[68-73]

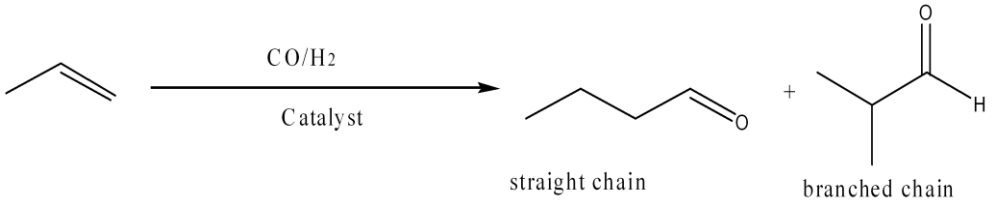

Equation 1.1

The formyl group can add either side of the C=C double bond depending on the substituents, hence the formation of two different aldehydes.[15a] In hydroformylation, the formyl group is added at the low substituted carbon atom of the double bond.[15a] This process is also an important process because since the resulting aldehydes are simply converted to secondary products, for examples alcohols. The *n*-aldehydes and the *iso*-aldehydes are the main products that form during hydroformylation, but there are also a number of side reactions such as isomerization and hydrogenation.[9b, 15a]

Hydroformylation involves important elemental reactions in the mechanism (**Figure 1.14**), which are: (**1)** dissociation of CO, (**2)** alkene coordination, **(3)** migratory insertion, **(4)** oxidative addition of CO and H_2, **(5)** alkyl migration and **(7)** reductive elimination.[9b, 73]

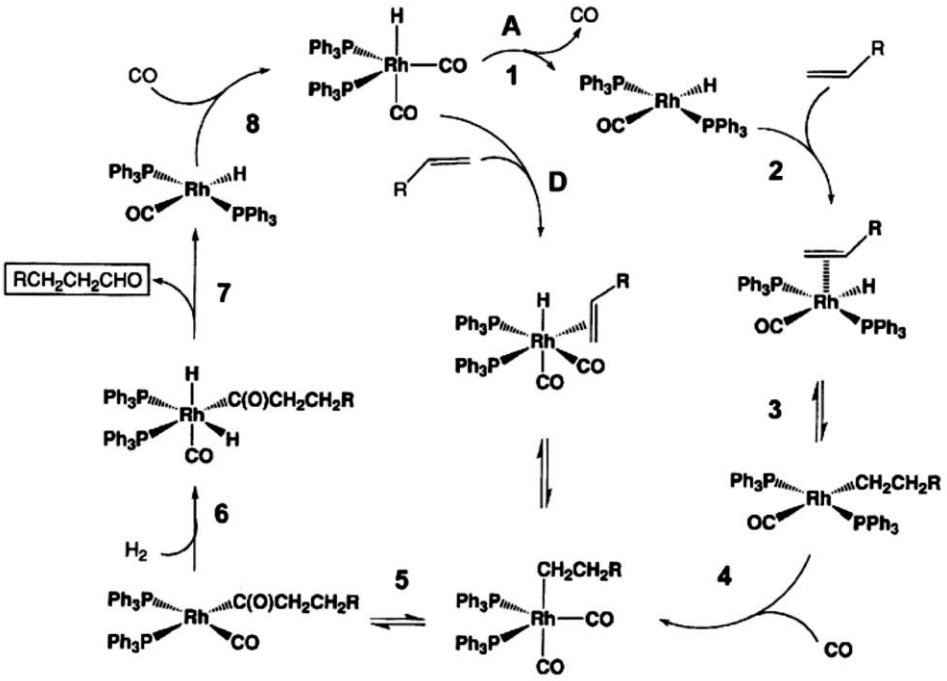

Figure 1.14: The mechanism of Rh-catalysed hydroformylation.[73]

Aldehydes are used in the manufacturing of detergents, surfactants and plasticisers.[15a, 16a, 72] They can also be used to manufacture other industrially important secondary compounds (**Figure 1.15**). [73]

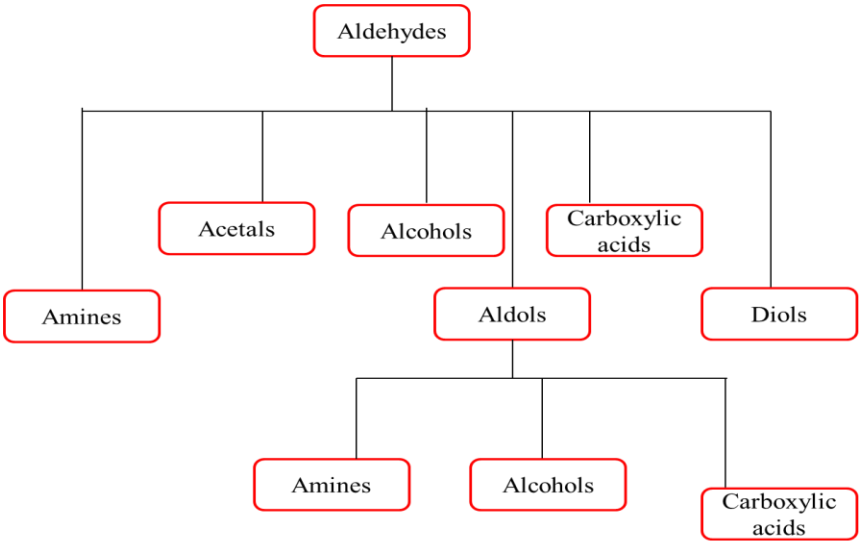

Figure 1.15: Products that are accessible *via* hydroformylation.[73]

1.4.1 Hydroformylation Catalysts

Hydroformylation catalysts contain transition-metals, and these can be modified by additional ligands such as phosphines. A number of transition metal-based catalysts (Ru, Pt, Pd, Ir or Os) have been reported, but the main interest in industry are Rh- and Co-based catalyst.[9b] Cobalt-based catalysts were the most used catalysts in the hydroformylation reaction until rhodium triarylphosphine catalysts were introduced in the early 1970's.[9b, 15b, 71] Cobalt and rhodium-based hydrides are the most used pre-catalysts for hydroformylation. This is due to the high selectivity for the preferred linear products displayed by rhodium pre-catalysts under milder reaction conditions compared to cobalt-based catalysts.[9b, 15] Rhodium catalyst normally work under mild conditions (25 bar, 100° C) which result in good activity and selectivity to the preferred linear product (aldehyde).[9b, 15, 16] For example, the hydroformylation of 1-octene (long-chain alkene) as shown in **Equation 1.2** uses a rhodium catalyst.

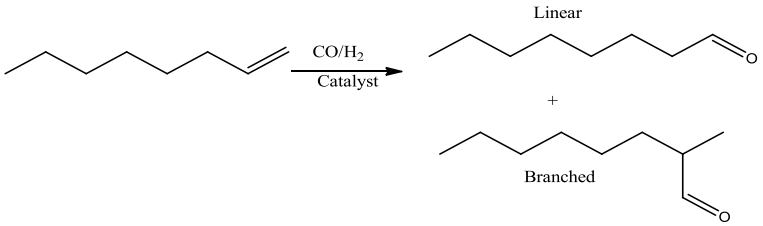

Equation 1.2

Commercially, hydroformylation of longer chain alkenes (e.g 1-octene) use cobalt catalysts even though they result in poor activity and selectivity for the desired linear aldehyde product.[15] Cobalt catalysts need much harsher conditions (normally 200°C, 100 bar).[15a] Nonetheless they are commercially favoured over rhodium catalyst because Rh catalysts decomposition when trying to distill them from the aldehyde product.[15a]

1.4.2 Hydroformylation in Fluorous Biphasic Catalysis

The first transition metal-catalysed reaction to be reported in fluorous biphasic system was hydroformylation;[44c] it was reported by Horvath and Rabai in 1994.[44c] Since then many studies have been carried out.[15b, 44c, 59-67] Fluorous biphasic systems were developed to improve the hydroformylation of higher olefins (C_8-C_{24}) to aldehydes using a rhodium-based catalyst.

Horvath and Rabai used fluorous biphasic system for the hydroformylation of 1-decene in a 1:1 mixture of toluene and $C_6F_{11}CF_3$.[15b, 44c, 59-67] The catalyst used was formed *in situ* from $Rh(CO)_2(acac)$ and $P[CH_2CH_2(CF_2)_5CF_3]_3$ and the reaction was conducted at 10 bar CO/H_2 and 100°C.[3b, 59] After the reaction went to completion phase separation occurred on cooling. The product was observed in the organic phase and decanted and the catalyst was recycled. Horvath demonstrated that rhodium catalysts of the fluorous-derivatised trialkylphosphine could give good activity and decreased leaching of the rhodium. A total turnover number of more than 35 000 was achieved upon recycling the catalyst phase nine successive times with only 4.2% loss of rhodium.[3b, 15b, 62-67]

The only problem experienced by Horvath is the decreased selectivity to the desired linear aldehyde product, this is due to the leaching of the free ligand into the organic phase.[15b, 59, 62] Nevertheless, this could be improved by fine-tuning the ligand/solvents: employing high concentrations of fluorous modified ligands.[59, 62-63] Isomerization of the alkene is a side reaction that occurs during hydroformylation, this result in approximately 10% loss of the starting alkene, therefore decreasing the (n/i) selectivity ratio.[3b, 15b, 59, 63]

Reports have shown that higher rates and selectivity for the desired linear product can be obtained if the organic solvent toluene is omitted and the ligand (trialkylphosphine) is substituted by the ligand (triaryl-phosphine or triarylphosphites). As a result rhodium leaching was reduced to 0.05% per run.[15b, 62-63] The energy requirements for separating the catalyst from the solvent were also reduced in the absence of toluene.[15b] Leaching of rhodium and phosphorous from the fluorous phase decreased significantly and slightly differ as the temperature is raised.[63] This suggests that the catalyst and ligand stability is increased significantly in the absence of toluene.[63] The authors concluded that[63, 65] triaryl-phosphines and phosphites containing fluorous ponytails can give great results in terms of rates, selectivity for the desired linear product, and retention in the fluorous phase at lower ligand loadings compared to trialkylphosines.[62-66]

1.5 Other Reactions Involving Fluorous Biphasic Catalysis

1.5.1 Alkene hydrogenation

Horvath and co-workers reported the hydrogenation of various alkenes (4-bromostyrene, cyclododecene, 2-cyclohexen-1-one and 1-dodecene) using a fluorous pre-catalyst similar to

Wilkinson's catalyst (**Figure 1.16**).[13a, 74] PFMC and toluene were used in the biphasic system. The catalyst was soluble in the fluorous solvent and insoluble in toluene.[74]

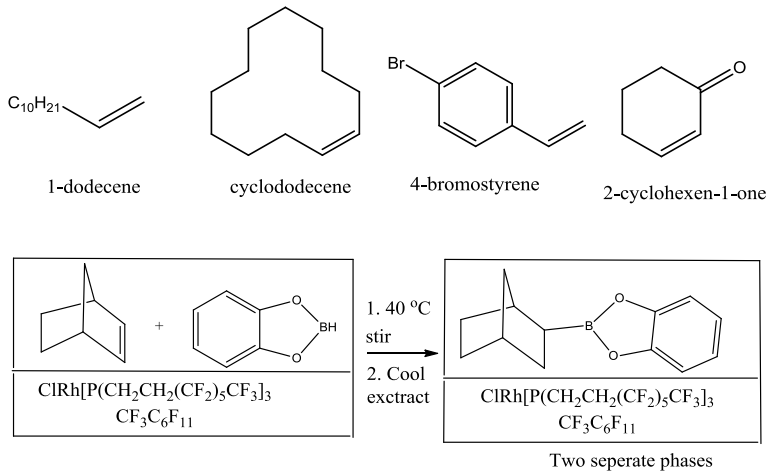

Figure 1.16: Hydrogenation reaction in fluorous biphasic system.[74]

Catalytic amounts (1.1 - 0.8 mol %) were used at 1 atm H_2 and 45 ºC. The GC analysis showed 87-98 % conversion of the hydrogenation products (4-bromoethylbenzene, cyclohexanone, cyclododecane and dodecane) with turnover numbers of 120.[74] The catalyst was recycled three times using 2-cyclohexen-1-one or 1-dodecene as substrates. There was no significant loss in the activity of a catalyst after the second run.[74]

1.5.2 Hydrosilation

The fluorous rhodium complex shown in **Equation 1.3** was used in the hydrosilation of 1-hexene in a biphasic system.[13a, 75] The reaction was carried out in PFMC without the addition of an organic solvent. The reaction was found to form a monophase at higher temperature and at lower temperatures phase separation occurred.[75]

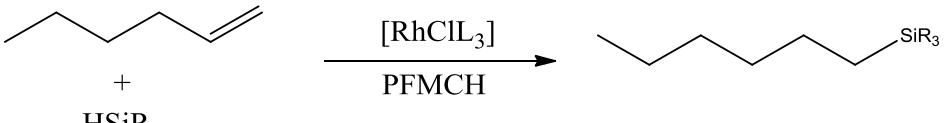

$L = P(4\text{-}C_6H_4SiMe_{3\text{-}n}(CH_2)_2C_8F_{17})_n$

Equation 1.3

The reactions were carried out for 15 minutes and the catalyst was recycled twice with 100 % conversions obtained each time. However, analysis of inductively coupled plasma atomic absorption (ICP-AA) showed leaching of rhodium and the ligand was high (12 and 19 %, respectively).[75]

1.5.3 Allylic Alkylation

Analogues of methoxynaphthyldiphenyl phosphine (**Figure 1.17**) and their application in palladium-catalyzed allylic alkylation have been reported by Maillard *et al*.[76] These ligands were used in the palladium-catalyzed allylic alkylation but they showed low enantioselectivities (0-37 %) for a range of solvent/base ligands.[13a] This was attributed to the low fluorine content which makes the ligands slightly soluble in the organic solvent and leaching of the ligand occurs. Efforts to recycle the catalyst were made, but the second run gave conversions of 24 % only compared 100% conversions in the first run.[76]

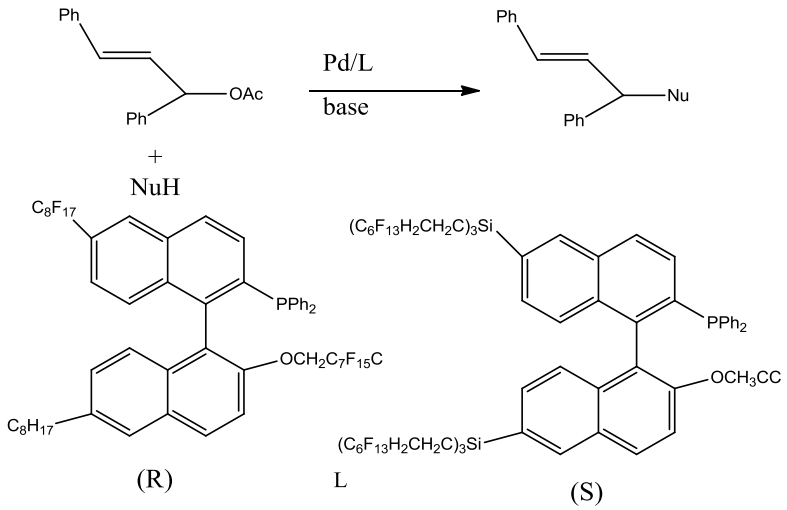

Figure 1.17: Palladium catalyzed reaction using fluorinated ligands.[13a, 76]

1.5.4 Suzuki cross-coupling reaction

Fluorous palladium complexes have also been applied in the Suzuki cross-coupling reaction (**Equation 1.4**) of various aromatic bromides with phenylboronic acid.[13a, 77, 78] Catalytic amounts (1.5 mol %) in perfluoromethylcyclohexane/ 1,2-dimethoxyethane were used at 75 ºC, and conversions greater than 90 % were obtained in 2 h.[13a]

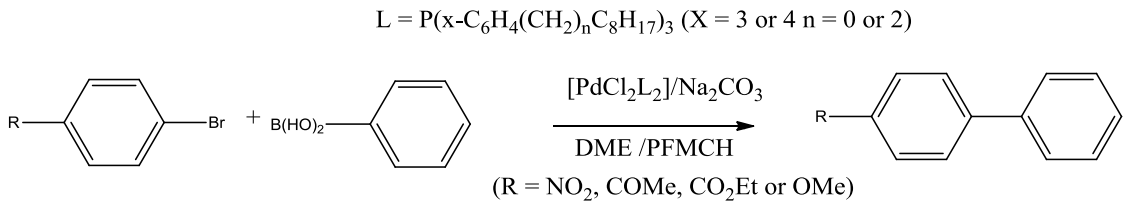

Equation 1.4

1.5 Concluding remarks

Extensive research has been reported in developing processes or systems in order to improve or address the separation of homogeneous catalysts from the products, recycling of the catalysts, activity, and selectivity and lessen and/or eliminate leaching of the metal. Immobilized catalysts on solid supports and multiphasic systems are some of the investigated techniques to improve homogeneous catalysts. Multiphasic systems include ionic liquids, supercritical fluids, aqueous and fluorous biphasic systems. Some of these systems have been employed in the various reactions of alkenes such as alkene hydroformylation, alkene hydrogenation and hydrosilation to name a few.

Herein, we focus on the hydroformylation of 1-octene using fluorous biphasic catalysis. Horvath and co-workers investigated hydroformylation of 1-decene in fluorous solvents using a catalyst formed *in situ* from $Rh(CO)_2(acac)$ and $P[CH_2CH_2(CF_2)_5CF_3]_3$. High turnover numbers upon recycling the catalyst were obtained and selectivity toward linear products decreased after each run.

Based on the research that has been reported for the hydroformylation reaction, we aim to potentially improve on the previously reported work on obtaining greater separation of the catalyst from the products and obtaining higher selectivities. We set out to synthesize and characterize well-defined fluorous catalysts based on rhodium and evaluate them in the hydroformylation of 1-octene. These catalysts contain *N,O*- and *N,P*- chelating ligands as compared to trialkyl phosphine ligands used previously.

1.6 Aims and Objectives

1.6.1 Aims

The aim of this project is to synthesize fluorocarbon-containing rhodium organometallic complexes that can be used as catalyst precursors in the hydroformylation of 1-octene using fluorous biphasic system.

1.6.2 Objectives

The main objectives for this research project are:

- To synthesize iminophosphine fluorocarbon-containing ligands and rhodium complexes and characterize them using various spectroscopic and analytical methods. (Series 1)

- To synthesize salicylaldimine-based ligands and fluorocarbon-containing Rh(I) complexes and characterize them using various spectroscopic and analytical methods. (Series 2)

- To conduct catalytic studies using series 1 and series 2 catalyst-precursors thus evaluating their potential as catalyst precursors in the hydroformylation of 1-octene reaction in a fluorous biphasic system.

1.7 References

1. a) J. H. Clark, D. Macquarrie, J. Rabai, Z. Szlavik and I. T. Horvath, *Handbook of Green Chemistry and Technology*, John Wiley and Sons, 2007, 1-26. b) P. T. Anastas, M. M. Kirchhoff and T. C. Williamson, *Appl. Catal. A Gen.*, **221**, 2001, 3.
2. P. T. Anastas, L. B. Bartlett, M. M. Kirchhoff and T. C. Williamson, *Catal. Today*, **55**, 2000, 11.
3. R. A Sheldon, *Chem. Commun. (Camb).*, 2008, 3352. b) R. A. Sheldon, I. Arends and U. Hanefeld, *Green Chemistry and Catalysis,* Wiley/VCH, Weinheim, Germany, 2007, 1-10, 295-324.
4. a) P. T. Anastas and M. M. Kirchhoff, *Acc. Chem. Res.*, **35**, 2002, 686. b) P. T. Anastas and J. C. Warner, *Green Chemistry: Theory and Practice*, Oxford University Press: New York, 1998, p. 30. c) P. T. Anastas and J. B. Zimmerman, *Design Through the 12 Principles of Green Engineering*, *Environmental Science and Technology*, ACS Publishing, Mar. 2003, 95-101.
5. D. L. Hjeresen, J. M. Boese and D. L. Schutt, *J. Chem. Educ.*, **77**, 2000, 1543.
6. a) J. A. Linthorst, *Found. Chem.*, **12**, 2009, 55. b) C. A. M. Afonso and J. G. Crespo, *Green Separation Processes,* WILEY-VCH Verlag GmbH & Co. KGaA, Weinheim, 2005, 1-18.
7. J. L. Tucker, *Org. Process Res. Dev.*, **10**, 2006, 2001.
8. a) K. I. Zamaraev, *Pure Appl. Chem.*, **68**, 1996, 357. b) J. Hagen, *Industrial Catalysis: A Practical Approach*, WILEY-VCH Verlag GmbH & Co. KGaA, Weinheim, 2006, 1-14, 59-62.
9. a) H. Clark, *Pure Appl. Chem.*, **73**, 2001, 103. b) O. Wiest and Y. Wu, *Comput. Organomet. Chem.*, Springer Heidelberg Dordrecht London New York, 2012, 219.
10. a) *Recognizing the Best In Innovation: Breakthrough Catalysts, R&D Magazine*, Sept. 2005, p. 20, *accessed 8th Feb. 2014*. b) *Types of Catalysis, Chemguide*, *accessed 25th Feb. 2014.*
11. a) B. R. Jagirdar, *General article, Resonance*, **4**, 1999, 63.
    b) http://alexandria.tue.nl/repository/freearticles/591529.pdf , *accssed 10th Feb, 2014.*

12. a) G. Centi, P. Ciambelli, S. Perathoner and P. Russo, *Catal. Today*, **75**, 2002, 3. b) http://eckert.chbe.gatech.edu/pdf/oats.pdf, *accessed 12th Feb 2014.*

13. a) D. J. Cole-Hamilton and R. P. Tooze, *Catalysis Separation, Recovery and Recycling*, Netherlands, 2006, 11-34. b) J. Matthey Plc, *The Catalyst Technical Handbook*, United Kingdom, 2008, 16-17, 43-44.

14. P. W. N. M. Van Leeuwen, *Homogeneous Catalysis Understanding The Art*, Kluwer Academic Publishers, The Netherlands, 2004, 1-25, 125-168.

15. a) A. Behr and P. Neubert, *Applied Homogeneous Catalysis*, First Edition, Wiley-VCH Verlag GmbH & Co. KGaA, 2012, 27-200. b) D. J. Cole-Hamilton, *Science*, **299**, 2003, 1702.

16. a) M. F. Sellin, I. Bach, J. M. Webster, F. Montilla, V. Rosa, T. Avilés and D. J. Cole-Hamilton, **9**, 2002, 4569. b) J. W. Rathke, R. J. Klingler and T. R. Krause, *Organometallics*, **10**, 1991, 1350.

17. B. C. E. Makhubela, A. Jardine and G. S. Smith, *Appl. Catal. A Gen.*, **393**, 2011, 231.

18. A. J. Sandee, R. S. Ubale, M. Makkee, J. N. H. Reek, P. C. J. Kamer, J. A. Moulijn and W. N. M. Van Leeuwen, *Adv. Synth. Cat.*, **343**, 2001, 201.

19. a) N. E. Leadbeater and M. Marco, *Chem. Rev.*, **102**, 2002, 3217. b) C. A. Mcnamara, M. J. Dixon and M. Bradley, *Chem. Rev.*, **102**, 2002, 3275.

20. a) A. J. Sandee, J. N. H. Reek, P. C. J. Kamer and P. W. N. M. van Leeuwen, *J. Am. Chem. Soc.*, **123**, 2001, 8468. b) A. J. Sandee, L. A. van der Veen, J. N. H. Reek, P. C. J. Kamer, M. Lutz, A. L. Spek and P. W. N. M. van Leeuwen, *Angew. Chem. Int. Ed. Engl.*, **38**, 1999, 3231. c) U. Deschler, P. Kleinschmit and P. Panster, *Angew. Chem. Int. Ed. Engl.*, **25**, 1986, 236.

21. E. Schwab and S. Mecking, *Organometallics*, **20**, 2001, 5504.

22. L. Ropartz, R. E. Morris, G. P. Schwarz, D. F. Foster and D. J. Cole-Hamilton, *Inorg. Chem. Commun.*, **3**, 2000, 714.

23. M. Reetz and D. Giebel, *Angew. Chem. Int. Ed. Engl.*, **39**, 2000, 2498.

24. a) L. Ropartz, R. E. Morris, D. J. Cole-Hamilton and D. F. Foster, *Chem. Commun.*, 2001, 361. b) L. Ropartz, K. J. Haxton, D. F. Foster, R. E. Morris and A. M. Z. Slawina, *J. Chem. Soc. Dalton Trans*. **2002**, 2002, 4323. c) B. Cornils, W. A. Herrmann, I. T. Horvath, W. Leitner, S. Mecking, H. Olivier-Bourbigou and D. Vogt, *Multiphase*

Homogeneous Catalysis, (Vol. 1), Wiley-VCH Verlag GmbH & Co. KGaA, Weinheim, 2005, 3.

25. E. A. Karakhanov and A. L. Maksimov, *Russ. J. Gen. Chem.*, **79**, 2009,1370.
26. a) E. Z. Jahromi and J. Gailer, *Dalton Trans.*, **39**, 2010, 329. b) P. L. Davis, *Gas Chromatogr.,* **6**, 1968, 518.
27. I. T. Horváth, *Green Chem.*, **10**, 2008, 1024.
28. R. A. Sheldon, *Green Chem.*, **7**, 2005, 267.
29. D. J. Adams and P. J. Dyson, *Chemistry In Alternative Reaction Media*, 2004, vol. 3, 33-146.
30. F. van Rantwijk, R. Madeira Lau and R. a Sheldon, *Trends Biotechnol.*, **21**, 2003, 131.
31. R. Sheldon, *Chem. Commun.,* 2001, 2399.
32. C. C. Tzschucke, C. Markert, W. Bannwarth, S. Roller, A. Hebel and R. Haag, *Angew. Chem. Int. Ed. Engl.*, **41**, 2002, 3964.
33. T. U. Eindhoven and R. Magnificus, *Homogeneously Catalyzed Hydroformylation in Supercritical Carbon Dioxide : Kinetics , Thermodynamics , and Membrane Reactor Technology for Continuous Operation*, Adrianus C. J. Koeken, 2007, 1.
34. P. B. Webb, M. F. Sellin, T. E. Kunene, S. Williamson, A. M. Z. Slawin and D. J. Cole-Hamilton, *J. Am. Chem. Soc.*, **125**, 2003, 15577.
35. M. F. Sellin, P. B. Webb and D. J. Cole-Hamilton, *Chem. Commun.*, 2001, 781.
36. T. E. Kunene, P. B. Webb and D. J. Cole-Hamilton, *Green Chem.*, **13**, 2011, 1476.
37. B. Cornils, W. A. Herrmann, *Aqueous-Phase Organometallic Catalysis*, Wiley-VCH Verlag GmbH & Co. KGaA, Weinheim, 2004, 71-82, 351-419.
38. E. B. Hager, B. C. E. Makhubela and G. S. Smith, *Dalton Trans.,* **41**, 2012, 13927.
39. B. Cornils, *J. Mol. Catal. A: Chem.*, **143**, 1999, 1.
40. O. Wachsen, K. Himmler and B. Cornils, *Catal. Today*, **42**, 1998, 373.
41. B. Cornils, *Org. Process Res. Dev.*, **2**, 1998, 121.
42 D. Vogt, *Applied Homogeneous Catalysis with Organometallic Compounds*, B. Cornils, W. A. Herr-Mann, Eds. VCH, Weinheim, Germany, 1996, vol. **1**, pp. 245–257.
43. X. L. Zheng, J. Y. Jiang, X. Z. Liu and Z. L. Jin, *Catal. Today*, **44**, 1998, 175.
44. a) J. H. Clark, D. Macquarrie, J. Rabai, Z. Szlavik and I. T. Horvath, *Handbook of Green Chemistry and Technology*, John Wiley and Sons, 2007, 1-26. b) I. T. Horvath, *Acc. Chem.*

Res., **31**, 1998, 641. c) I. T. Horvath and J. Rabai, *Science*, **266**, 1994, 72. d) J. A. Gladysz, D. P. Curran and I. T. Horvath, *Handbook of Fluorous Chemistry*, Wiley-VCH Verlag GmbH & Co. KGaA, 2003, 24-35, 272-350.

45. M. A. Ubeda, *J. Chem. Educ.*, **83,** 2006, 84.
46. A. P. Dobbs and M. R. Kimberley, *J. Fluorine Chem.*, **118**, 2002, 3.
47. E. G. Hope and A. M. Stuart, *J. Fluorine Chem.*, **100**, 1999, 75.
48. R. H. Fish, *Chem. Eur. J.,* **5**, 1999, 1677.
49. D. J. Flannigan, *Fluorous Biphasic Catalysis,* Literature Seminar, 21st Nov. 2001, 49-52.
50. L. P. Barthel-Rosa and J. A. Gladysz, *Coord. Chem. Rev.*, **190–192**, 1999, 587.
51. P. Bhattacharyya, B. Croxtall, J. Fawcett, J. Fawcett, D. Gudmunsen, E. G. Hope, R. D. W. Kemmitt, D. R. Paige, D. R. Russell, A. M. Stuart and D. R. W. Wood, *J. Fluorine Chem.*, **101**, 2000, 247.
52. P. Bhattacharyya, D. Gudmunsen, E. G. Hope, R. D. W. Kemmitt, D. R. Paige and A. M. Stuart, *J. Chem. Soc. Perkin Trans.,* **1**, 1997, 3609.
53. D. J. Adams, D. Gudmunsen, J. Fawcett and E. G. Hope A. M. Stuart, *Tetrahedron*, **58**, 2002, 3827.
54. S. Kawaguchi, Y. Minamida, T. Ohe, A. Nomoto, M. Sonoda and A. Ogawa, *Angew. Chem. Int. Ed*, **52**, 2013, 1.
55. T. Mathivet, E. Monflier, Y. Castanet, A. Mortreux and J. Couturier, *Tetrahedron*, **40**, 1999, 3885.
56. M. Wende, F. Seidel and J. A. Gladysz, *J. Fluorine Chem.*, **124**, 2003, 45.
57. T. Soos, B. L. Bennett, D. Rutherford, L. P. Barthel-Rosa and J. A. Gladysz, *Organometallics*, **20**, 2001, 3079.
58. P. Bhattacharyya, B. Croxtall, J. Fawcett, J. Fawcett, D. Gudmunsen, E. G. Hope, R. D. W. Kemmitt, D. R. Paige, D. R. Russell, A. M. Stuart and D. R. W. Wood, *J. Fluorine Chem.*, **101**, 2000, 247.
59. E. Perperi, Y. Huang, P. Angeli, G. Monos, C. R. Mathison, D. J. Cole-Hamilton, D. A. Adams and E. G. Hope, *Chem. Eng. Sci*., **59**, 2004, 4983.
60. I. T. Horvath, G. Kiss, R. A. Cook, J. E. Bond, P. A. Stevens, J. Rabai and E. J. Mozeleski, *J. Am. Chem. Soc.*, **120**, 1998, 3133.

61. D. J. Adams, D. J. Cole-Hamilton, E. G. Hope, P. J. Pogorzelec and A. M. Stuart, *J. Organomet. Chem.*, **689**, 2004, 1413.

62. D. F. Foster, D. Gudmunsen, D. J. Adams, A. M. Stuart, E. G. Hope, D. J. Cole-Hamilton, G. P. Schwarz and P. Pogorzelec, *Tetrahedron*, **58**, 2002, 3901.

63. D. F. Foster, D. J. Adams, D. Gudmunsen, A. M. Stuart, E. G. Hope and D. J. Cole-Hamilton, *Chem. Commun.,* 2002, 722.

64. Y. Huang, E. Perperi, G. Manos and D. J. Cole-Hamilton, *J. Mol. Catal. A: Chem.,* **210**, 2004, 17.

65. A. Aghmiz, C. Claver, A. M. Masdeu-Bulto, D. Maillard and D. Sinou, *J. Catal. A: Chem.*, **208**, 2004, 97.

66. T. Mathivet, E. Monflier, Y. Castanet, A. Mortreux and J-L. Couturier, *Tetrahedron*, **58**, 2002, 3877.

67. D. J. Adams, J. A. Bennett, D. J. Cole-Hamilton, E. G. Hope, J. Hopewell, J. Kight, P. Pogorzelec and A. M. Stuart, *J. Organomet. Chem.*, **689**, 2004, 1413.

68. a) J. Falbe, *New syntheses with carbon Monoxide*, Springer-Verlag Berlin Heidelberg, New York. 1980, p 31, 274, 304. b) P. Pino, I. G. Wender, *Organic Syntheses via Metal Carbonyls*; John Wiley and Sons: New York, 1977, Vol. 2, p 446, 457, 504.

69. a) K. Mukhopadhyay, A. B. Mandale, R. V. Chaudhari, *Chem. Mater*, **15**, 2003, 1766; b) K. Mukhopadhyay, B. R. Sarkar, R. V. Chaudhari, J. *Am. Chem. Soc*., **124**, 2002, 9692. c) W. A. Herrmann, B. Cornils, *Angew. Chem. Int. ed.*, **36**, 1997, 1048.

70. a) G. W. Parshall, in *Homogenous Catalysis*, Wiley, New York, 1980, 12-24. b) S. Bhaduri and D. Mukesh, *Homogenous Catalysis: Mechanisms and Industrial Applications*, John Wiley and Sons Inc., New York, 2000, 85-88.

71. M. A. Rida and A. K. Smith, *J. Mol. Catal. A: Chem*., **202**, 2003, 87.

72. M. Haumann, H. Koch b, P. Hugo and R. Schomäcker, *Appl. Catal. A: Gen.*, **225**, 2002, 239.

73. D. Rutherford, J. J. J. Juliette, C. Rocaboy, I. T. Horvath and J. A. Gladysz, *Catal. Today*, **42**, 1998, 381.

74. E. de Wolf, E. A. Speets, B. Deelman and G. Van Koten, *Organometallics*, **20**, 2001, 3686.

75. M. Cavazzini, G. Pozzi, S. Quici, D. Maillard and D. Sinou, *Chem. Commun.*, 2001, 1220.

76. C. C. Tzschucke, C. Markert, H. Glatz and W. Bannwarth, *Angew. Chem. Int. Ed*., **41**, 2002, 4500.

77. M. Moreno-Man, R. Pleixats and S. Villarroya, *Organometallics*, **20**, 2001, 4524.

78. J. Falbe; *New Syntheses With Carbon Monoxide*, Springer-Verlag Berlin Heidelberg, New York. 1980, p. 31, 274, 304.

Synthesis and Characterization of Fluorocarbon-Containing Schiff Base Ligands

2.1 Introduction

Schiff base ligands and their complexes have been widely studied due to their structural features and coordination properties.[1, 2a] Schiff base compounds mainly contain nitrogen, oxygen, sulphur and phosphorous donor atoms or sites and also possess an imine group (C=N).[1] They are prepared *via* simple condensation between amines and aldehydes to form imine ligands (**Scheme 2.1**).[1b, 3, 4] These ligands are of importance in chemistry, particularly in the development of Schiff base complexes. This is because of their potential to form stable complexes by chelating different metal ions and they are also easy to synthesize and can be obtained in excellent yields.[2b]

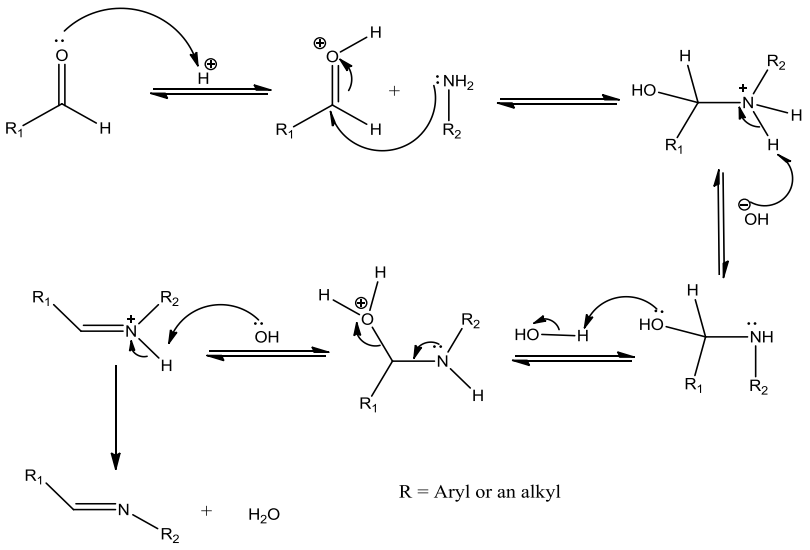

Scheme 2.1

Due to easy preparation of Schiff bases, various ligands with different design and characteristics can be obtained by selecting suitable reactants.[3] Schiff base ligands of *o*-hydroxyaromatic aldehydes (i.e salicylaldehyde) with aliphatic and aromatic mono- or di-amines are the most commonly prepared ligands.[2] The salicylaldimine Schiff base bidentate chelating ligands can contain *N,O*- donor sites. The nitrogen atom is a soft donor atom which stabilizes the lower oxidation state metal ions upon coordination and oxygen is a strong donor atom which stabilizes high oxidation state metal ions.[5]

Iminophosphine-based ligands are also commonly used and they possess *N,P*- donor atoms which are soft donor atoms known to bind with soft metals such as palladium which makes these precursors good for catalytic processes.[6] These ligands can also stabilize metal ions with different oxidation states.

This chapter describes the synthesis and characterization of fluorous-containing salicylaldimine and iminophosphine bidentate chelating ligands. The synthesized ligands were characterized using a range of spectroscopic and analytical techniques, these include 1-D NMR (^{1}H, $^{13}C\{^{1}H\}$, $^{31}P\{^{1}H\}$ and $^{19}F\{^{1}H\}$ NMR spectroscopy), 2-D NMR (COSY and HSQC) spectroscopy, EI-mass spectrometry, FT-IR spectroscopy and elemental analysis.

2.2 Results and Discussion

2.2.1 Synthesis and characterization of fluorocarbon-containing iminophosphine ligands L1 and L2

The synthesized ligands in this section contain fluorous-substituted aryl rings. The iminophosphine ligands (**L1** and **L2**) were synthesized *via* a Schiff base condensation reaction of 2-diphenylphosphino(benzaldehyde) with various primary amines (**Scheme 2.2**). These compounds and their synthetic methods have been previously reported in literature.[7, 8] Ligands **L1** and **L2** both were isolated as yellow solids in good yields (71 % and 82 %, respectively). The ligands were characterized using various spectroscopic and analytical methods.

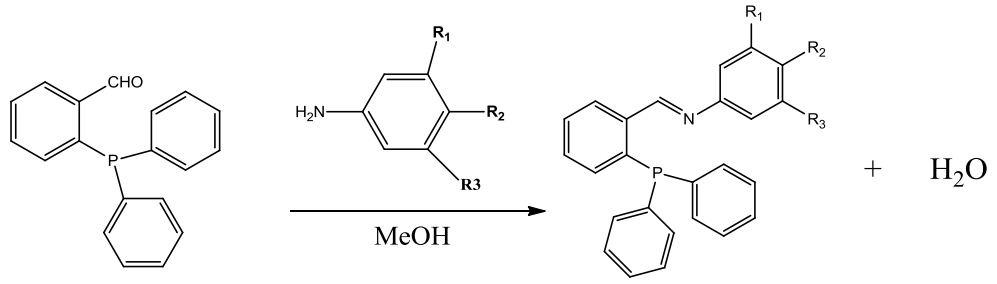

Scheme 2.2

^{1}H NMR Spectroscopy

^{1}H NMR spectroscopy was used to characterize and confirm the formation of ligands **L1** and **L2**. The ^{1}H NMR spectra display a doublet assigned to the imine proton at δ 9.02 ppm with a coupling constant of ^{4}J = 5.2 Hz for **L1** and δ 8.94 ppm ($^{4}J_{HP}$ = 4.6 Hz) for **L2**. The coupling constants suggest that the imine proton is coupling to the phosphorous and is consistent with $^{4}J_{HP}$ o pli ng on n (5.1 z .[7,8] The imine assignments for both ligands were also compared to the assignments reported in the literature.[7, 8] The ^{1}H NMR spectrum of ligand **L2** in **Figure 2.1** is used as a model. Full assignment of the proton NMR was made using 2-D NMR (COSY) correlation spectroscopy.

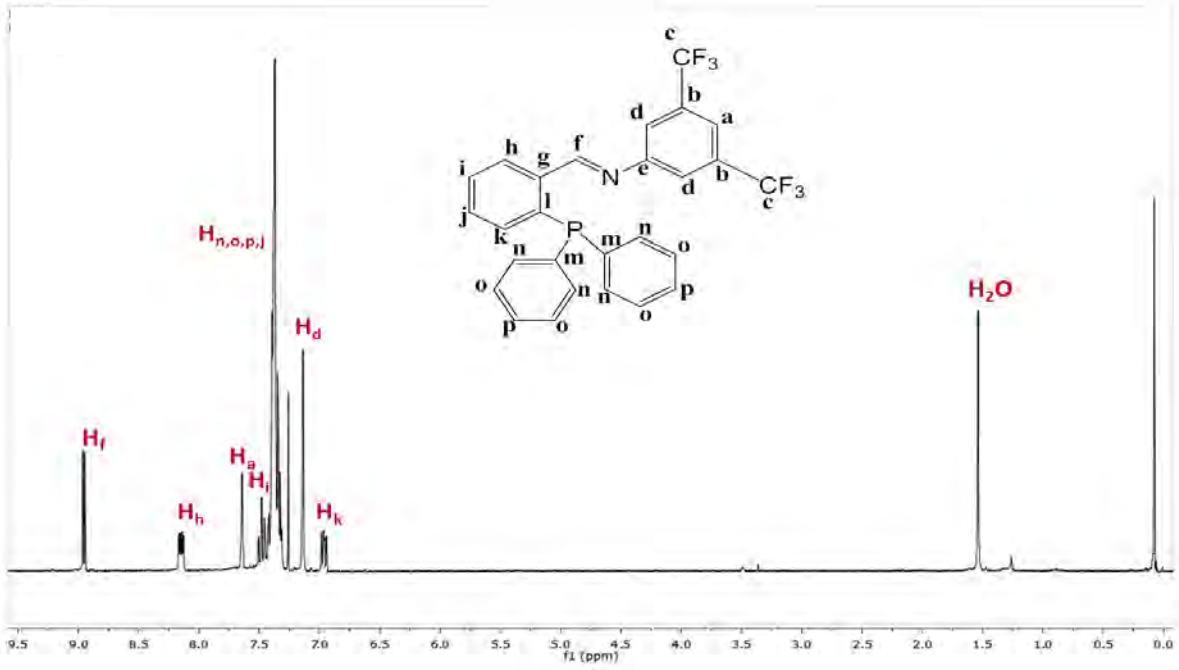

Figure 2.1: ^{1}H NMR spectrum of iminophosphine ligand **L2** in $CDCl_3$.

The COSY spectrum permits assignments of the neighboring connectivities in a compound *via* proton-proton scalar coupling. The cross peaks in the COSY generally signify that the protons providing the connected resonances on the diagonal are either vicinally or geminally coupled.[9] The COSY can also provide cross peaks indicative of long-range coupling. The COSY spectrum assisted in the peak assignments and confirms the formation of the synthesized ligand. **Figure 2.2** is a COSY spectrum of **L2** which is used as an illustration on assigning the full proton NMR spectrum.

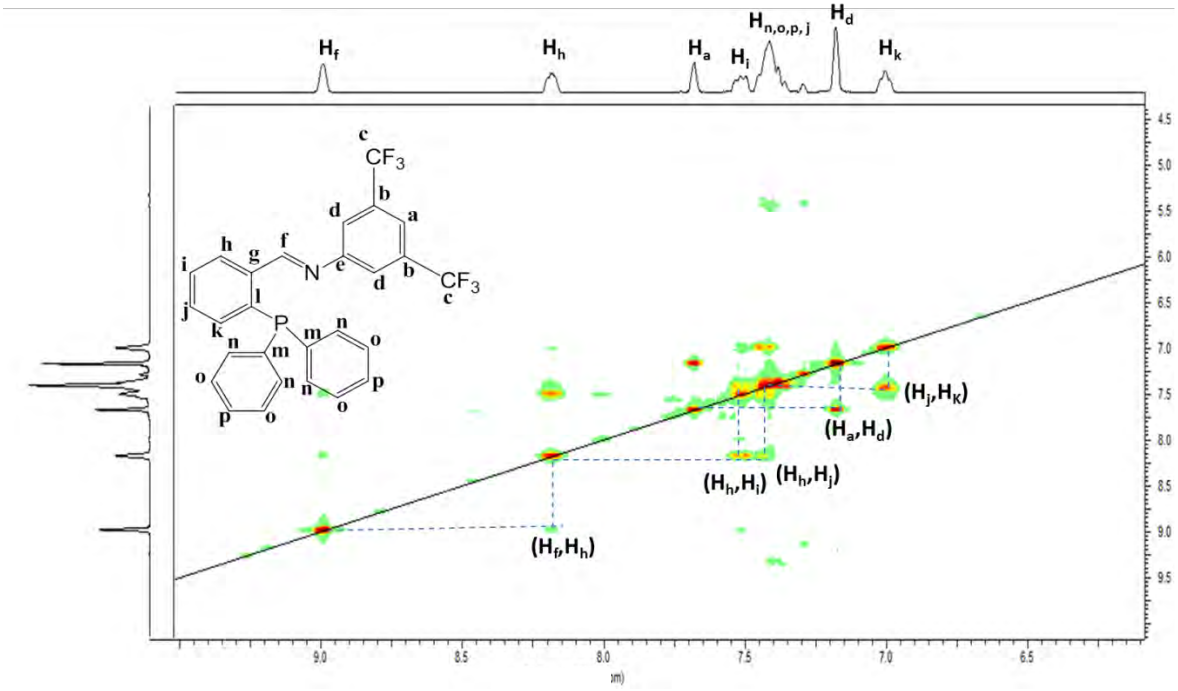

Figure 2.2: ^{1}H-^{1}H COSY 2D-NMR spectrum of ligand **L2** in $CDCl_3$.

The COSY spectrum (**Figure 2.2**) contains three spin systems: the ring attached to the phosphorous and carbon (f), the ring containing fluorocarbon groups and the imine carbon and lastly the other two rings attached to the phosphorous. On inspection of the COSY spectrum (**Figure 2.2**) the most downfield signal (H_f) whi h i i gned o he imine pro on (δ 8.94 ppm as assigned above is coupling to (H_h), this is indicative of long-range coupling between the two protons. Proton (H_h) correlates to the adjacent/vicinal proton (H_i) which further couples to the proton (H_j) *via* long-range coupling, as shown by the cross peak in COSY spectrum (**Figure 2.2**). The spectrum also indicates a cross peak between (H_j) and its coupling partner (H_k). The COSY also shows that in the second spin system protons (H_a) and (H_d) couple to each other with (H_a) being more deshielded due to the fluorine electron-withdrawing groups and also integrates for one proton. Lastly, the protons of the diphenyl rings attached to the phosphorous are observed ro nd δ 7.36 ppm nd i n egr e for en pro on .

$^{13}C\{^{1}H\}$ NMR Spectroscopy

The 2D-NMR Heteronuclear Spin-Quantum Coupling Spectroscopy (HSQC) was used to assist in assigning the carbon peaks. HSQC detects correlation between the proton and attached ^{13}C

nuclei.[10] The full ^{1}H NMR spectrum was used to label the proton/carbon cross peaks in order to assign the carbon peaks. **Figure 2.3** displays the HSQC spectrum of **L2** as an illustration.

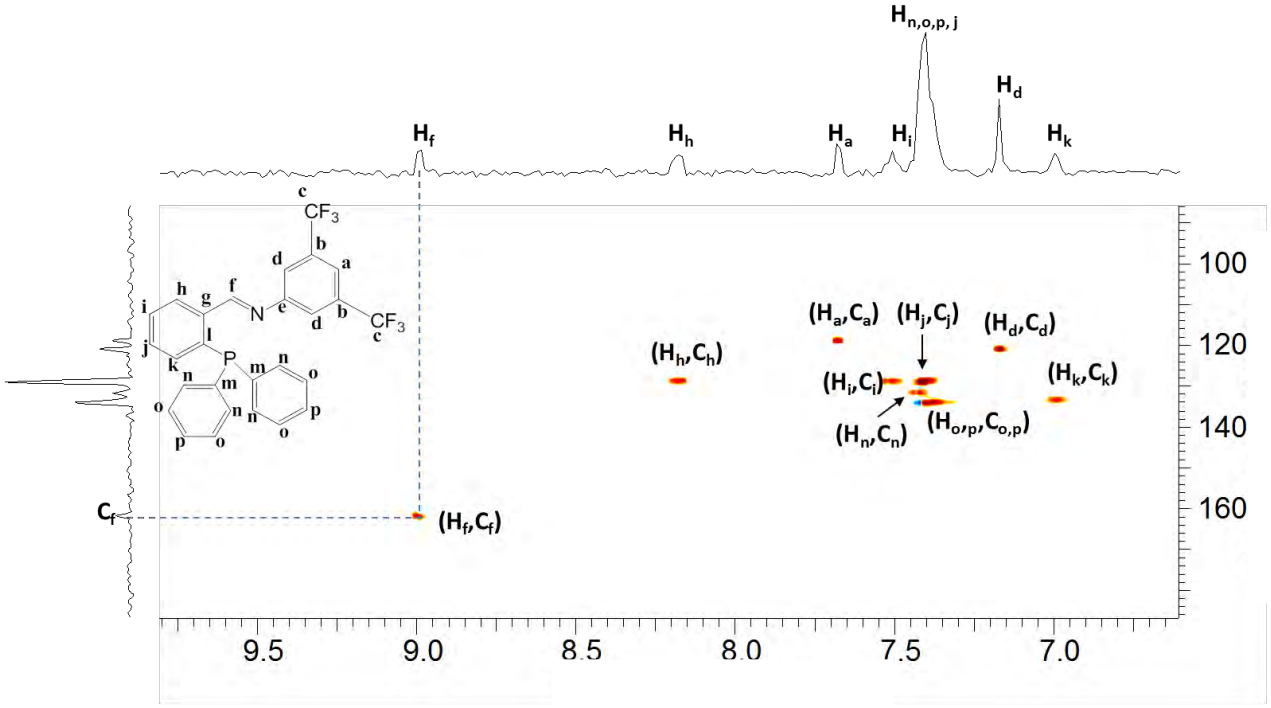

Figure 2.3: ^{1}H-^{13}C HSQC 2D NMR spectrum of ligand **L2** in $CDCl_3$.

The HSQC spectrum (**Figure 2.3**) shows that the most deshielded signal (H_f) corresponds to the most deshielded carbon signal (C_f δ 161.7 ppm, whi h i do ble wi h o pli ng on n of ^{3}J = 19.7 Hz. Carbon (C_f) is a doublet because of its coupling to the phosphorous and the coupling constant is comparable with what is reported in the literature.[11-13] **L1** also displays its carbon shift (C_f δ 160.5 ppm (^{3}J = 21.3 Hz). The remaining carbon signals were also assigned by correlating them to the assigned protons. The aromatic carbons appear in the expected region, for **L1** (δ 120.8-134.1 ppm) and **L2** (δ 120.8-134.2 ppm).

$^{31}P\{^{1}H\}$ NMR and $^{19}F\{^{1}H\}$ NMR spectroscopy

$^{31}P\{^{1}H\}$ NMR spectroscopy was also used to prove the formation of the ligands. The $^{31}P\{^{1}H\}$ NMR pe r exhibi ing le pfie ld δ -12.7 ppm nd δ -11.36 for **L1** and **L2**, respectively. The peak is assigned to the phosphorous atom of the (diphenylphosphino)benzaldehyde moiety of the ligand. These values are comparable with values reported in literature.[7,8]

$^{19}F\{^1\}$ NMR di pl y he fl or ine om pe k δ 78.1 ppm for **L1** nd wo pe k δ 79.7 nd 78.9 ppm for **L2** each assigned to the -CF_3 moieties.

Fourier Transform-Infrared Spectroscopy (FT-IR)

The FT-IR spectra were obtained using KBr pellets. Infrared spectroscopy was used to further corroborate the formation of the ligands **L1** and **L2**. The IR spectra shows an absorption band at 1613 cm^{-1} for **L1** and at 1632 cm^{-1} for **L2** which is assigned to the imine stretching frequency. The C-F frequencies were also observed in the IR spectrum around 1105 - 1200 cm^{-1} for both ligands. These values are comparable to values reported in literature.[7,8]

Elemental Analysis and Electron Impact Mass Spectrometry

The mass spectral data shows a molecular ion peak $[M]^+$ at 433.1 (*m/z*) for ligand **L1** and at 500.9 (*m/z*) for **L2**. The calculated elemental analysis results correlate with the obtained experimental values **L2** and there is a slight deviation from the theoretical value of carbon compared to that of the experimental value. This might be due to traces of moisture or solvent in the compound.

2.2.2 Synthesis and characterization of Perfluoroalkyl Azide (L3), Pefluoroalkyl amine (L4) and N-(2-(diphenylphosphino)benzylidene)-3,3,4,4,5,5,6,6,7,7,8,8,8-tridecafluorooctan-1-amine (L5)

This section discusses the synthesis and characterization of compounds containing perfluoroalkyl chains. Compound **L5** is accessible by multistep syntheses (**Scheme 2.3**) starting from the perfluorooctyl iodide. Following the literature method used by Palomo and co-workers,[14] pefluoroalkyl iodide was first reacted with sodium azide in the presence of a phase transfer catalyst methyltridecylammonium chloride (Aliquat® 336) to yield the intermediate perfluoroalkyl azide (**L3**), which was then reduced to afford the perfluoroalkyl amine[14-21] (**L4**) which was isolated as yellow oil in excellent yield (96 %). Compound **L4** was then reacted with 2-diphenylphosphino(benzaldehyde) *via* Schiff base condensation reaction to yield a new compound **L5**, which was obtained as a yellow oil in good yield (83 %).

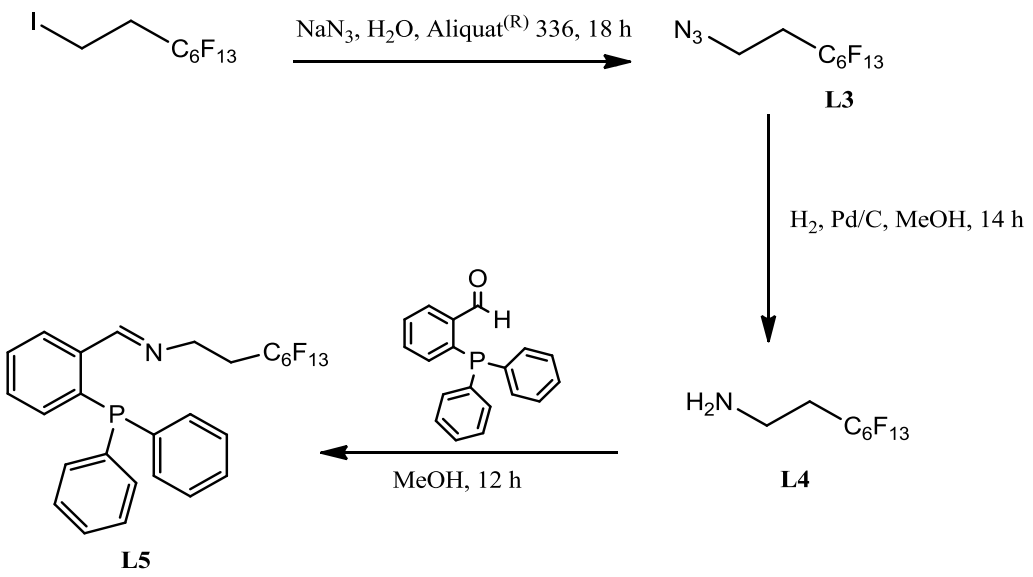

Scheme 2.3

^{1}H NMR Spectroscopy

The ^{1}H NMR spectrum of compound **L3** exhibi wo pe k , riple δ 3.60 ppm ($^{3}J_{HH}$ = 7.19 z nd m l iple δ 2.40, while h of he pre r or di pl yed m l iple δ 2.73 ppm nd riple δ 3.26 ppm. The riple i i gned o he me hylene pro on dj en o he zide (N_3) and the multiplet is assigned to the protons next to the carbons attached to the fluorine atoms -CF_2-CH_2.

The proton NMR spectrum of compound **L4** h ow ing le δ 1.65 ppm rib e d o he mine pro on, riple δ 3.03 ppm ($^{3}J_{HH}$ = 7.19 Hz) assigned to -CH_2 next to the amine (NH_2) and a m l iple δ 2.23 ppm i gned o -CH_2 next to -CF_2. The triplet assigned to –CH_2-NH_2 hif ed pfie ld from δ 3.60 ppm (-CH_2-N_3 o δ 3.03 ppm (-CH_2-NH_2). The resulting shifts indicate the formation of the amine. Furthermore, a D_2O wash experiment was also used to v lid e he form ion of he mine. Thi i how n by he di ppe r n e of he mine pe k δ 1.65 ppm after the D_2O wash experiment.

The ^{1}H NMR spectrum of compound **L5** di pl y wo liph i ign l , riple δ 3.71 ppm (J = 7.6 Hz) assigned to -CH_2 next to -NH_2 nd m l iple δ 2.16 ppm i gned o -CH_2 adjacent to -CF_2. The pe r m ho w n imine pe k δ 8.87 ppm ($^{4}J_{HP}$ = 4.4 Hz). The aromatic protons ppe r in he expe ed region δ 6.91 – 7.91 ppm.

$^{13}C\{^1H\}$ NMR Spectroscopy

$^{13}C\{^1H\}$ NMR spectrum of compound **L3** di pl y i gn l δ 43.2 ppm i gned o –CH_2 carbon next to -N_3 nd δ 30.7 ppm llo ed o -CH_2 carbon adjacent to –CF_2. The spectrum l o how m l iple δ 122.2-104.9 ppm attributed to the carbons attached to the fluorine atoms.

Similarly, the $^{13}C\{^1H\}$ NMR spectrum of **L4** di p l y he liph i rbon ig n l δ 34.4 ppm nd riple δ 34.7 ppm. The e ig n l re igned o he rbon om hed o he mine and the carbon adjacent to the fluorocarbon, respectively. The spectrum also shows multiplets at δ 120.9 - 107.9 ppm characteristic for the carbon atoms attached to the fluorine atoms. The $^{13}C\{^1H\}$ NMR spectrum of the target compound **L5** how ig n l downfield δ 161.7 ppm which is assigned to the imine carbon. Signals for the aromatic carbon atoms occur in the region δ 128.5-134.1 ppm.

$^{19}F\{^1H\}$ NMR and $^{31}P\{^1H\}$ NMR spectroscopy

The $^{19}F\{^1H\}$ NMR spectra of compound **L3**, **L4** and **L5** display six signals which have comparable chemical shifts. For example, the spectrum of compound **L5** shows signals at δ -81.7, -126.9, -124.4, -123.6, -122.7 and -114.4 ppm. The m l iple en ered δ -81.7 corresponds to -CF_3, he ig n l δ -126.9, -124.4, -123.6, -122.7 are assigned to -CF_2 moieties and lastly the multiplet at -114.4 ppm corresponds to -CF_2 adjacent to the -CH_2.
The $^{31}P\{^1\}$ NMR pe r exhibi ingle δ -12.6 ppm characteristic of the phosphorous of the (diphenylphosphino)benzaldehyde moiety.

FT-IR Spectroscopy

The FT-IR spectrum of compound **L3** displays an absorption band at 2107 cm^{-1} characteristic of the azide (-N_3) group. In the IR spectrum of **L4** the absorption band (2107 cm^{-1}) characteristic of the azide does not appear, this is expected as this further proves that the reduction of the azide to an amine has occurred. The spectrum of **L5** shows an absorption band at 1638 cm^{-1} assigned to the imine moiety (C=N). The spectra of **L3**, **L4** and **L5** display similar bands at around 1105 - 1208 cm^{-1} corresponding to the C-F frequencies.

Elemental Analysis and Electron Impact Mass Spectrometry

The EI Mass spectrum of **L5** shows a molecular ion peak $[M]^+$ at 635.10 (*m/z*). The calculated elemental analysis results for C, H and N were in agreement with the obtained experimental values.

2.3 Synthesis and characterization of fluorocarbon-containing salicylaldimine ligands

2.3.1 Synthesis and characterization of 2-((4-(trifluoromethyl)phenyl)imino)methyl)phenol (L6) and 2-((3,5-bis(trifluoromethyl)phenyl)imino)methyl)phenol (L7)

This section discusses the series of compounds containing fluorous-substituted aryl rings. The known salicylaldimine ligands **L6** and **L7** (**Scheme 2.4**) were synthesized *via* a Schiff base condensation reaction following methods reported in literature.[22-27] In separate reactions, salicylaldehyde was reacted with 4-trifluoromethyl aniline by refluxing at 78 ^oC in ethanol to form **L6** and reacted with 3,5-bis(trifluoromethyl)aniline at room temperature to form **L7**. Both ligands were isolated as bright yellow solids in 85 % yield for **L6** and 66 % for **L7**

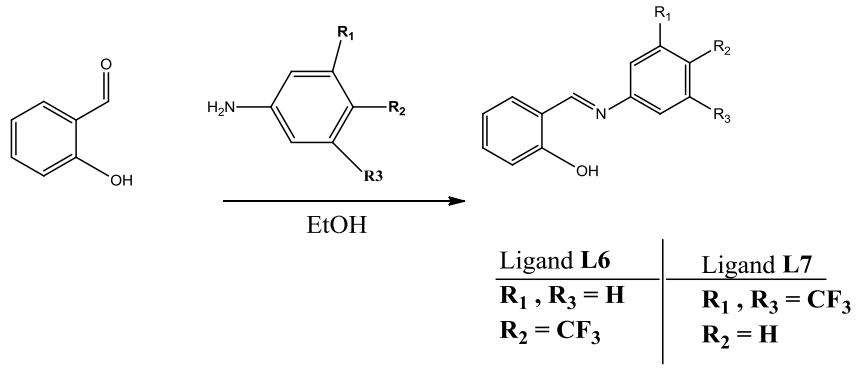

Scheme 2.4

^1H NMR Spectroscopy

^1H NMR spectrum shows distinctive peaks associated with the proposed structures. The proton NMR pe r di pl y imine pro on ing le ro nd δ 8.54 ppm nd δ 8.58 ppm for **L6** and **L7**, re pe ively. The hydroxyl pro on i l o ob er ved bro d ing le δ 12.7 ppm for **L6** nd δ 12.2 ppm for **L7**. The aromatic protons appear in the expected region for both compounds. The chemical shifts are comparable with literature values.[23.26] **Figure 2.4** shows the proton spectrum of **L6** as a typical example for the salicylaldimine based ligands.

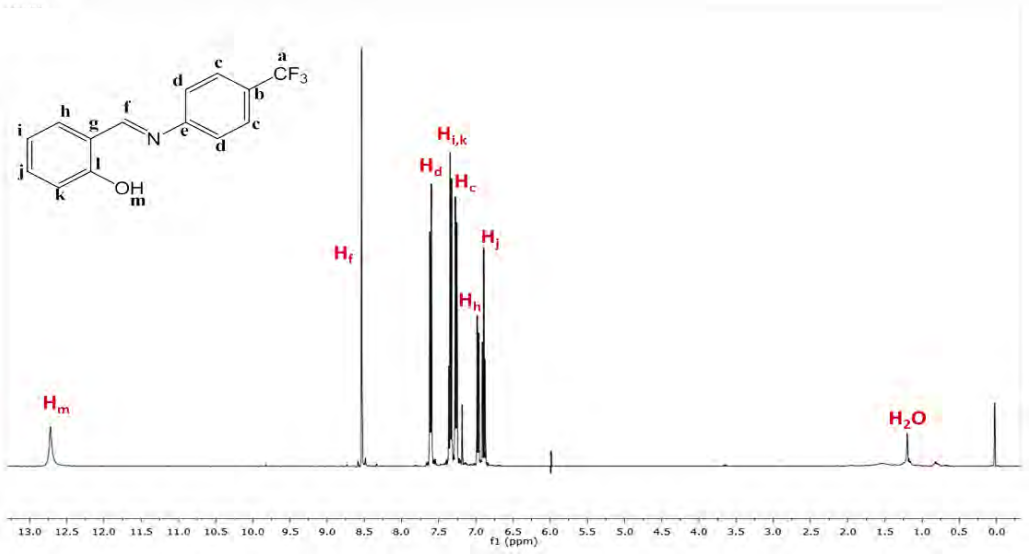

Figure 2.4: ^{1}H NMR of iminophosphine ligand **L6** in $CDCl_3$.

Full proton NMR assignments were made using the same methodology describe is **Section 2.3** using the COSY spectrum (**Figure 2.5**). The COSY spectrum also assisted in assigning the remaining protons in the ligands. The COSY spectrum (**Figure 2.5**) shows long-range coupling between (H_f) and (H_h, H_i and H_k). Proton H_i couples to the vicinal protons (H_h) and (H_j). Lastly protons (H_d) correlates to proton (H_c) in the ring containing fluorine groups.

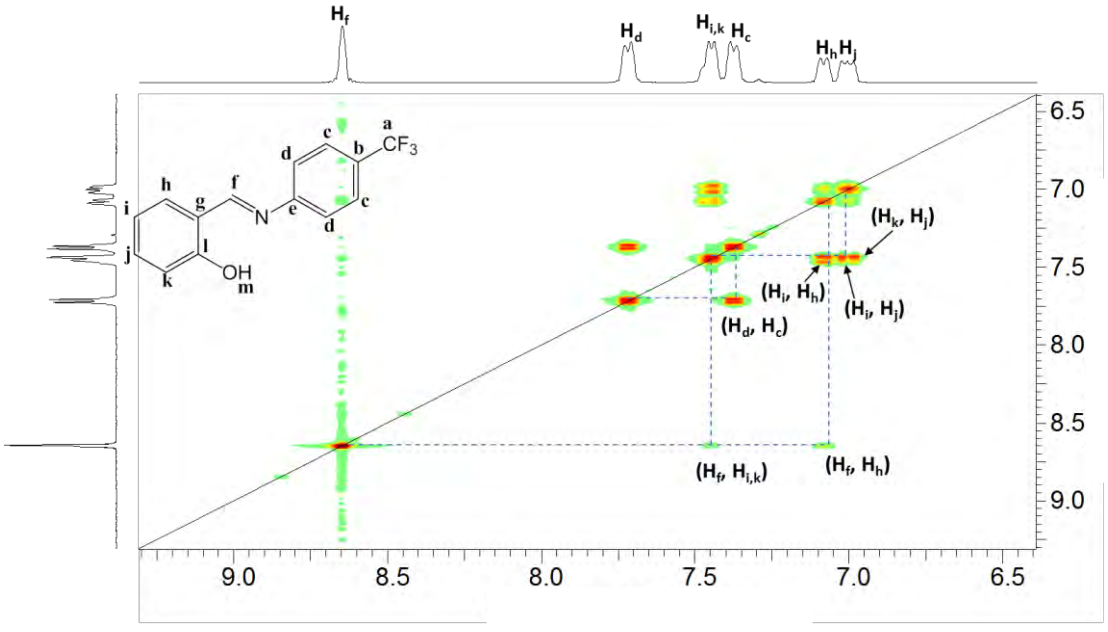

Figure 2.5: ^{1}H-^{1}H COSY 2D-NMR spectrum of ligand **L6** in $CDCl_3$.

$^{13}C\{^1H\}$ NMR Spectroscopy

The $^{13}C\{^1\}$ NMR pe r of he lig nd how ign l downfield δ 164.5 for **L6** nd δ 165.7 for **L7** ppm which is assigned to the imine carbon. The HSQC spectrum was used to assist in assigning the remaining carbon signals. **Figure 2.6** displays the HSQC spectrum of ligand **L6** as an example to illustrate the carbon assignments.

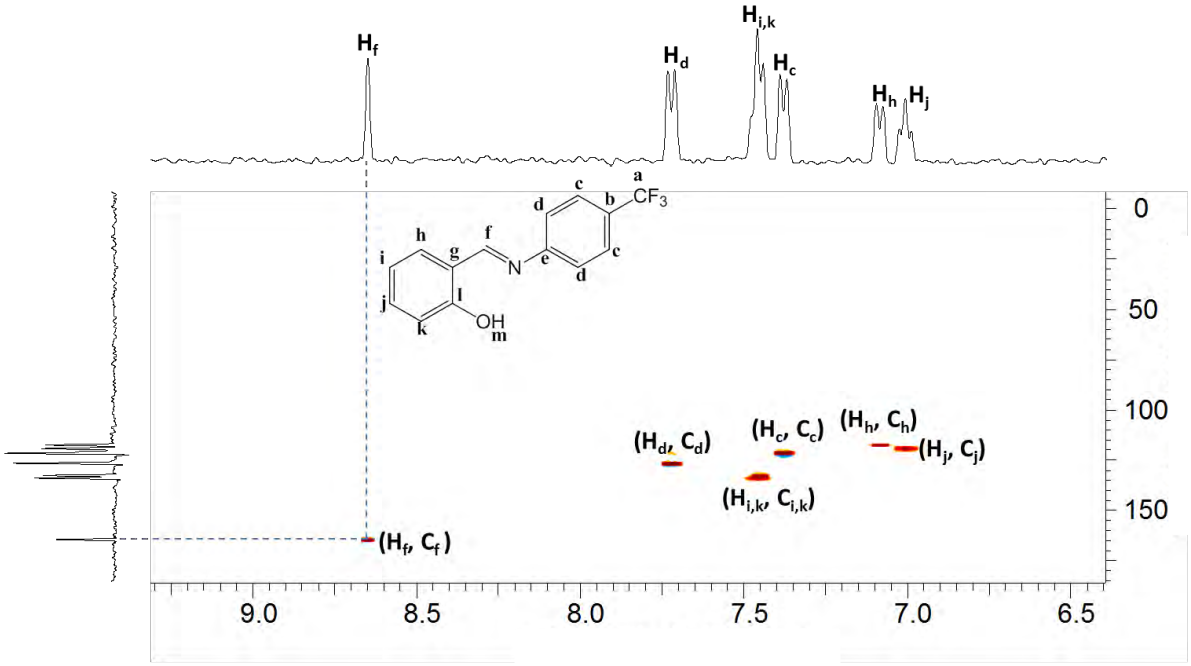

Figure 2.6: ^1H-^{13}C HSQC 2D NMR spectrum of ligand **L6** in $CDCl_3$.

The most downfield signal (imine proton H_f δ 8.85 ppm o ple o he mo downfield rbon whi h i i gned o he imine rbon (δ 164.5 ppm, C_f). The fully assigned proton NMR spectrum permitted the assignment of the remaining carbons of the ligand (**Figure 2.6**). The aromatic carbons occur in he expe ed region (δ 117-133 ppm) for both ligands **L6** and **L7**.

$^{19}F\{^1H\}$ NMR spectroscopy

The $^{19}F\{^1\}$ NMR pe r how one pe k δ 78.7 ppm for **L6** nd δ 78.0 ppm for compound **L7**. The peaks are attributed to the fluorine atoms of the $–CF_3$ moiety.

FT-IR Spectroscopy

FT-IR spectroscopy was used to further corroborate the formation of the ligands. This is indicated by the imine absorption band that appears at 1623 cm^{-1} for **L6** and 1628 cm^{-1} for **L7**. The C-F frequencies were also observed in the IR spectrum around 1100 cm^{-1}.

Elemental Analysis and Electron Impact Mass Spectrometry

The mass spectrum shows a molecular ion peak $[M]^+$ at 264.03 (*m/z*) for **L6** and 333.03 (*m/z*) for **L7**. The calculated elemental analysis results correlate to the obtained experimental values for **L6** and **L7**.

2.3.2 Synthesis and Characterization of 2-(((3,3,4,4,5,5,6,6,7,7,8,8,8-tridecafluorooctyl)imino)methyl)phenol (L8)

In this section, the synthesis and characterization of the compound containing the perfluoroalkyl chain will be discussed. The Ligand **L8** was prepared by refluxing 1H, 1H, 2H, 2H-Perfluorooctyl amine (**L4**) and salicylaldehyde in methanol for 1h (**Scheme 2.5**).[28] The solvent was removed, and DCM was added followed by anhydrous magnesium sulfate to remove water and then removed by gravitational filtration. The desired product was obtained as a yellow solid in 89 % yield.

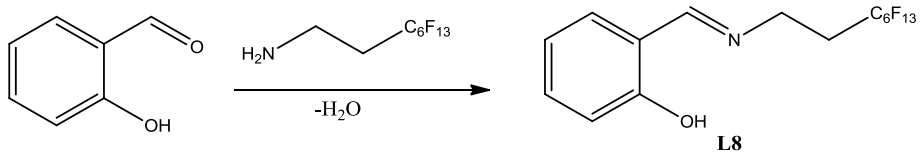

Scheme 2.5

^{1}H NMR Spectroscopy

The ^{1}H NMR spectrum shows a single peak at δ 8.35 ppm, assigned to the imine proton. A triplet at δ 3.84 ppm and a multiplet at δ 2.47 ppm were also observed in the spectrum. The multiplet is assigned to the protons attached to the carbon adjacent to the carbon attached to the fluorine atoms ($-CH_2-CF_2$) while the triplet is assigned to the protons next to the imine nitrogen.

$^{13}C\{^1H\}$ NMR Spectroscopy

The $^{13}C\{^1\}$ NMR pe r m of he lig nd how ig n l downfield δ 166.7 ppm whi h i i gned o he imine rbon. The rom i rbon ig n l o r in he region δ 128.6-134.1 ppm as expected.

$^{19}F\{^1H\}$ NMR spectroscopy

The $^{19}F\{^1\}$ NMR pe r m how pe k δ -81.6 ppm assigned to $–CF_3$ moiety, also peaks at δ – 126.9, -124.3, -123.6, -122.7 assigned to $–CF_2$ gro p nd l l y pe k δ -114.3 ppm assigned to $–CF_2$ adjacent to $-CH_2$.

FT-IR Spectroscopy

FT-IR spectroscopy was used to further confirm Schiff base condensation. This is indicated by he imine b orp ion b nd h ppe r δ 1638 m^{-1}. Absorption bands for the C-F frequencies were also observed in the IR spectrum around 1200 cm^{-1}.

Elemental analysis and Electron Impact Mass Spectrometry

The mass spectra shows a molecular ion peak $[M]^+$ at 466.84 (*m/z*). The calculated elemental results are in agreement with the obtained experimental values.

2.4 Conclusion

A series of Schiff base fluorocarbon-containing iminophosphine ligands (**L1, L2** and **L5**) and salicylaldimine ligands (**L6 – L8**) were successfully synthesized *via* Schiff base condensation reaction. Ligands (**L1 - L2** and **L6 - L8**) were isolated as air stable solids in moderate to high yields.

The ligands were fully characterized using a number of spectroscopic techniques and analytical methods which include ^1H NMR, $^{13}C\{^1H\}$ NMR, $^{31}P\{^1H\}$ NMR and $^{19}F\{^1H\}$ NMR, 2-D NMR (COSY and HSQC) spectroscopy, mass spectrometry, infrared spectroscopy and elemental analysis.

2.5 Experimental

2.5.1 General

All the reagents were purchased from Sigma-Aldrich and were used without any further purification.

All NMR spectra (^{1}H, $^{13}C\{^{1}H\}$, $^{31}P\{^{1}H\}$, and $^{19}F\{^{1}H\}$ NMR) were recorded using Varian mercury XR300 MHz (^{1}H at 300.08 MHz, $^{31}P\{^{1}H\}$ at 121.47 MHz), Varian Unity XR400 spectrometer (^{1}H at 399.95 MHz, $^{13}C\{^{1}H\}$ 100.58 MHz, $^{19}F\{^{1}H\}$ 376.9 MHz) or Bruker Biospin GmbH (^{1}H at 400.22 MHz, $^{13}C\{^{1}H\}$ 100.60 MHz, $^{31}P\{^{1}H\}$ at 162.00 MHz) spectrometer at ambient temperature using tetramethylsilane (TMS) for ^{1}H NMR, trifluoroacetic acid (TFA) for the $^{19}F\{^{1}H\}$ NMR and phosphoric acid for $^{31}P\{^{1}H\}$ NMR as internal standards. Fourier Transform Infrared spectra (FT-IR) were obtained using the Perkin-Elmer Spectrum 100 FT-IR spectrometer as KBr pellets or in a solution of dichloromethane using NaCl cells. Elemental analysis (EA) for C, H and N were carried out using a Thermo Flash 1112 Series CHNS-O Analyser. Electron Impact mass spectrometry was carried out on an Agilent 6890 N spectrometer. Melting points were determined using a Büchi Melting Point B-540 and are uncorrected.

2.5.2 Preparation of Compound ***L1***[7]

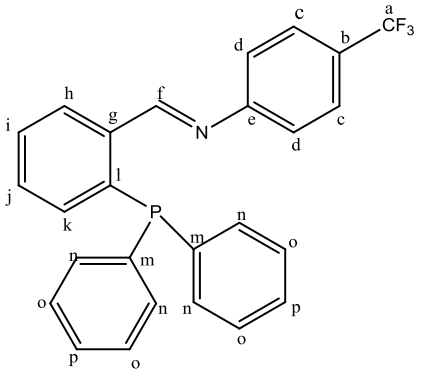

4-(Trifluoromethyl) aniline (0.110 g, 0.682 mmol) and 2-(diphenylphosphino)benzaldehyde (0.200 g, 0.689 mmol) were dissolved in methanol (20 ml). The reaction mixture was stirred for 24 h at room temperature. After 24 h, the solvent was removed and DCM was added followed by anhydrous magnesium sulfate. The mixture was stirred for 10 min, $MgSO_4$ was removed by

gravitational filtration and the solvent was removed under reduced pressure. The resulting residue was dried under vacuum. The yellow solid was the desired product. (Yield: 0.243 g, 82 %). **IR**: KBr pelle , υ/ m^{-1}: 1613 (s, imine, C=N), 1105-1200 (C-F). **^{1}H NMR** (400 MHz, $CDCl_3$): δ (ppm) = 6.90 (m, 2H, H_d), 6.97 (m, 1H, H_k), 7.35 (m, 11H, $H_{j,o,p,\ n}$), 7.49 (m, 3H, $H_{c,i}$), 8.20 (m, 1H, H_h), 9.02 (d, $^{4}J_{HP}$ = 5.2 Hz, 1H, H_f). **^{13}C{^{1}H} NMR** (100 MHz, $CDCl_3$): δ (ppm) = 113.9 (C_d), 120.8 (C_a), 126.1 (C_c), 128.6 ($C_{i,j,h}$), 131.2 (C_o), 133.4 (C_k), 134.1 (C_p), 136.1 (C_g), 138.7 (C_m), 154.6 (C_e), 160.5 (d, ^{3}J = 21.3 Hz, C_f). **^{31}P{^{1}H} NMR** (121 MHz, $CDCl_3$): δ (ppm) = -12.7 (s). **^{19}F{^{1}H} NMR** (377 MHz, $CDCl_3$): δ (ppm) = 78.5. **MS** (EI, m/z): 433.12 $[M]^+$. **Elemental analysis** (%): Anal. Calc: $C_{26}H_{19}F_3NP$: C, 72.05; H, 4.42; N, 3.23. Found: C, 66.81; H, 4.26; N, 3.35. **Melting point**: 91.8 – 95.3 ºC.

*2.5.3 Preparation of Compound **L2***[8]

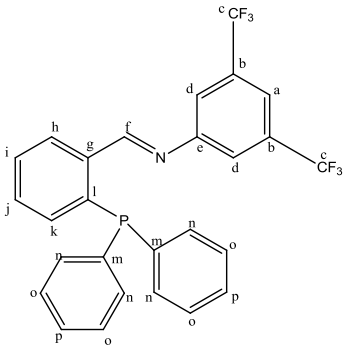

3,5-bis(Trifluoromethyl) aniline (0.238 g, 1.04 mmol) and 2-(diphenylphosphino) benzaldehyde (0.201 g, 0.692 mmol) were dissolved in methanol (20 ml). The yellow solution was refluxed at 65 ^{0}C for 4 h. After 4 h the solvent was removed and DCM (20 ml) was added followed by anhydrous $MgSO_4$. The mixture was stirred for 10 min; $MgSO_4$ was removed using gravitational filtration. The solvent was removed using rotary evaporation and cold methanol was added, the mixture was put on ice and a yellow precipitate formed. The solid was filtered and dried under vacuum. The desired product was isolated as a yellow solid. (Yield: 0.246 g, 71 %). **IR**: KBr pellets, ν/cm^{-1}: 1632 (s, imine, C=N), 1105 (C-F). **^{1}H NMR** (300 MHz, $CDCl_3$): δ (ppm) = 6.96 (m, 1H, H_k), 7.14 (m, 2H, H_d), 7.36 (m, 11H, $H_{j,o,p}$), 7.47 (m, 1H, H_i), 7.64 (s, 1H, H_a), 8.15 (m, 1H, H_h), 8.94 (d, $^{4}J_{HP}$ = 4.6 Hz, 1H, H_f). **^{13}C{^{1}H} NMR** (100 MHz, $CDCl_3$): δ (ppm) = 161.7 (d, C=N, ^{3}J = 19.7 Hz, C_f), 152.9 (s, C_e), 139.7 (d, C_m), 137.7 (d, C_g), 135.9 (C_b), 134.2 (C_p), 133.3 (C_k), 132.20 (C_l), 131.6 (C_o), 128.9 ($C_{j,n,o,p}$), 124.4 (C_c), 120.9 (C_d), 118.6 (C_a). **^{13}P{^{1}H} NMR**

(162.00, $CDCl_3$): δ (ppm) = -11.36. **MS** (EI, m/z): 500.92 $[M]^+$. **$^{19}F\{^1H\}$ NMR** (377 MHz, $CDCl_3$): δ (ppm) = 78.2. **Elemental analysis** (%): Anal. Calc: $C_{27}H_{18}F_6NP$: C, 64.68; H, 3.62; N, 2.79. Found: C, 64.33; H, 3.93; N, 2.39. **Melting point**: 120.4 – 122.5 ºC.

*2.5.4 Preparation of Compound **L3***[14-21]

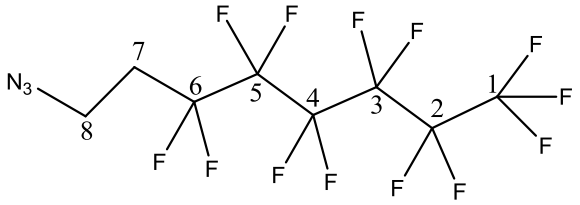

To a round-bottom flask equipped with a magnetic stirrer, NaN_3 (2.62 g, 40.3 mmol), water (6 ml), 1H, 1H, 2H, 2H-Perfluorooctyl iodide (4.90 ml, 20.0 mmol) and methyltridecylammonium chloride (Aliquat®336) (0.400 g, 1.00 mmol) were added. The mixture was stirred and refluxed for 18 hours at 90 ^oC using an oil bath. The reaction was monitored by TLC; after the reaction was complete the two layers were separated using a separating funnel. The bottom layer gave rise to a light yellow oil of 1H, 1H, 2H, 2H-Perfluorooctyl azide. (Yield: 6.32 g, 81 %). The product was used in the next step without further purification. **IR**: CH_2Cl_2, ν/cm^{-1}: 2107 (s, N_3), 1105-1200 (C-F). **^1H NMR** (300 MHz, $CDCl_3$): δ (ppm) = 2.40 (m, 2H, H_7), 3.60 (t, ^3J = 7.01 Hz, 2H, H_8). **$^{13}C\{^1H\}$ NMR** (100 MHz, $CDCl_3$): δ (ppm) = 30.8 (t, C_7), 43.2 (s, C_8), 122.2-104.9 (m, C-F), **$^{19}F\{^1H\}$ NMR** (377 MHz, $CDCl_3$): δ (ppm) = -81.7 (m, 3F, F_1), -126.9 (m, 2F, F_2), -124.3 (m, 2F, F_3), -123.7 (m, 2F, F_4), -122.6 (m, 2F, F_5), -114.7 (m, 2F, F_6).

*2.5.5 Preparation of Compound **L4***[14-21]

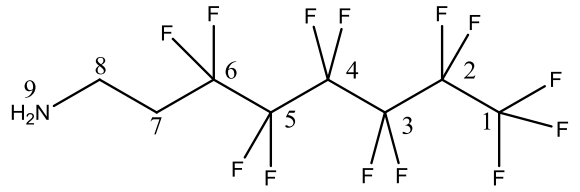

A 90 ml stainless steel pipe reactor equipped with a magnetic stirrer was charged with 1H, 1H, 2H, 2H-Perfluorooctyl azide (**L3**) (3.01 g, 7.13 mmol). To the reactor, 10 % Pd/C (0.50 g) in methanol (25 ml) was added. The pipe reactor was flushed with nitrogen three times, followed by flushing with H_2 once. The reaction mixture was pressurized with H_2 (7 bar) and stirred at

room temperature for 14 h. After 14 h, the catalyst was filtered through Celite®. The solvent was removed from the filtrate under reduced pressure and the desired product **L4** was isolated as light yellow oil. (Yield: 2.48 g, 96 %). **IR**: CH_2Cl_2, ν/cm^{-1}: 887 (s, NH), 1144-1208 (C-F). **^{1}H NMR** (300 MHz, $CDCl_3$): δ (ppm) = 1.65 (s, 2H, H_9), 2.23 (m, 2H, H_7), 3.03 (t, ^3J = 7.19 Hz, 2H, H_8). **^{13}C{^{1}H} NMR** (100 MHz, $CDCl_3$): δ (ppm) = 34.4 (s, C_8), 34.7 (t, J_{CF} = 21, C_7), 120.9-107.9 (m, C-F), **^{19}F{^{1}H} NMR** (377 MHz, $CDCl_3$): δ (ppm) = -81.7 (m, 3F, F_1), -126.9 (m, 2F, F_2), -124.5 (m, 2F, F_3), -123.6 (m, 2F, F_4), -122.7 (m, 2F, F_5), -114.4 (m, 2F, F_6).

*2.5.6 Preparation of Compound **L5***

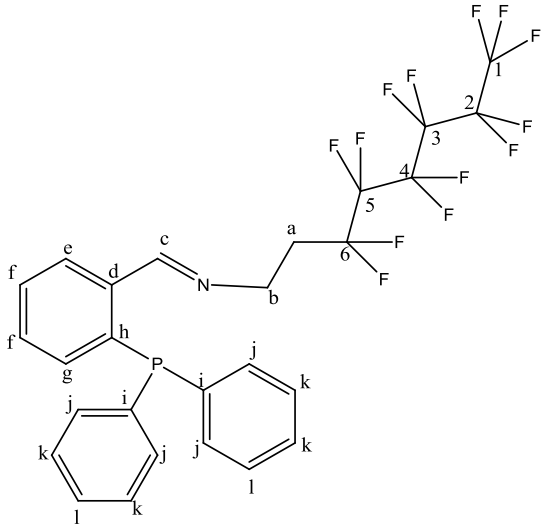

1H, 1H, 2H, 2H-Perfluorooctyl amine (**L4**) (0.0580 g, 0.160 mmol) and 2-(diphenylphosphino) benzaldehyde (0.0460 g, 0.159 mmol) were dissolved in methanol (10 ml). The yellow solution was stirred at room temperature for 12 h. After 12 h the solvent was removed and DCM (20 ml) was added followed by anhydrous $MgSO_4$. The mixture was stirred for 10 min; $MgSO_4$ was removed using gravitational filtration. The solvent was removed using rotary evaporator. The residue was dried under vacuum for 8 h. The product was obtained as yellow oil. (Yield: 0.0838 g, 83 %). **IR**: CH_2Cl_2, ν/cm^{-1}: 1638 (s, imine, C=N), 1144-1208 (C-F). **^{1}H NMR** (300MHz, $CDCl_3$): δ (ppm) = 2.16 (m, 2H, H_a), 3.71 (t, ^3J = 7.63 Hz, 2H, H_b), 6.91 (m, 1H, H_g), 7.33 (m, 12H, $H_{f,j,k,l}$), 7.91 (m, 1H, H_e), 8.87 (d, J = 4.38, 1H, H_c). **^{13}C{^{1}H} NMR** (100 MHz, $CDCl_3$): δ (ppm) = 32.1 (t, $^2J_{CF}$ = 21. 2 Hz, C_a), 52.5 (s, C_b), 128.87, 128.65, 130.49, 134.12 ($C_{f,j,k,l}$), 128.58 (s, C_e), 133.42 (s, C_g), 137.43 (s, C_h), 138.20 (s, C_i), 139.01 (s, C_d), 161.7 (d, imine, C=N). **^{13}P{^{1}H} NMR** (162.00, $CDCl_3$): δ (ppm): -12.63. **^{19}F{^{1}H) NMR** (377 MHz, $CDCl_3$): δ (ppm) =

-81.7 (m, 3F, F_1), -126.9 (m, 2F, F_2), -124.4 (m, 2F, F_3), -123.6 (m, 2F, F_4), -122.7 (m, 2F, F_5), -114.4 (m, 2F, F_6). **MS** (EI, m/z): 635.10 $[M]^+$. **Elemental analysis** (%): Anal. Calc: $C_{27}H_{19}F_{13}NP$: C, 51.04; H, 3.01; N, 2.20. Found: C, 51.96; H, 3.03; N, 1.47.

2.5.7 Preparation of Compound ***L6***[22-24]

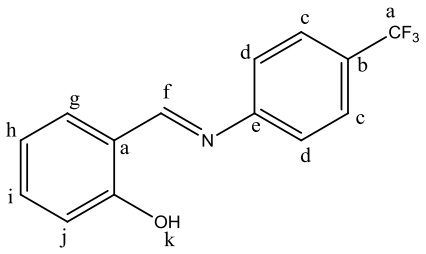

To a solution of salicylaldehyde (0.100 g, 0.819 mmol) in ethanol (10 ml), 4-trifluoromethylaniline (0.132 g, 0.819 mmol) was added dropwise at room temperature. The solution was stirred at room temperature for 1 h. After 1 h the mixture was refluxed at 78 ^oC until the consumption of starting material was complete. The solvent was reduced using rotary evaporator, a yellow precipitate formed and it was filtered and washed with cold ethanol. The product was dried under vacuum. A yellow solid was obtained as the desired product. (Yield: 0.185 g, 85 %). **IR**: KBr pellets, ν/cm^{-1}: 3418, 3405 (s_{br}, OH), 1623 (s, imine, C=N), 1071-1103 (C-F). **^{1}H NMR** (400 MHz, $CDCl_3$): δ (ppm) = 6.90 (m, 1H, H_h), 6.97 (m, 1H, H_j), 7.27 (m, 2H, H_c), 7.35 (m, 2H, $H_{i,\ k}$), 7.61 (m, 2H, H_d), 8.54 (s, 1H, H_f), 12.72 (s_{br}, 1H, H_m). **^{13}C{^{1}H} NMR** (100 MHz, $CDCl_3$): δ (ppm) = 117.4 (s, C_h), 118.9 (s, C_g), 119.1 (s, C_j), 121.5 (C_c), 122.8 (s, C_a), 125.5 (s, C_b), 126.6 (C_d), 132.7 (C_i), 133.9 (C_k), 151.7 (s, C_e), 161.3 (s, C_l), 164.5 (C_c). **^{19}F{^{1}H} NMR** (377 MHz, $CDCl_3$): δ (ppm) = 78.7 (s, 3F). **MS** (EI, m/z): 264.03 $[M]^+$. **Elemental analysis** (%): Anal. Calc: $C_{14}H_{10}F_3NO$: C, 63.40; H, 3.80; N, 5.28. Found: C, 63.57; H, 4.20; N, 4.62. **Melting point**: 93.2 – 94.2 ºC.

*2.5.8 Preparation of Ligand **L7***[25-27]

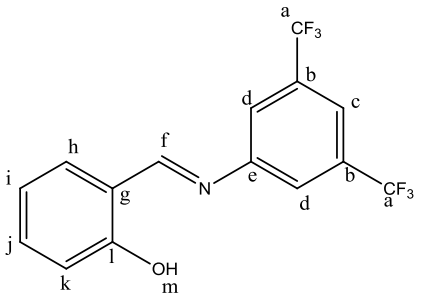

To a solution of salicylaldehyde (0.305 g, 0.250 mmol) in ethanol (10 ml), 3,5-bis(trifluoromethyl)aniline (0.573 g, 0.250 mmol) was added at room temperature. The solution was stirred at room temperature for 3 h. The solvent was reduced using a rotary evaporator, then cold ethanol was added and a yellow precipitate formed. The precipitate was filtered and washed with cold ethanol. The product was dried under vacuum. A yellow solid was obtained as the desired product. (Yield: 0.551 g, 66.1 %). **IR**: KBr pellets, ν/cm^{-1}: 3064 (s_{br}, OH), 1628 (s, imine, C=N), 1174-1221 (C-F). **^{1}H NMR** (400 MHz, $CDCl_3$): δ (ppm) = 6.92 (t, J = 7.57 Hz, 1H, H_j), 6.98 (m, 1H, H_h), 7.38 (m, 2H, $H_{i,\,k}$), 7.61 (s, 2H, H_d), 7.72 (s, 1H, H_c), 8.58 (s, 1H, H_f), 12.27 (s_{br}, 1H, H_m). **^{13}C{^{1}H} NMR** (100 MHz, $CDCl_3$): δ (ppm) = 117.6 (s, C_h), 118.6 (s, C_g), 119.6 (s, C_j), 120.1 (C_c), 121.5 (C_d), 124.4 (s, C_a), 127.2 (s, C_c), 132.9 (C_i), 133.5 (C_k), 150.3 (s, C_e), 161.3 (s, C_l), 165.7 (C_f). **^{19}F {^{1}H} NMR** (377 MHz, $CDCl_3$): δ (ppm) = 78.0 (s, 6F). **MS** (EI, m/z): 333.01 $[M]^+$. **Elemental analysis** (%): Anal. Calc: $C_{15}H_9F_6NO$: C, 54.07; H, 2.72; N, 4.20. Found: C, 53.62; H, 2.66; N, 3.53. **Melting point**: 105.4 – 107.4 ºC.

*2.5.9 Preparation of ligand **L8***[28]

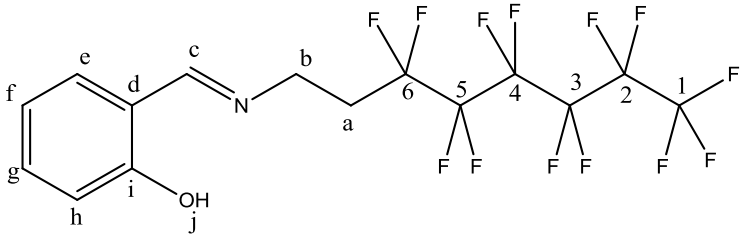

To a solution of salicylaldehyde (0.0530 g, 0.435 mmol) in methanol (20 ml), 1H, 1H, 2H, 2H-Perfluorooctyl amine (**L4**) (0.158 g, 0.435 mmol) was added dropwise at room temperature. The resulting yellow solution was refluxed at 65^{o}C for 1 h. After 1 h the solvent was removed and

DCM (15 ml) was added followed by anhydrous $MgSO_4$. The mixture was stirred for 10 min; and $MgSO_4$ was removed using gravitational filtration. The solvent was removed, cold methanol was added and a yellow precipitate formed. The precipitate was filtered and dried under vacuum. A light yellow solid was obtained as the desired product. (Yield: 0.181 g, 89 %). **IR**: KBr pellets, ν/cm^{-1}: 3405 (s_{br}, OH), 1638 (s, imine, C=N), 1082-1236 (C-F). **^{1}H NMR** (400 MHz, $CDCl_3$): δ (ppm) = 2.47 (m, 2H, H_a), 3.84 (t, ^3J = 7.19 Hz, 2H, H_b), 6.83 (td, 1H, H_g), 6.91 (m, 1H, H_e), 7.19 (m, 1H, H_h), 7.26 (m, 1H, H_f), 8.35 (s, 1H, H_c), 12.70 (s, 1H, H_j). **^{13}C{^{1}H} NMR** (100 MHz, $CDCl_3$): δ (ppm) = 32.4 (t, J_{CF} = 21, C_a), 51.4 (s, C_b), 117.0 (C_e), 118.5 (s, C_d), 118.7 (C_g), 131.5 (C_h), 132.7 (C_f), 160.9 (s, C_i), 166.7 (C_c). **^{19}F{^{1}H} NMR** (377 MHz, $CDCl_3$): δ (ppm) = -81.6 (m, 3F, F_1), -126.9 (m, 2F, F_2), -124.3 (m, 2F, F_3), -123.6 (m, 2F, F_4), -122.6 (m, 2F, F_5), -114.3 (m, 2F, F_6). **MS** (EI, m/z): 466.84 $[M]^+$. **Elemental analysis** (%): Anal. Calc: $C_{15}H_{10}F_{13}NO$: C, 38.54; H, 2.16; N, 3.00. Found: C, 38.24; H, 1.32; N, 2.56. **Melting point** (ºC): Decomposes without melting at 265.0 ºC.

2.6 References

1. a) R. N. Patel, V. L. N. Gundla and D. K. Patel, *J. Indian Chem*., **47**, 2008, 353. b) K. C. Gupta and A. K. Sutar, *Coord. Chem. Rev.*, **252**, 2008, 1420.
2. a) P. A. Vigato and S. Tamburini, *Coord. Chem. Rev.*, **248**, 2004, 1717. b) P. Souza, J.A. Garcia-Vazquez and J. R. Masaguer, *Transition Met. Chem*., **10**, 1985, 410.
3. B. Bosnerb, *Inorg. Chim. Acta.,* **343**, 1997, 145.
4. K. C. Gupta and A. K. Sutar, *Coord. Chem. Rev.*, **252**, 2008, 1420.
5. R. Drozdzak, B. Allaert, N. Ledoux, I. Dragutan, V. Dragutan and F. Verpoort, *Coord. Chem. Rev.*, **249**, 2005, 3055.
6. G. Sanchez, *Polyhedron*, **18**, 1999, 3057.
7. A. Scrivanti, U. Matteoli, V. Beghetto, S. Antonaroli and B. Crociani, *Tetrahedron*, **58**, 2002, 6881.
8. Best, J. M. Wilson, H. Adams, L. Gonsalvi, M. Peruzzini and A. Haynes, *Organometallics*, **26**, 2007, 1960.
9. K. James (2010). *Understanding NMR Spectroscopy* (2nd ed.), Wiley. pp. 190-191.
10. K. James (2010). *Understanding NMR Spectroscopy* (2nd ed.), Wiley. pp. 209-215.
11. S. Antonaroli and B. Crociani, *J. Organomet. Chem.*, **560**, 1998, 137.
12. G. Bandoli and A. Dolmella, *Transition Met. Chem.*, **25**, 2000, 17.
13. J. Best, J.M. Wilson, H. Adams, L. Gonsalvi, M. Peruzzini and A. Haynes, *Organometallics*, **26**, 2007, 1960.
14. a) C. Palomo, J. M. Aizpurua, I. Loinaz, M. J. Fernandez-Berridi and L. Irusta, *Org. Lett.*, **3**, 2001, 2361. b) J. A. Gladysz, D. P. Curran and I. T. Horvath, *Handbook of Fluorous Chemistry*, Wiley-VCH Verlag GmbH & Co, K GcA, pp 457-458.
16. A. Soules, C. P. Vazquez, B. Ameduri, C. J. Duhamel, M. Essahli and B. Boutevin, *J. Polym. Sci A Polym. Chem.*, **46**, 2008, 3214.
17. Z. Lu, X. Zhou, S. Hu, X. Shu, Y. Tian and J. Zhu, *J. Phys. Chem. C.,* **114**, 2010, 13546.
18. S. R. Patil, M. Turmine, V. Peyre, G. Duran and B. Pucci, *Talanta*, **74**, 2007, 72.
19. A. Abulikemu, G. Halasz, A. Csampai, A. Gomony and J. Rabai, *J. Fluorine Chem.,* **125**, 2004, 1143.
20. 24. C.A. Ghilardi, S. Midollini, S. Moneti, A. Orlandini and G. Scapacci, *J. Chem. Soc., Dalton Trans.*, 1992, 3371.

21. M. A. Torzilli, *Polyhedron*, **21**, 2002, 697.
22. P. Altmann, M. Cokoja and F. E. Kühn, *J. Organomet. Chem*., **701**, 2012, 51.
23. G. Bilgehan and A. Gokturk, *Inorg. Chem: An Indian Journal*, **3**, 2008, 1.
24. M. Carril, P. Altmann, M. Dress, W. Bonrath, T. Netscher, J. Schutz and F. E. Kuhn, *J. Catal*., **283**, 2011, 55.
25. Y. Cheng, X. Hu, S. Gao, L. Lu and J. Chen, W. Xiao, *Tetrahedron*, **69**, 2013, 3810.
26. D. J. Darensbourg, P. Rainey and J. Yarbrough, *Inorg. Chem.*, **40**, 2001, 986.
27. L. M. Hui, T. H. Yangi, L. H. Yi, F. S. Kai and C. K. Yu, *Chin. Chem. Lett*., **23**, 2012, 1279.
28. F. Guenouni, F. Szonyi and A. Cambon, *J. Fluorine Chem*., **104**, 2000, 143.

Synthesis and Characterization of Fluorocarbon-Containing iminophosphine and salicylaldimine-based Rh(I) Complexes

3.1 Introduction

A number of Schiff base transition metal complexes display excellent catalytic activity in many reactions at temperatures above 100 ºC.[1a] There have been various reports on applications on Schiff base complexes in heterogeneous and homogeneous catalysis.[1a] The Schiff bases usually contain *N,P*- and *N,O*- donor atoms. The steric and electronic properties of these ligands can be tuned and which can influence the rate of key steps in the hydroformylation cycle.[1a]

This chapter will describe and discuss the synthesis and characterization of Schiff base fluorous-containing salicylaldimine and iminophosphine rhodium(I) complexes. The synthesized complexes were characterized using a range of spectroscopic and analytical techniques, these include 1-D NMR (^{1}H, $^{13}C\{^{1}H\}$, $^{31}P\{^{1}H\}$ and $^{19}F\{^{1}H\}$ NMR), 2-D NMR (COSY and HSQC) spectroscopy, EI or ESI mass spectrometry, elemental analysis, FT-IR spectroscopy and single crystal X-ray diffraction.

3.2 Results and Discussion

3.2.1 Synthesis and characterization of iminophosphine Rh(I) complexes 3.1 and 3.2

The new Rh(I) iminophosphine-based complexes **3.1** and **3.2** (**Scheme 3.1**) were prepared by reacting the dimeric rhodium(I) precursor $[RhCl(CO)_2]_2$ (0.5 eqv.) with ligands **L1** and **L2** (1 eqv.) respectively following a procedure obtained from the literature.[1]. Both complexes (**3.1** and **3.2**) were isolated as orange solids in good yields (64 % and 74 % respectively) and were characterized using a combination of analytical and spectroscopic methods. Both complexes are stable at room temperature and decompose without melting at temperatures above 160 ºC.

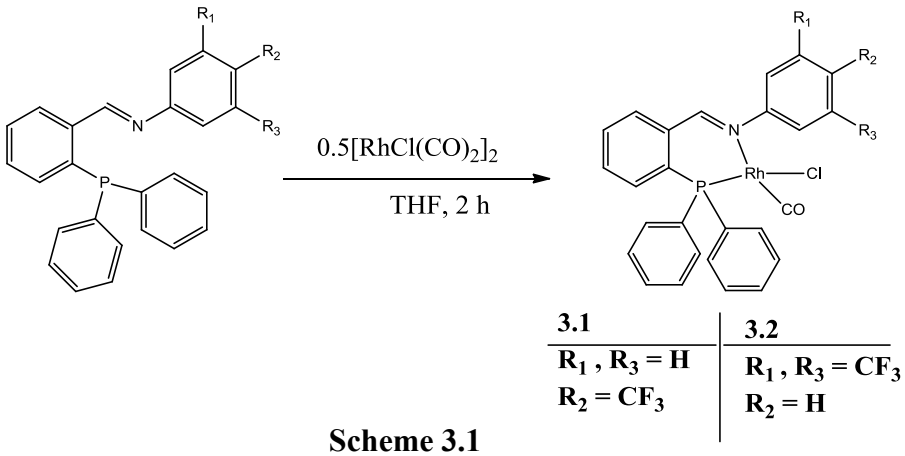

3.1	3.2
R_1 , R_3 = H R_2 = CF_3	R_1 , R_3 = CF_3 R_2 = H

Scheme 3.1

^{1}H NMR Spectroscopy

The ^{1}H NMR spectra display a singlet assigned to the imine proton at δ 8.07 and δ 8.04 for complex **3.1** and **3.2**, respectively. The imine protons for both complexes (**3.1** and **3.2**) shifted upfield from δ 9.02 ppm (**L1**) and δ 8.94 ppm (**L2**) respectively in the uncoordinated ligands. This shift provided evidence that the coordination of the ligand to the metal had occurred. The ^{1}H NMR spectrum of complex **3.2** in **Figure 3.1** is used to show a typical spectrum for these complexes. Other proton assignments were made using 2-D NMR (COSY).

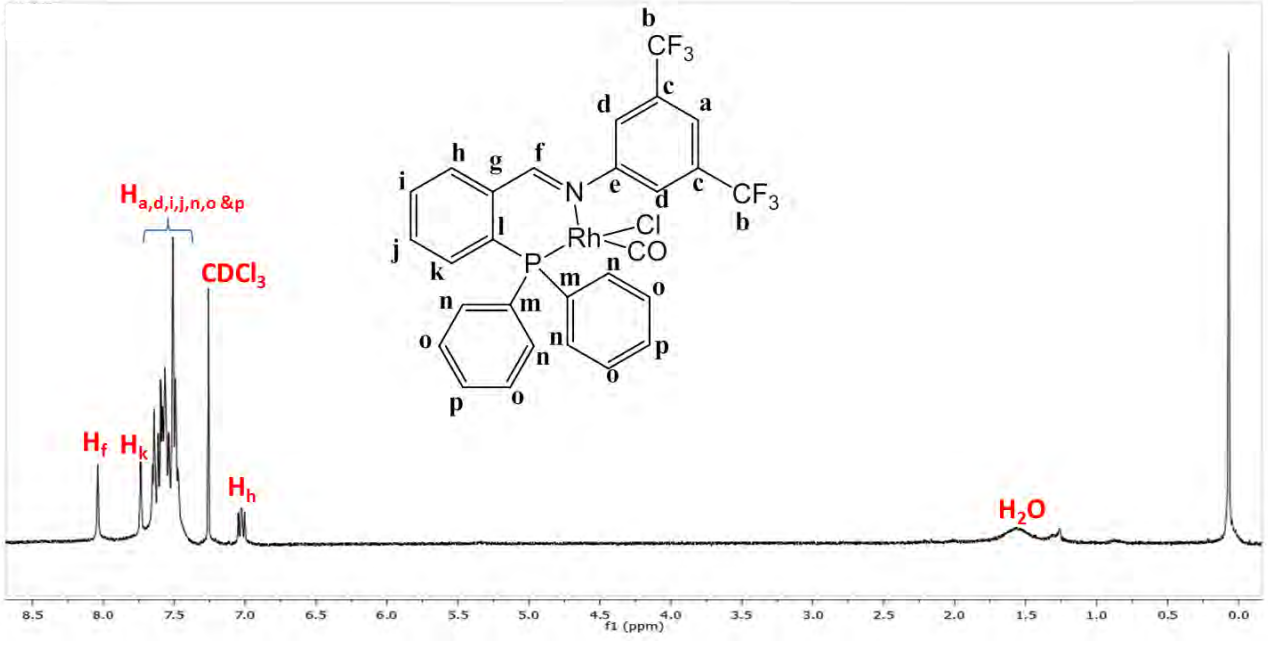

Figure 3.1: ^{1}H NMR spectrum of complex **3.2** in $CDCl_3$.

On inspection of the COSY spectrum for complex **3.2** (**Figure 3.2**), it is confirmed that the most deshielded signal is the imine proton (H_f) at δ 8.04 and it couples to H_h, (δ 7.03 ppm) *via* long range coupling. The COSY spectrum also illustrates that proton (H_h) couples to its adjacent proton (H_i) and similarly (H_i) correlates to the vicinal proton (H_j). The proton (H_j) also couples to its neighboring proton (H_k).

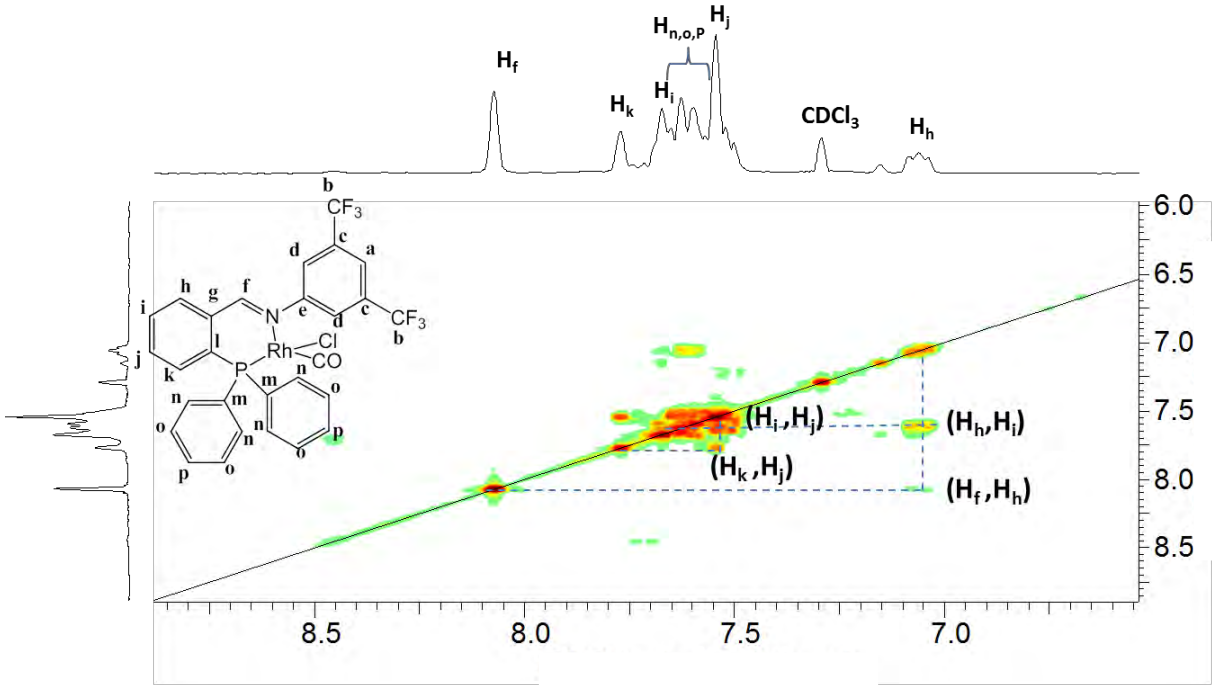

Figure 3.2: ^{1}H-^{1}H COSY 2D-NMR spectrum of complex **3.2** in $CDCl_3$.

$^{13}C\{^{1}H\}$ NMR spectroscopy

The $^{13}C\{^{1}H\}$ NMR spectrum displays an imine carbon peak at δ 160.5 ppm for complex **3.1** and at δ 167.9 pm for **3.2**. The carbon spectrum also exhibits a doublet of doublets at δ 188.5 ppm for the carbonyl carbon of complex **3.1** with coupling constants ($^{2}J_{PC}$ = 15.0 Hz and $^{1}J_{RhC}$ = 74.9 Hz). The moderately small $^{2}J_{PC}$ coupling constant (15.0 Hz) indicates that the CO moiety is *cis* to phosphorous,[1b-3] as a larger coupling constant (> 100 Hz) would be expected for a carbonyl *trans* to the phosphorous.[1b-3]

The HSQC 2-D NMR spectrum was also used to assign the remaining carbons and also assisted in further validation of the carbon assignments. **Figure 3.3** displays the HSQC NMR spectrum of complex **3.2** as an example to illustrate typical carbon assignments. **Figure 3.3** shows that the

most downfield signal (δ 8.04, H_f) is coupling to the carbon signal assigned to the imine carbon (δ 167.9 ppm, C_f). The HSQC spectrum also permitted the assignment of the aromatic carbons which appear in the expected region around (δ 123.2 – 136.3 ppm).

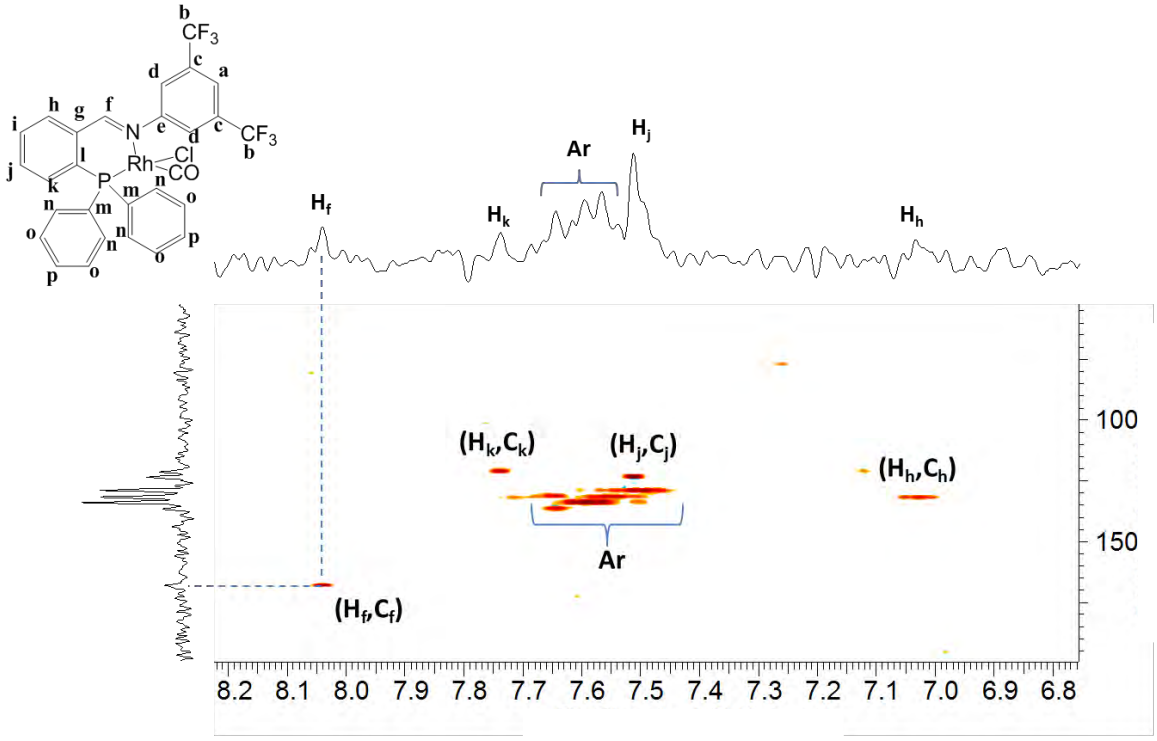

Figure 3.3: ^{1}H-^{13}C HSQC 2D-NMR spectrum of complex **3.2** in $CDCl_3$.

$^{31}P\{^{1}H\}$ NMR and $^{19}F\{^{1}H\}$ NMR spectroscopy

For both complexes **3.1** and **3.2** the $^{31}P\{^{1}H\}$ NMR spectra display doublets at δ 47.9 ppm ($^{1}J_{PRh}$ = 163.3 Hz) for complex **3.1** and at δ 48.1 ppm ($^{1}J_{PRh}$ = 161.3 Hz) for complex **3.2**. The observed coupling constants are comparable with the literature reported $^{1}J_{PRh}$ coupling constants.[1b-3] The doublet in the $^{31}P\{^{1}H\}$ spectrum at (δ 47.9 ppm, ^{1}J = 163.2 Hz for **3.1** and at δ 48.1 ppm, ^{1}J = 161.3 Hz for **3.2**) further proves that the rhodium metal has coordinated to the ligand and also indicates the formation of a single isomer for each complex. This is the complex where phosphorous is *trans* to the chloro group. The coupling constants are consistent with the rhodium phosphorous coupling constants reported in literature.[2-3]

The $^{19}F\{^{1}H\}$ NMR spectra show a peak δ 78.5 ppm for complex **3.1** and at δ 78.2 ppm for complex **3.2**. The observed peaks are assigned to the CF_3 moieties in both complexes.

FT-IR spectroscopy

FT-IR spectroscopy was further used to confirm the formation of the complexes. Generally, the FT-IR spectra for **3.1** and **3.2** shows a shift in the wavelength of the (C=N) absorption band towards lower wavenumbers compared to the uncoordinated ligands (*ca*. 1613 *vs* 1604 cm^{-1} for **3.1** and *ca*. 1632 *vs* 1602 cm^{-1} for **3.2**). This decrease in stretching frequency is due to the strengthening Rh-N bond and weakening of the C=N bond upon rhodium coordination due to donation and back donation of electrons through the synergic effect. This results in the lower frequency of C=N bond compared to the free ligand. This shift confirms that coordination of rhodium to nitrogen has occurred. The FT-IR also shows the stretching frequency for the terminal carbonyl (CO) at 2000 cm^{-1} for **3.1** and at 2008 cm^{-1} for **3.2**. This further corroborates the formation of one isomer.

Elemental Analysis and Electrospray Ionization Mass Spectrometry

The experimental values obtained from elemental analysis agree well with the calculated values for C, N and H in both complex **3.1** and **3.2**. In the mass spectrum of complex **3.1**, a peak assigned to $[M\text{-}Cl]^+$ is observed at *m/z* 564. A molecular ion peak $[M]^+$ is observed at *m/z* 666.9 in the mass spectrum of complex **3.2**.

*Molecular Structures of Complex **3.1** and **3.2***

Single crystals of complexes **3.1** and **3.2** (**Figure 3.4**) were grown by slow diffusion of petroleum ether into a concentrated DCM solution of **3.1** and **3.2**. The crystallographic data for the molecular structures of **3.1** and **3.2** are presented in **Table 1** as well as selected bond lengths and angles are given in **Table 2**.

Complex **3.1** (**Figure 3.4**) crystallizes in P1 space group with a triclinic system, while complex **3.2** (**Figure 3.4**) crystallizes in the P21/c space group in a monoclinic system. Both complexes **3.1** and **3.2** crystallize with a molecule of DCM. The crystal colour of complex **3.1** and **3.2** is red they both possess a block crystal shape.

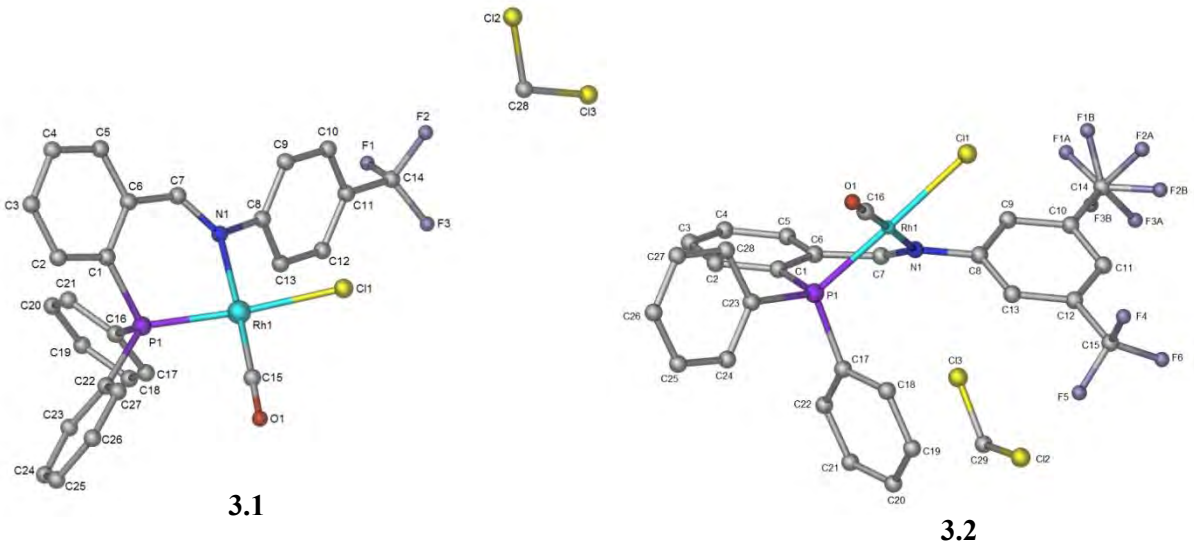

Figure 3.4: Molecular structures of complex **3.1** and **3.2**.

The molecular structures of compounds **3.1** and **3.2** both confirm a four-coordinate square planar geometry about the rhodium center and the bidentate P-N binding mode of the iminophosphine ligands. The CO moiety is located *trans* to the N-donor fragment and *cis* to P-donor fragment in both complexes **3.1** and **3.2**. The geometric parameters shown in **Table 2** are comparable with those of similar systems reported in literature.[4-11]

The P(1)-Rh(1)-Cl(1) angles are 175.16(3)° and 173.19(4) ° for **3.1** and **3.2**, respectively. These deviate from the expected 180° which indicates distortion caused by the 6-membered chelate ring which includes the rhodium atom. Similar deviation is also seen for the angle N(1)-Rh(1)-P(1) 84.04(6)° and 84.54(10) ° for **3.1** and **3.2**, respectively, which deviates from the expected 90°. The CF_3 group of complex **3.2** appears to be disordered over two positions as F1A, F2A, and F3A) and F1B, F2B and F3B. The site occupancy factors for F1A, F2A and F3A were refined to be 0.721; whereas for F1B, F2B and F3B were 0.189. The bond lengths for Rh(1)-P(1) and Rh(1)-N(1) are 2.1926(6) Å and 2.1320(2) Å, respectively for complex **3.1** and 2.2054(10) Å and 2.1360(4) Å for complex **3.2**. The Rh(1)-C(15) bond distance in complex **3.1** measures at 1.8150(3) Å and at 1.8160(4) Å for complex **3.2**.

Table 1: Crystallographic data and structure refinement details for complexes **3.1** and **3.2**.

	Complex 3.1	**Complex 3.2**
Molecular formula	$C_{27}H_{19}ClF_3NOPRh.CH_2Cl_2$	$C_{28}H_{18}Cl\ F_6NOPRh.CH_2Cl_2$
Molar mass g/mol	684.69	752.69
Crystal shape	Block	Block
Crystal colour	Red	Red
Temperature (K)	173(2)	133(2)
λ (Å)	0.71073	0.71073
Crystal system	Triclinic	Monoclinic
Space group	P-1	P21/c
Z	2	4
V/ $Å^3$	1371.9(2)	3109.1(3)
a (Å)	10.0724(8)	18.0398(11)
b (Å)	10.7398(10)	10.2049(6)
c (Å)	14.2923(13)	17.4809(11)
α (^{o})	68.841(2)	90
β (^{o})	72.9010(10)	104.9600(10)
γ (^{o})	88.779(2)	90
Dc / $g.cm^{-3}$	1.658	1.608
μ (Mo Kα) mm^{-1}	1.017	0.919
F(000)	684	1496.0
Theta Min-Max/ °	1.61-28.46	2.3, 28.4
Index ranges (h, k, l)	-13:13, -14:14, -19:19	-24:24; -13:13; -23:23
No. of reflections	6917	7754
No. reflections with I > 2σ(I)	5448	6354
wR2 (all data)	0.0774(6917)	0.1534(7754)
Unique reflections	24087	51744
Goodness-of-fit	1.029	1.094
Min, Max density/ e $Å^{-3}$	-0.56, 0.64	-1.85, 1.70

Table 2: Selected bond lengths and bond angles for complexes **3.1** and **3.2**.

Complex 3.1		**Complex 3.2**	
Bond lengths (Å)		Bond lengths (Å)	
Rh(1)-Cl(1)	2.3928(6)	Rh(1)-Cl(1)	2.3735(10)
Rh(1)-C(15)	1.8150(3)	Rh(1)-C(16)	1.8160(4)
Rh(1)-P(1)	2.1926(6)	Rh(1)-P(1)	2.2054(10)
Rh(1)-N(1)	2.1320(2)	Rh(1)-N1	2.1360(4)
Bond angles (^{o})		Bond angles (^{o})	
C(15)-Rh(1)-Cl(1)	90.74(8)	C(16)-Rh(1)-Cl(1)	91.90(12)
C(15)-Rh(1)-P(1)	93.78(8)	C(16)-Rh(1)-P(1)	93.99(12)
P(1)-Rh(1)-N(1)	84.04(6)	P(1)-Rh(1)-N(1)	84.54(10)
N(1)-Rh(1)-Cl(1)	91.38(6)	N(1)-Rh(1)-Cl(1)	89.67(10)
C(15)-Rh(1)-N(1)	176.94(10)	C(16)-Rh(1)-N(1)	177.70(15)
P(1)-Rh(1)-Cl(1)	175.16(3)	P(1)-Rh(1)-Cl(1)	173.19(4)

3.2.2 Synthesis and Characterization of iminophosphine Rh(I) complex 3.3

Complex **3.3** exhibits a fluorous aliphatic chain and an aliphatic ($(CH_2)_2$) spacer unlike the complexes discussed in the previous section containing fluorocarbon bonded to an aromatic ring. The reaction between ligand **L5** with dimeric the rhodium(I) $[RhCl(CO)_2]_2$ complex afforded a new complex **3.3** (**Scheme 3.2**). The complex was isolated as an orange solid in excellent yield (49 %) and is thermally stable up to 164.8 ºC above which it decomposes without melting.

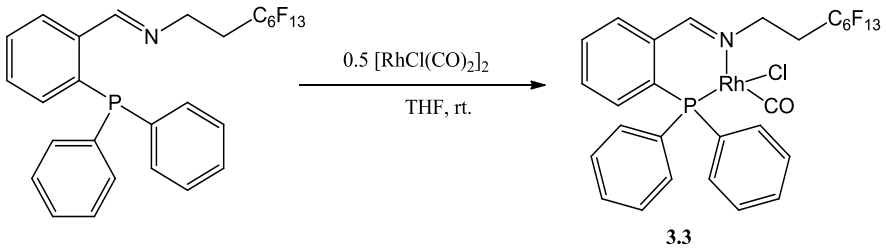

3.3

Scheme 3.2

^{1}H NMR Spectroscopy

The ^{1}H NMR spectrum displays a singlet at δ 8.04 assigned to the imine proton; the upfield shift from δ 8.87 of the uncoordinated ligand suggests that coordination of nitrogen to rhodium occurred, which suggests that the complex has been obtained. The ^{1}H NMR spectrum also exhibits two peaks upfield, a multiplet at δ 2.53 ppm and a triplet at δ 4.47 ppm ($^{3}J_{HH}$ = 7.63 Hz) and these are assigned to the -CH_2 next to –CF_2 and –CH_2 adjacent to the nitrogen, respectively. The triplet and the multiplet shifted downfield in comparison to the uncoordinated ligand (*ca*. δ 3.71 ppm and *ca*. δ 2.16 ppm, respectively). The aromatic protons occur between δ 6.86 and δ 7.41 ppm.

$^{13}C\{^{1}H\}$ NMR spectroscopy

The $^{13}C\{^{1}H\}$ NMR spectrum shows an imine carbon signal at δ 166.2 ppm. The spectrum also displays a doublet of doublets at δ 188.2 ppm ($^{2}J_{PC}$ = 15.5 Hz, $^{1}J_{RhC}$ = 73.4 Hz) assigned to the carbonyl carbon. The small J_{PC} coupling constant confirms that the carbonyl carbon is *trans* to the imine nitrogen. The aromatic carbon atoms signals appear in the expected region (δ 126.8 – 136.3 ppm).

$^{31}P\{^{1}H\}$ NMR and $^{19}F\{^{1}H\}$ NMR spectroscopy

$^{31}P\{^{1}H\}$ NMR spectroscopy was used to further ascertain the coordination of rhodium to the phosphorous atom. The spectrum of complex **3.3** illustrated a downfield shift of the phosphorous peak from δ -12.63 ppm in the free ligand to δ 47.9 ppm in the complex. The phosphorous peak observed in the $^{31}P\{^{1}H\}$ spectrum is a doublet with a coupling constant of $^{1}J_{PRh}$ = 163.3 Hz, consistent with a rhodium phosphorous coupling constant.[1-3] The $^{19}F\{^{1}H\}$ NMR spectrum exhibits six peaks at δ -81.6, – 126.9, -124.4, -123.6, -122.6, -114.2 ppm. The peak at δ -81.6 is assigned to –CF_3, δ -114.2 is assigned to -CF_2 next to –CH_2 and the remaining peaks are assigned to the –CF_2-CF_2 moieties in the chain.

FT-IR spectroscopy

Furthermore, FT-IR spectroscopy was used to confirm the formation of complex **3.3**. In this spectrum a shift of the imine stretching band from 1638 cm^{-1} in the free ligand to 1625 cm^{-1} in the complex is seen. A carbonyl stretching band is also observed in the FT-IR spectrum at 2008

cm^{-1}. Other characteristic C-F bands are observed around 1144-1202 cm^{-1}, which corresponds to perfluorohexyl moiety.

Elemental Analysis and Electrospray Ionization Mass Spectrometry (ESI-MS)

The ESI spectrum of complex **3.3** displays a peak at *m/z* 766.00 assigned to $[M\text{-}Cl]^+$ and the calculated elemental analysis for C, N and H correspond well with the obtained results confirming purity.

3.3 Synthesis and characterization of fluorocarbon-containing salicylaldimine-based Rh(I) complexes

3.3.1 Synthesis and characterization of salicylaldimine Rh(I) complexes 3.4 and 3.5

The new complexes **3.4** and **3.5** (**Scheme 3.3**) were prepared by stirring ligands **L6** and **L7** (1 eqv.), respectively with a base triethylamine in ethanol for 1 h. After 1 h, and ethanolic solution of the rhodium dimer $[RhCl(COD)]_2$ (0.5 eqv.) was added and the reaction mixture was stirred overnight at room temperature. Both complex **3.4** and **3.5** were isolated as bright yellow solids in excellent yields of 41 % and 47 %, respectively. Complex **3.4** decomposes without melting at 205.6 ºC, while complex **3.5** melts in the range of 228.2 – 231.8 ºC.

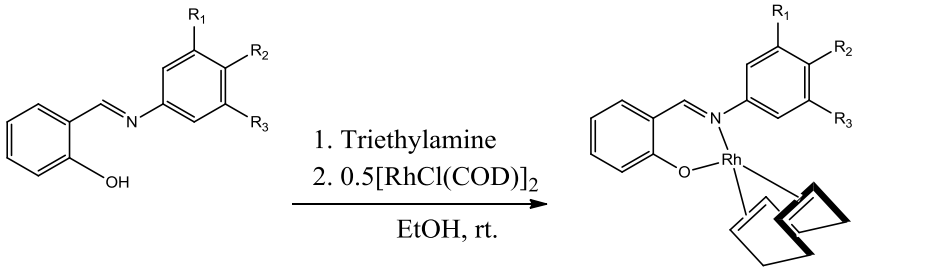

Complex **3.4**	Complex **3.5**
R_1 , R_3 = H	**R_1 , R_3 = CF_3**
R_2 = CF_3	**R_2 = H**

Scheme 3.3

^{1}H NMR spectroscopy

The ^{1}H NMR spectrum (**Figure 3.5** shown as an example) shows an imine peak at δ 7.87 ppm for complex **3.4**, this confirms metal to ligand coordination. The spectra also exhibits the

expected endo- and exo- methylene[12-26] as well as olefin proton peaks characteristic of the 1,5-cyclooctadiene (COD) moiety. The spectra show a multiplet at around δ 1.75 ppm for both complexes assigned to the exo-methylene protons. The endo-methylene signal appears as a multiplet at δ 2.32 ppm and at δ 2.34 ppm for complex **3.4** and **3.5**, respectively. The multiplets of the olefinic protons appear at δ 3.05 ppm and at δ 4.56 ppm for **3.4** and at δ 2.89 ppm and δ 4.60 ppm for **3.5**. The olefinic multiplet at around δ 4.5 ppm is assigned to the proton *trans* to the nitrogen and the upfield multiplet at around δ 3.00 ppm is assigned to the proton *trans* to the oxygen.[12] The different signals for the methylene and olefinic protons are due to the *trans effect* of the coordinated *N,O*-chelate on the proton resonance.[12-26] The COSY permitted full assignment of the proton spectrum and was also used to further corroborate the assigned signals. The proton NMR spectrum of complex **3.4** is used as an example (**Figure 3.5**).

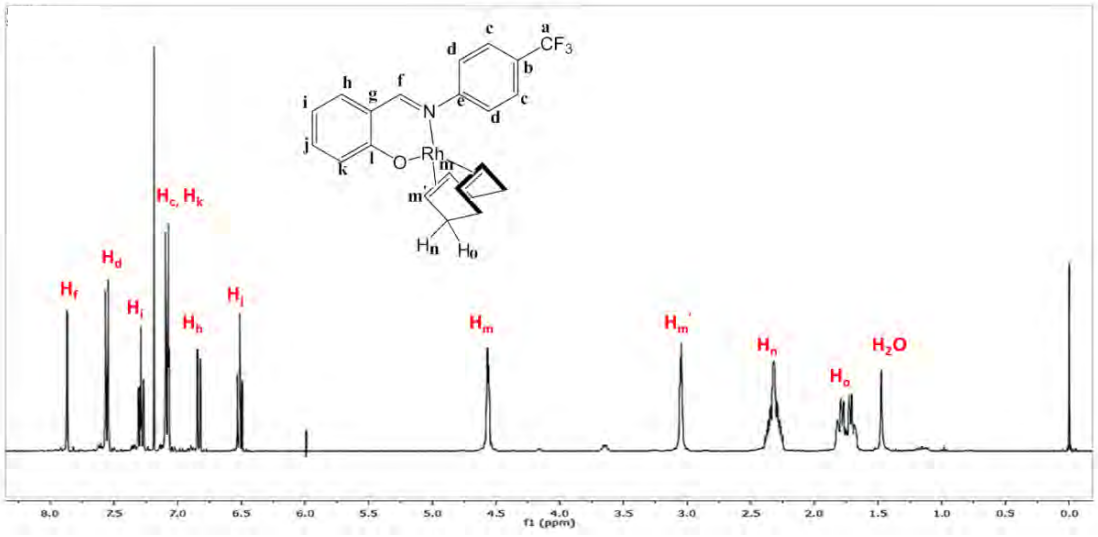

Figure 3.5: ^{1}H NMR spectrum of complex **3.4** in $CDCl_3$.

The expanded COSY spectrum in **Figure 3.6** for complex **3.4** shows the correlations within the aromatic rings of the complex. The imine proton H_f couples to H_h *via* long-range coupling, then H_h couples to a proton at 7.89 ppm assigned to H_i because it is adjacent to H_h. Proton H_i correlates to its neighboring proton H_j, which in turn couples to the vicinal proton H_k. Lastly, the proton H_c couples to its neighboring proton H_d.

Figure 3.7 shows the full COSY for complex **3.4** which illustrates the proton correlations in the COD moiety of the complex. The COSY spectrum shows that the proton ($H_{m'}$) *trans* to nitrogen couples to both the endo- (H_n) and *via* long-range coupling to the exo- (H_o) methylene protons.

Similarly, the proton (H_m) *trans* to oxygen also couples both to the endo- and *via* long-range coupling to exo- methylene protons. Lastly the exo- and endo protons couple to each other.

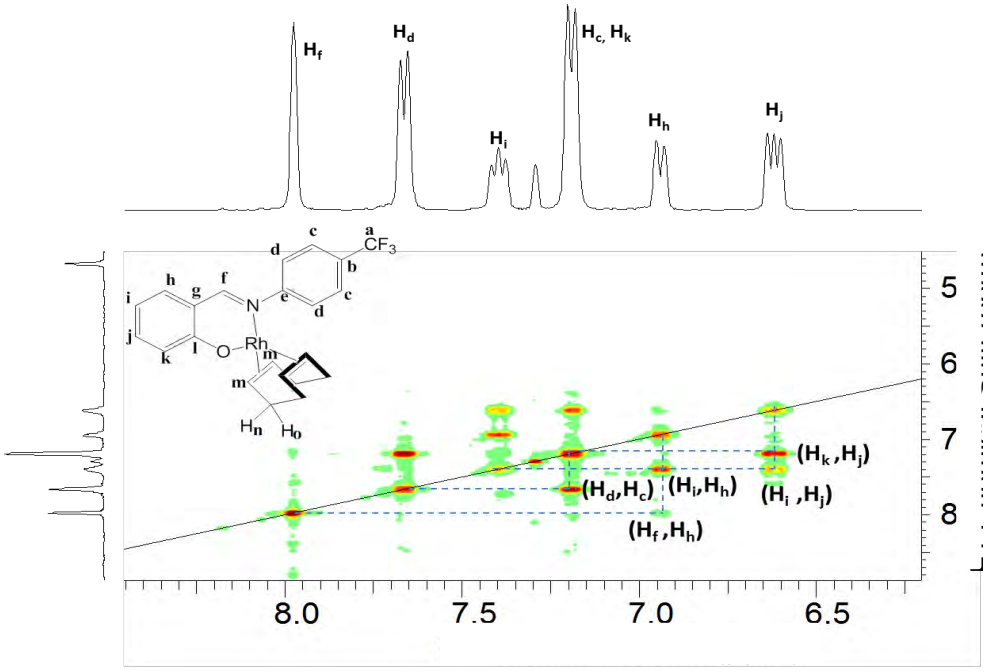

Figure 3.6: Expanded ^{1}H-^{1}H COSY 2D-NMR spectrum of complex **3.4** in $CDCl_3$.

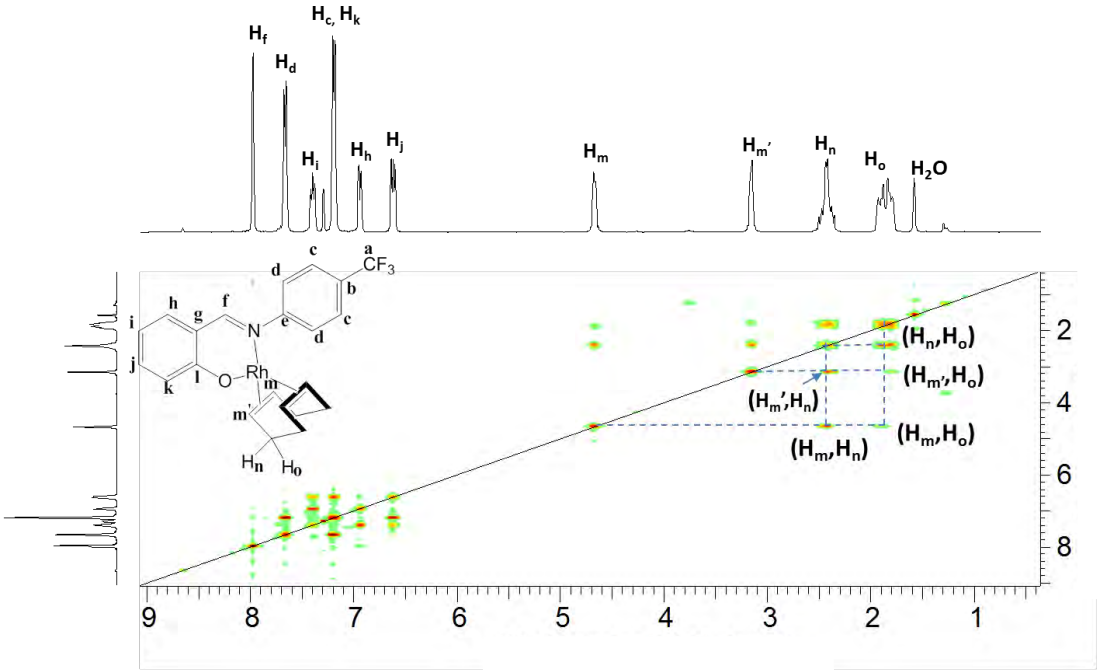

Figure 3.7: Full ^{1}H-^{1}H COSY 2D-NMR spectrum of complex **3.4** in $CDCl_3$.

$^{13}C\{^1H\}$ NMR spectroscopy

The $^{13}C\{^1H\}$ NMR spectrum shows an imine carbon signal at δ 166.4 ppm for **3.4** and at δ 166.8 ppm for **3.5**. The HSQC spectrum was used to fully assign the carbon spectrum by correlating the fully assigned proton NMR spectrum with the carbon NMR spectrum. **Figure 3.8** shows the HSQC spectrum of complex **3.4** which is used as an example to illustrate the carbon assignments.

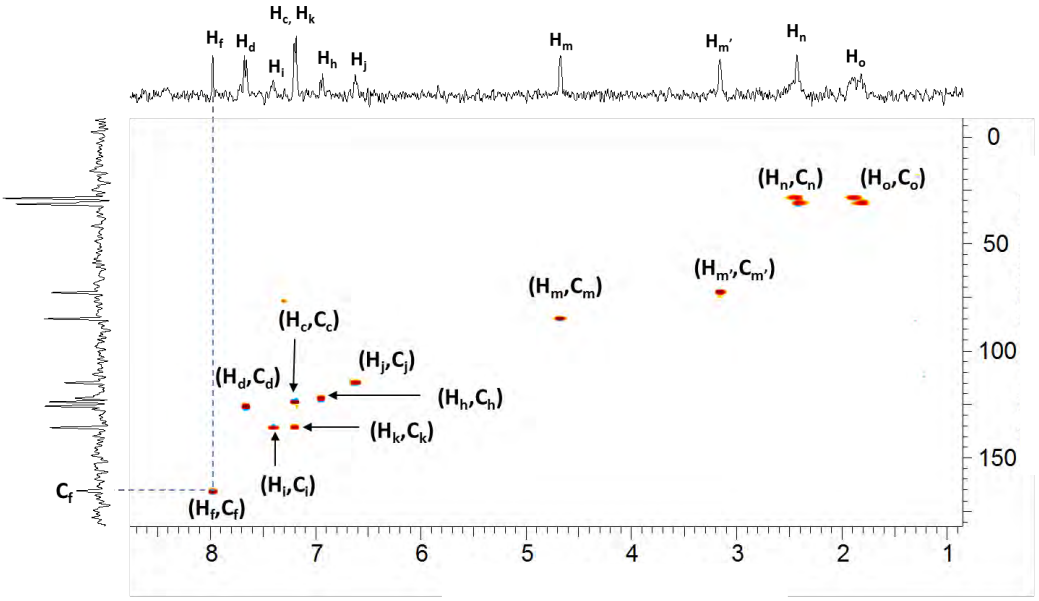

Figure 3.8: ^1H-^{13}C HSQC 2D-NMR spectrum of complex **3.4** in $CDCl_3$.

The HSQC spectrum in **Figure 3.8** shows that the most deshielded signal (H_f) couples to the most deshielded signal (C_f) in the ^{13}C NMR spectrum. The remaining aromatic carbon atoms were also assigned using this technique (**Figure 3.8**).

The $^{13}C\{^1H\}$ and HSQC NMR spectrum (**Figure 3.8**) also displays two singlets at δ 28.9 ppm and δ 31.8 ppm having equal intensities characteristic for the COD moiety, in contrast to only one singlet in the spectrum of the $[RhCl(COD)]_2$ dimer. The observed differences in the signals can be explained by the *trans* effect of the coordinated *N,O*-chelate on the carbons resonances. [12-26] The spectrum also exhibits two doublets at δ 85.1 ppm, ($^1J_{RhC}$ = 12.3 Hz) and at δ 72.7 ppm, ($^1J_{RhC}$ = 14.0 Hz) assigned to the carbon *trans* to the nitrogen ($C_{m'}$) and carbon *trans* to oxygen (C_m), respectively.[13-14] The doublets are due to coupling of the olefinic carbons to rhodium and

the ^{103}Rh-^{13}C (olefin) coupling constants are in good agreement with those found in literature (*ca*. *trans* to N: J = 12-13 Hz and trans to O: J = 14-15 Hz).[12-14]

$^{19}F\{^{1}H\}$ NMR spectroscopy

The $^{19}F\{^{1}H\}$NMR spectra show a peak around δ 78.7 ppm for complex **3.4** and at δ 78.1 ppm for **3.5**. The peaks are assigned to the $-CF_3$ moieties. There is no significant shift of the peaks in the complex compared to the free ligand (*ca*. 78.7 ppm and 78.0 ppm).

FT-IR spectroscopy

FT-IR spectra of complexes **3.4** and **3.5** further confirms the formation of the complexes. This is indicated by the shift of the imine band from a high (1623 cm^{-1} **L6** and 1628 cm^{-1} **L7**) to a lower frequency (1604 cm^{-1} **3.4** and **3.5**) upon coordination of the metal to the imine nitrogen. The FT-IR spectra also exhibit bands at around 1013-1275 cm^{-1} for the C-F bonds and are characteristic for the perfluorohexyl group.

Elemental analysis and Electron impact mass spectrometry (EI-MS)

The EI-Mass spectra show the parent molecular ion peak $[M]^+$ at 475.02 (*m/z*) for **3.4** and at 543.09 (*m/z*) for complex **3.5**. The obtained elemental analysis data are comparable with the calculated values, confirming the formation of the desired compounds.

3.3.2 Synthesis and Characterization of complex 3.6

The new complex **3.6** was prepared by stirring ligand **L8** (1 eqv.) with a base (triethylamine) in ethanol for 1 h. After 1 h, the rhodium dimer $[RhCl(COD)]_2$ (0.5 eqv.) in ethanol was added and the reaction mixture was stirred overnight (**Scheme 3.4**). The product was isolated as a yellow solid in good yield (65 %).

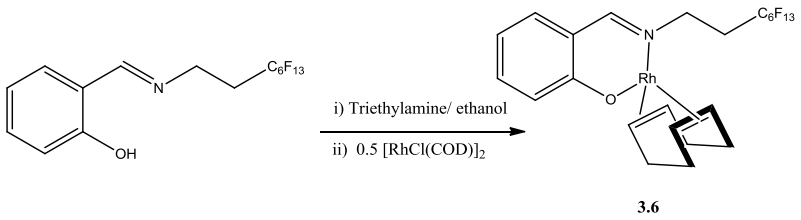

3.6

Scheme 3.4

^{1}H NMR spectroscopy

The upfield shift of the imine peak to δ 7.89 ppm from δ 8.35 ppm in the free ligand confirms metal to ligand coordination. The ^{1}H NMR spectrum shows a triplet at δ 3.39 ppm, ($^{3}J_{HH}$ = 7.60 Hz) assigned to the $–CH_2$ next to nitrogen as well as a multiplet at δ 2.39 ppm assigned to the -CH_2 next to the $–CF_2$.

In the proton NMR spectrum new peaks at δ 1.85, δ 2.39, δ 3.58 and δ 4.45 ppm are observed. The signals upfield at δ 1.85 and δ 2.39 ppm are assigned to the methylene protons, the signals downfield at δ 3.58 and δ 4.45 ppm are assigned to the olefinic protons characteristic for the COD protons. The COD methylene protons split into two compared to the starting rhodium COD dimer. This is due to the asymmetric environment induced by the *N,O*- chelating ligand (*trans* effect).[12-26] The aromatic protons appear in the expected region (δ 6.50 – 7.54 ppm).

$^{13}C\{^{1}H\}$ NMR spectroscopy

The $^{13}C\{^{1}H\}$ NMR spectrum displays a signal at δ 166.7 ppm, characteristic of the carbon atoms of the imino group. The methylene COD carbon peaks are observed as singlets at δ 71.4 and δ 85.8 ppm and the different methylene environments can be explained by the *trans effect*.[12-26] The spectrum also exhibits two doublets at δ 7.14 and at δ 31.8 ppm, the doublets are due to coupling of the rhodium to the olefinic carbons.

$^{19}F\{^{1}H\}$ NMR spectroscopy

The $^{19}F\{^{1}H\}$ NMR spectrum displays six peaks at (δ -81.6 ppm) assigned to $–CF_3$-, (δ – 126.9, -124.2, -123.6, -122.6 ppm) assigned to $–CF_2$-CF_2- and a peak at (-114.1 ppm) assigned to $–CF_2$-CH_2-. There is no significant shift of the peaks in the complex compared to the free ligand.

FT-IR spectroscopy

The FT-IR spectrum of complex **3.6** confirms coordination of the metal to the imine nitrogen, where the imine absorption band shifted to 1608 cm^{-1} from 1638 cm^{-1} in the free ligand. The spectrum also displays absorption bands around 1075-1236 cm^{-1}, attributed to the ν(C-F) of the perfluorohexyl group.

Elemental Analysis and Electron Impact Mass Spectrometry (EI-MS)

The obtained elemental analysis data are in agreement with the calculated values. The EI-MS spectrum shows a molecular ion peak $[M]^+$ at 677.02 (m/z) and a peak at 568.94 (*m/z*) for $[M\text{-}COD]^+$.

3.4 Conclusion

A series of new Schiff base fluorocarbon-containing iminophosphine (**3.1** - **3.3**) and salicylaldimine (**3.4** - **3.6**) Rh(I) based complexes were synthesized. All the complexes were isolated as yellow or orange solids in moderate to high yields and are air stable. Complex **3.1** and **3.2** have a crystal system of monoclinc and triclinic, respectively. The synthesized complexes were fully characterized using a number of spectroscopic techniques and analytical methods which include ^{1}H NMR, ^{13}C{^{1}H} NMR, ^{31}P{^{1}H} NMR and ^{19}F{^{1}H} NMR, 2-D NMR (COSY and HSQC) spectroscopy, mass spectrometry, infrared spectroscopy and elemental analysis and single crystal X-ray diffraction for complexes **3.1** and **3.2**.

3.5 Experimental

3.5.1 General

All solvents were purchased from Sigma-Aldrich and were used without any further purification. Dry THF was used for the reactions and all compounds were dried under vacuum. Rhodium chlorocarbonyl dimer ($[RhCl(CO)_2]_2$ and $[RhCl(COD)]_2$) were prepared using literature methods.[27-29]

All NMR spectra (^{1}H, ^{13}C{^{1}H}, ^{31}P{^{1}H}, and ^{19}F{^{1}H} NMR) were recorded using Varian mercury XR300 MHz (^{1}H at 300.08 MHz, ^{31}P{^{1}H} at 121.47 MHz) or Varian Unity XR400 spectrometer (^{1}H at 399.95 MHz, ^{13}C{^{1}H} 100.58 MHz, ^{19}F{^{1}H} 376.9 MHz) or Bruker Biospin GmbH (^{1}H at 400.22 MHz, ^{13}C{^{1}H} 100.60 MHz, ^{31}P{^{1}H} at 162.00 MHz) spectrometer at ambient temperature using tetramethylsilane (TMS) for ^{1}H NMR, trifluoroacetic acid (TFA) for ^{19}F{^{1}H} NMR and phosphoric acid for ^{31}P{^{1}H} as internal standards. Fourier Transform Infrared spectroscopy (FT-IR) was obtained using the Perkin-Elmer Spectrum 100 FT-IR spectrometer as KBr pellets or in a solution of dichloromethane using NaCl cells. Elemental

analysis (EA) for C, H and N were carried out using a Thermo Flash 1112 Series CHNS-O Analyser. Melting points were determined using a Büchi Melting Point B-540. Mass spectrometry was carried out at the University of Stellenbosch on a Waters API Quattro Micro Triple Quadrupole mass spectrometer and at the University of Cape Town using an Agilent 6890 N spectrometer.

Single-crystal X-ray diffraction data were collected on a Bruker KAPPA APEX II DUO diffractometer using graphite-monochromated Mo-Kα radiation (χ = 0.71073 Å). Data collection was carried out at 173(2)/ 133(2) K. Temperature was controlled by an Oxford Cryostream cooling system (Oxford Cryostat). Cell refinement and data reduction were performed using the 64 program SAINT.[30] The data were scaled and absorption correction performed using SADABS. The structure was solved by direct methods using SHELXL-97[31] and refined by full-matrix least-squares methods based on F using SHELXL-97[31] and graphic interface X-Seed program[32]. The X-Seed and POV-Ray[33] programs were both used to prepare graphic images.

*3.5.2 Preparation of Complex **3.1***

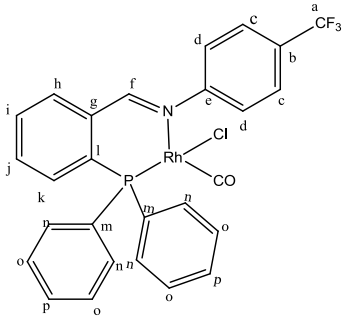

Compound (**L1**) (0.0541 g, 0.125 mmol) dissolved in 5 ml THF was added dropwise to a stirring solution of $[RhCl(CO)_2]_2$ (0.0242 g, 0.0625 mmol) in 5 ml of THF. An orange solution resulted. The mixture was stirred at room temperature for 2 h. After 2 h, the solvent was removed and the resulting orange solid was washed with diethyl ether and filtered. The orange solid was dried under vacuum. This was the desired product **3.1**. (Yield: 0.0486 g, 64 %). **IR**: KBr pellets, υ/cm^{-1}: 1604 (s, imine, C=N), 2000 (C=O). **^{1}H NMR** (300 MHz, $CDCl_3$): δ (ppm) = 7.01 (m, 1H, H_k), 7.32 (m, 2H, H_d), 7.53 (m, 15H, Ar), 8.07 (s, 1H, H_f). **^{13}C{^{1}H} NMR** (100 MHz, $CDCl_3$): δ (ppm) = 123.2 (s, C_d), 125.7 (C_a), 128.8 ($C_{i,jo,p}$), 131.5 ($C_{c,g,k,n}$), 133.6 (C_m), 136.3 (C_l), 153.8 (s, C_e), 166.7 (s, imine, C=N), 188.5 (dd, $^2J_{PC}$ = 15.0 Hz, $^1J_{RhC}$ = 74.9 Hz).**^{31}P{^{1}H} NMR** (121 MHz,

$CDCl_3$): δ (ppm) = 47.9 (d, $^1J_{RhP}$ = 163.3 Hz). **$^{19}F\{^1H\}$ NMR** (377 MHz, $CDCl_3$): δ (ppm) = 78.5 (s, 6F). **MS** (ESI, m/z): 564.1$[M\text{-}Cl]^+$. **Elemental analysis** (%): Calc. For: $C_{27}H_{19}ClF_3NOPRh$: C, 54.07; H, 3.19; N, 2.34. Found: C, 53.37; H, 3.00; N, 1.79. **Melting point**: Decomposes without melting at 180.4 ºC.

*3.5.3 Preparation of Complex **3.2***

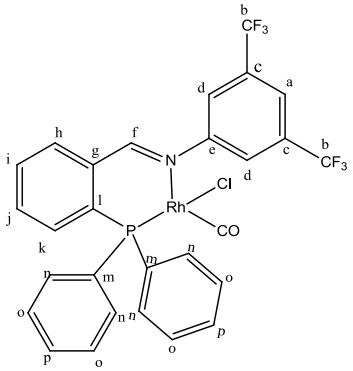

Compound (**L2**) (0.0500 g, 0.0991 mmol) in 6 ml THF was added dropwise to stirring solution of $[RhCl(CO)_2]_2$ (0.0193 g, 0.0490 mmol) in 6 ml of THF. The mixture resulted in an orange solution. The mixture was stirred at room temperature for 2 h. After 2 h, the solvent was removed and the resulting orange solid was dried under vacuum. The product **3.2** was isolated as an orange solid. (Yield: 0.0490 g, 74 %). **IR**: KBr pellets, (υ/cm^{-1}): 1602 (s, imine, C=N), 2008 (C=O). **^1H NMR** (300 MHz, $CDCl_3$): δ (ppm) = 7.03 (m, 1H, H_h), 7.57 (m, 15H, Ar), 7.64 (s, 1H, H_k), 8.04 (s, 1H, H_f). **$^{13}C\{^1H\}$ NMR** (100 MHz, $CDCl_3$): δ (ppm) = 121.2 (s, C_k), 123.5 (s, C_a), 133.9, 131.7, 129.1 ($C_{b,c,d,g,i,j,n,o,p}$), 131.3 (C_m), 132.0 (C_h), 134.3 (C_l), 136.6 (C_e),167.9 (s, imine, C=N), 188.6 (dd, $^2J_{PC}$ = 15.4 Hz, $^1J_{RhC}$ = 73.7 Hz). **$^{31}P\{^1H\}$ NMR** (121 MHz, $CDCl_3$): δ (ppm) = 48.1 (d, $^1J_{RhP}$ = 161.3 Hz). **$^{19}F\{^1H\}$ NMR** (377 MHz, $CDCl_3$): δ (ppm) = 78.2 (s, 6F). **MS** (ESI, m/z): 666.9 $[M]^+$. **Elemental analysis** (%):Calc. For: $C_{28}H_{18}ClF_6NOPRh$: C, 50.36; H, 2.72; N, 2.10. Found: C, 50.57; H, 3.65; N, 1.00. **Melting point**: Decomposes without melting at 160.2 ºC.

*3.5.4 Preparation of Complex **3.3***

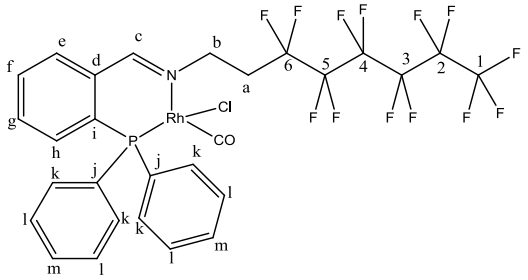

$[RhCl(CO)_2]_2$ (0.0178 g, 0.0457 mmol) was dissolved in THF (7 ml). **L5** (0.0581 g, 0.0914 mmol) in THF (7 ml) was added slowly to the $[RhCl(CO)_2]_2$ THF solution. The reaction mixture was stirred at room temperature for 2 h. After 2 h, the solvent was removed using rotary evaporator. An orange solid resulted as the product **3.3**. (Yield: 0.0358 g, 49 %). **IR**: CH_2Cl_2, ν/cm^{-1}: 2008 (C=O), 1625 (s, imine, C=N), 1144-1202 (C-F). **^{1}H NMR** (300 MHz, $CDCl_3$): δ (ppm) = 2.53 (m, 2H, H_a), 4.47 (t, $^3J_{HH}$ = 6.80 Hz, 2H, H_b), 6.86 (m, 1H, H_h), 7.41 (m, 13H, $H_{e,f,g,k,l,m}$), 8.04 (s, 1H, H_c). **^{13}C{^{1}H} NMR** (100 MHz, $CDCl_3$): δ (ppm) = 32.1 (t, $^2J_{CF}$ = 21.5 Hz, C_a), 56.2 (s, C_b), 120.5-105.9 (m, C-F), 130.7, 131.9, 132.6, 133.5 ($C_{f,k,l,m}$), 131.9 (s, C_h),135.8 (s, C_j),136.6 (s, C_d), 166.2 (s, imine, C=N), 188.5 (dd, $^2J_{PC}$ = 15.5 Hz, $^1J_{RhC}$ = 73.4 Hz). **^{13}P{^{1}H} NMR** (162 MHz, $CDCl_3$): δ (ppm) = 47.9 (d, $^1J_{RhP}$ = 161.1 Hz). **^{19}F{^{1}H} NMR** (377 MHz, $CDCl_3$): δ (ppm) = -81.6 (m, 3F, F_1), -126.9 (m, 2F, F_2), -124.4 (m, 2F, F_3), -123.9 (m, 2F, F_4), -122.6 (m, 2F, F_5), -114.2 (m, 2F, F_6). **MS** (ESI, m/z): 766.00 $[M\text{-}Cl]^+$. **Elemental analysis** (%): Calc. For $C_{27}H_{18}F_6NP$: C, 64.68; H, 3.62; N, 2.79. Found: C, 64.33; H, 3.93; N, 2.39. **Melting point**: Decomposes without melting at 164.8 ºC.

*3.5.5 Preparation of Complex **3.4***

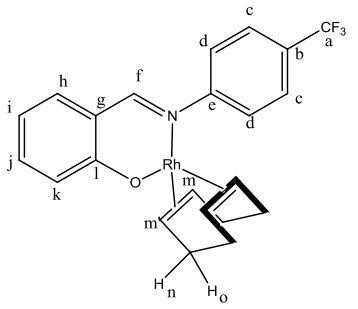

To a stirring solution of compound **L6** (0.100 g, 0.377 mmol) in ethanol (10 ml) triethylamine (0.0110 g, 0.105 mmol) was added dropwise and the mixture was stirred at room temperature for 1 h. After 1 h, $[RhCl(COD)]_2$ (0.0930 g, 0.189 mmol) in ethanol (5 ml) was added. The mixture was further stirred at room temperature for 24 h. After 24 h solvent was removed and a yellow solid resulted. The desired yellow solid was washed with cold ethanol, filtered and dried under vacuum. (Yield: 0.0740 g, 41 %). **IR**: KBr pellets, ν/cm^{-1}: 1604 (s, imine, C=N), 1013-1168 (C-F). **^{1}H NMR** (400 MHz, $CDCl_3$): δ (ppm) = 1.75 (m, 4H, CH_{2exo}, H_o), 2.32 (m, 4H,$CH_{2endo,}$ H_n), 3.05 (m, 2H, CH_{COD}, H_m), 4.56 (m, 2H, CH_{COD}, $H_{m'}$), 6.51 (m, 1H, H_j), 6.83 (m, 1H, H_h), 7.08 (m, 3H, $H_{c,\,k}$), 7.29 (m, 1H, H_i), 7.56 (d, J = 8.14 Hz, 2H, H_d), 7.87 (s, 1H, H_f). **^{13}C{^{1}H} NMR** (100 MHz, $CDCl_3$): δ (ppm) = 28.9 (s, CH_{2COD}, $C_{n,o}$), 31.8 (s, CH_{2COD}, $C_{n,o}$), 72.7 (d, $^1J_{RhC}$ = 14.0 Hz, CH_{COD}, C_m), 85.1 (d, $^1J_{RhC}$ = 12.3 Hz, CH_{COD}, $C_{m'}$), 114.9 (s, C_j), 118.3 (s, C_g), 122.2 (s, C_g), 123.9 (s, C_c), 125.9 (s, C_d), 135.6 (s, $C_{i,\,k}$), 155.2 (s, C_e), 165.5 (s, C_f), 167.2 (s, C_l). **^{19}F{^{1}H} NMR** (377 MHz, $CDCl_3$): δ (ppm) = 78.7 (s, 3F). **MS** (EI, m/z): 475.02 $[M]^+$. **Elemental analysis** (%): Calc. For $C_{22}H_{21}F_3NORh$: C, 55.59; H, 4.45; N, 2.45. Found: C, 55.15; H, 5.18; N, 2.47. **Melting point**: Decomposes without melting at 205.6 ˚C.

*3.5.6 Preparation of Complex **3.5***

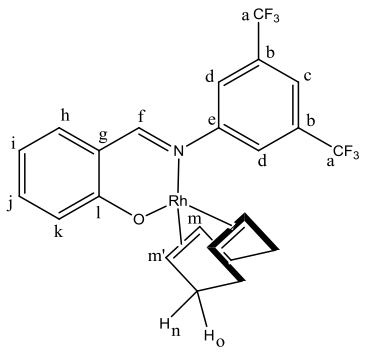

To a stirring solution of compound **L7** (0.103 g, 0.309 mmol) in ethanol (10 ml) triethylamine (0.0302 g, 0.300 mmol) was added dropwise and the mixture was stirred at room temperature for 1 h. After 1 h, a solution of $[RhCl(COD)]_2$ (0.0765 g, 0.155 mmol) in ethanol (5 ml) was added. The mixture was stirred at room temperature for 24 h. After 24 h solvent was removed by rotary evaporation and a yellow solid resulted. The desired yellow solid was washed with cold ethanol, filtered and dried under vacuum for 7 h. (Yield: 0.0790 g, 47 %). **IR**: KBr pellets, ν/cm^{-1}: 1604 (s, imine, C=N), 1131-1275 (C-F). **^{1}H NMR** (400 MHz, $CDCl_3$): δ (ppm) = 1.76 (m, 4H, CH_{2exo}, H_o), 2.34 (m, 4H, CH_{2endo}, H_n), 2.89 (m, 2H, CH_{COD}, H_m), 4.60 (m, 2H, CH_{COD}, $H_{m'}$), 6.53 (m, 1H, H_j), 6.82 (dd, J = 9.38 Hz, 1H, H_h), 7.09 (dt, J = 9.80, 1H, H_k), 7.31 (m, 1H, H_i), 7.45 (m, 2H, H_d), 7.64 (s, 1H, H_b), 7.87 (s, 1H, H_f). **^{13}C{^{1}H} NMR** (100 MHz, $CDCl_3$): δ (ppm) = 28.9 (s, CH_{2COD}, $C_{n,o}$), 31.4 (s, CH_{2COD}, $C_{n,o}$), 72.1 (d, $^1J_{RhC}$ = 14.0 Hz, CH_{COD}, C_m), 85.6 (d, $^1J_{RhC}$ = 12.3 Hz, CH_{COD}, $C_{m'}$), 115.2 (s, C_j), 118.1 (s, C_b), 121.5 (s, C_g), 119.8 (s, C_c), 122.4 (s, C_h), 123.9 (s, C_d), 132.2 (s, C_a), 135.6 (s, $C_{g,k}$), 136.2 (s, C_i), 153.5 (s, C_e), 166.0 (s, C_f), 167.6 (s, C_l) **^{19}F{^{1}H} NMR** (377 MHz, $CDCl_3$): δ (ppm) = 78.1 (s, 6F). **MS** (EI, m/z): 543.09 $[M]^+$. **Elemental analysis** (%): Calc. For $C_{23}H_{20}F_6NORh$: C, 50.85; H, 3.71; N, 2.58. Found: C, 50.62; H, 3.91; N, 2.08. **Melting point**: 228.2-231.8 ºC.

*3.5.7 Preparation of Complex **3.6***

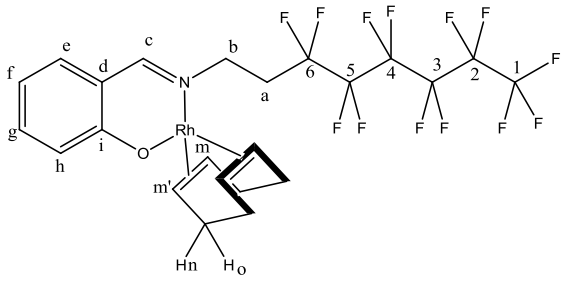

To a solution of compound **(L8)** (0.105 g, 0.147 mmol) in ethanol (10 ml) triethylamine (0.0115 g, 0.114 mmol) was added dropwise and the mixture was stirred at room temperature for 1 h. After 1 h a solution of $[RhCl(COD)]_2$ (0.0363 g, 0.0735 mmol) in ethanol (5 ml) was added. The mixture was further stirred at room temperature for 24 h. A precipitate formed during the reaction. The yellow precipitate was filtered and washed with ethanol to give the product as a yellow solid. (Yield: 0.0648 g, 65 %). **IR**: KBr pellets, ν/cm^{-1}: 1608 (s, imine, C=N), 1075-1236 (C-F). **^{1}H NMR** (400 MHz, $CDCl_3$): δ (ppm) = 1.85 (m, 4H, CH_{2exo}, H_o, 2.39 (m, 6H, H_a, CH_{2endo}, H_n), 3.39 (t, 2H, H_b), 3.58 (d, 2H, $H_{m'}$), 4.45 (d, 2H, H_m), 6.50 (t, 1H, H_g), 6.77 (d, 1H, H_e), 7.09 (d, 1H, H_h), 7.24 (t, 1H, H_f), 7.89 (s, 1H, H_c). **^{13}C{^{1}H} NMR** (100 MHz, $CDCl_3$): δ (ppm) = 28.7 (s, CH_{2COD}, $C_{n,o}$), 31.8 (s, CH_{2COD}, $C_{n,o}$), 35.4 (t, C_a), 50.9 (s, C_b), 71.4 (d, $^1J_{RhC}$ = 14.1 Hz, CH_{COD}, C_m), 85.8 (d, $^1J_{RhC}$ = 12.5 Hz, CH_{COD}, $C_{m'}$), 114.7 (s, C_g), 121.6 (s, C_e), 134.9 (s, C_f), 135.3 (s, C_h), 166.8 (d, C_c). **^{19}F{^{1}H} NMR** (377 MHz, $CDCl_3$): δ (ppm) = -81.6 (m, 3F, F_1), -126.9 (m, 2F, F_2), -124.2 (m, 2F, F_3), -123.6 (m, 2F, F_4), -122.6 (m, 2F, F_5), -114.1 (m, 2F, F_6). **MS** (EI, m/z): 677.02 $[M]^+$, 568.94 $[M\text{-}COD]^+$. **Elemental analysis** (%): Calc. For $C_{23}H_{21}F_{13}NORh$: C, 40.78; H, 3.17; N, 2.07. Found: C, 40.79; H, 3.72; N, 1.52. **Melting point**: 184.1-186.1 ˚C.

3.6 References

1. a) N. Kumar, P. Sharma and A. Pareek, *iJARS*, **2**, 2013, 307. b) Best, J. M. Wilson, H. Adams, L. Gonsalvi, M. Peruzzini and A. Haynes, *Organometallics*, **26**, 2007, 1960.
2. J. Rankin, A. D. Poole, C. Benyei and D. J. Cole-Hamilton, *Chem. Commun*., 1997, 1835.
3. G. S. Rodman and K. R. Mann, *Inorg. Chem.*, **27**, 1988, 3338.
4. Y. Cheng, X. Hu, S. Gao, L. Lu, J. Chen and W. Xiao, *Tetrahedron*, **69**, 2013, 3810.
5. P. Altmann, M. Cokoja and F. E. Kühn, *J. Organomet. Chem*., **701**, 2012, 51.
6. D. J. Darensbourg, P. Rainey and J. Yarbrough, *Inorg. Chem.*, **40**, 2001, 986.
7. M. H. Luo, H. Y. Tsai, H. Y. Lin, S. K. Fang and K. Y. Chen, *Chinese Chem. Lett*., **23**, 2012, 1279.
8. N. C. Antonels, B. Therrien, J. R. Moss and G. S. Smith, *Inorg Chem. Commun.,* **12**, 2009, 716.
9. S. Burling, L.D. Field, B.A. Messerle, K.Q. Vuong and P. Turner, *Dalton Trans.,* 2003, 4181.
10. P. W. Dyer, J. Fawcett and M. J. Hanton, *J. Organomet. Chem*., **690**, 2005, 5264.
11. K. N. Gavrilov, O. G. Bondarev, R. V. Lebedev, A. A. Shiryaev, S. E. Lyubimov, A. I. Polosukhin, G. V. Grintselev-Knyazev, K. A. Lyssenko, S. K. Moiseev, N. S. Ikonnikov, V. N. Kalinin, V. A. Davankov, A.V. Korostylev and H. Gais, *Eur. J. Inorg. Chem.* 2002, 1367.
12. M. Enamullah, K. M. Royhan Uddin, G. Hogarth and C. Janiak, *Inorg. Chim. Acta*, **387**, 2012, 173.
13. M. Enamullah, A. Sharmin, M. Hasegawa, T. Hoshi, A. C. Chamayou and C. Janiak, *Eur. J. Inorg. Chem.*, **2006**, 2006, 2146.
14. C. Janiak, A. C. Chamayou, K. M. Royhan Uddin, M. Uddin, K. S. Hagen and M. Enamullah, *Dalton Trans.*, **9226**, 2009, 3698.
15. A. P. Mart, F. J. Lahoz and L. A. Oro, *Inorg. Chem. Commun*., **5**, 2002, 245.
16. S. Heterocycles, R. Aumann, I. Göttker-schnetmann, R. Fröhlich and P. Saarenketo, *Chem. Eur. J*., **7**, 2001, 711.
17. M. Enamullah, M. Uddin and W. Linert, *J. Coord. Chem.*, **60**, 2007, 2309.

18. B. C. E. Makhubela, A. M. Jardine, G. Westman and G. S. Smith, *Dalton Trans.*, **41**, 2012, 10715.
19. E. B. Hager, B. C. E. Makhubela and G. S. Smith, *Dalton Trans.*, **41**, 2012, 13927.
20. L. De Chimie, O. Structurale, R. Bonnaire and D. Davoustic, *Inorg. Chem.*, **21**, 1982, 2032.
21. R. Bonnaire, J. M. Manoli, C. Potvin, I. N. Platzer and N. Goasdoueib, *Inorg. Chem.*, **20**, 1981, 2691.
22. C. Tejel, M. Ciriano, M. Bordonaba, J. López , F. J. Lahoz and L. A. Oro, *Inorg. Chem.*, **41**, 2002, 2348.
23. P. G. Rasmussen and J. B. Kolowich, *J. Chem. Soc., Dalton Trans*., 1987, 3003.
24. D. W. Krassowski, J. H. Nelson, K. R. Brower, D. Hauenstein and R. A. Jacobsonlc, *Inorg. Chem*., **27**, 1988, 4294.
25. R. Dreos, G. Nardin, L. Randaccio, P. Siega and G. Tauzher, *Inorg. Chem.*, **43**, 2004, 3433.
26. S. L. James, D. M. P. Mingos, X. Xu, A. J. P. White and D. J. Williams, *J. Chem. Soc., Dalton Trans*., 1998, 1335.
27. A. J. Deeming and P.J Sharrat, *J. Organomet. Chem*., **99**, 1975, 447.
28. S. H. Hong and R. H. Grubbs, *J. Am. Chem. Soc*., **128**, 2006, 3508.
29. J. Chatt and L. M. Venanzi, *J. Chem. Soc.,* 1957, 4735.
30. SAINT Version 7.60a, Bruker AXS Inc., Madison, WI, USA, 2006.
31. G. M. Sheldrick, SHELXS-97, SHELXL-97 and SADABS version 2.05, University of Göttingen, Germany, 1997.
32. a) L. J. Barbour, *J. Supramol. Chem.*, **1**, 2001, 189. b) J. L. Atwood and L. J. Barbour, *Cryst. Growth Des*., **3**, 2003, 3.
33. http://www.povray.org., *accessed on 10th March 2014.*

Catalytic Evaluation of Fluorocarbon-containing Rh(I) Complexes in Fluorous Biphasic Hydroformylation of 1-Octene

4.1 Introduction

The hydroformylation reaction (or Oxo process) is an important industrial homogeneous catalyzed reaction for the production of aldehydes.[1-3] The reaction entails the addition of CO/H_2 (syngas) across the double bond of an alkene in the presence of a catalyst to produce aldehydes (**Equation 4.1**).[4] These aldehydes are used in the production of alcohols, ethers, diols, carboxylic acids, esters, aldols and acroleins.[5-7] The aldehydes formed can be linear aldehydes or branched aldehydes, and these are both important in the industry. Linear aldehydes are mostly used for manufacturing surfactants and plasticizers, while branched aldehydes are significant in the pharmaceutical and agrochemical industries.[8] In 2012, more than 12 million tons of aldehydes were produced in industry.[9]

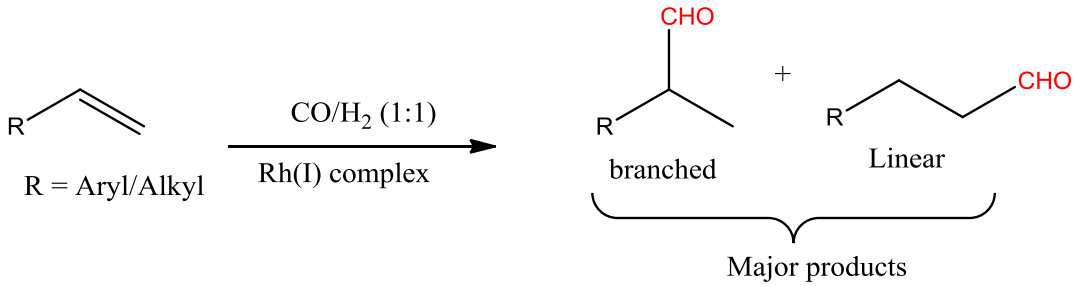

Equation 4.1

Transition metal catalysts are required for the hydroformylation reaction. The commercially used metals in this reaction are Co and Rh, Rh being the most active metal and gives high rates and selectivities.[10-13] Also, reactions using rhodium-based catalysts are performed under milder conditions compared to the Co-based catalysts.[10-13] However, rhodium is one of the most expensive metals hence the recovery of the catalysts after reactions is important and this is the main challenge in homogeneous catalysis.[14] Fluorous biphasic catalysis is one of the methods that will allow immobilizing catalysts in the fluorous phase while the products/reactants are in the organic phase; this provides a facile approach for separation of catalyst from products and the catalyst might be reused.[14]

This chapter discusses the evaluation of fluorocarbon-containing bidentate iminophosphine and salicylaldimine Rh(I)-based complexes described in Chapter 3 as catalyst precursors in the fluorous biphasic hydroformylation of 1-octene.

4.2 Results and Discussion

The synthesized iminophosphine Rh(I) complexes **3.1** – **3.3** and salicylaldimine **3.4** - **3.6** (**Figure 4.1**) were evaluated as catalysts in the hydroformylation of 1-octene. The iminophosphine Rh(I) complex **3.3** and salicylaldimine complex **3.6** were used in preliminary testing to find the optimum reaction conditions for the fluorous hydroformylation experiments. These were chosen due to their high fluorine content. The reaction products were monitored by GC and the products that formed were generally aldehydes (linear and branched). Small quantities of isomers such as *cis*- and *trans*-2-octene and *cis*- and *trans*-3-octene were also observed. These are formed *via* isomerization.

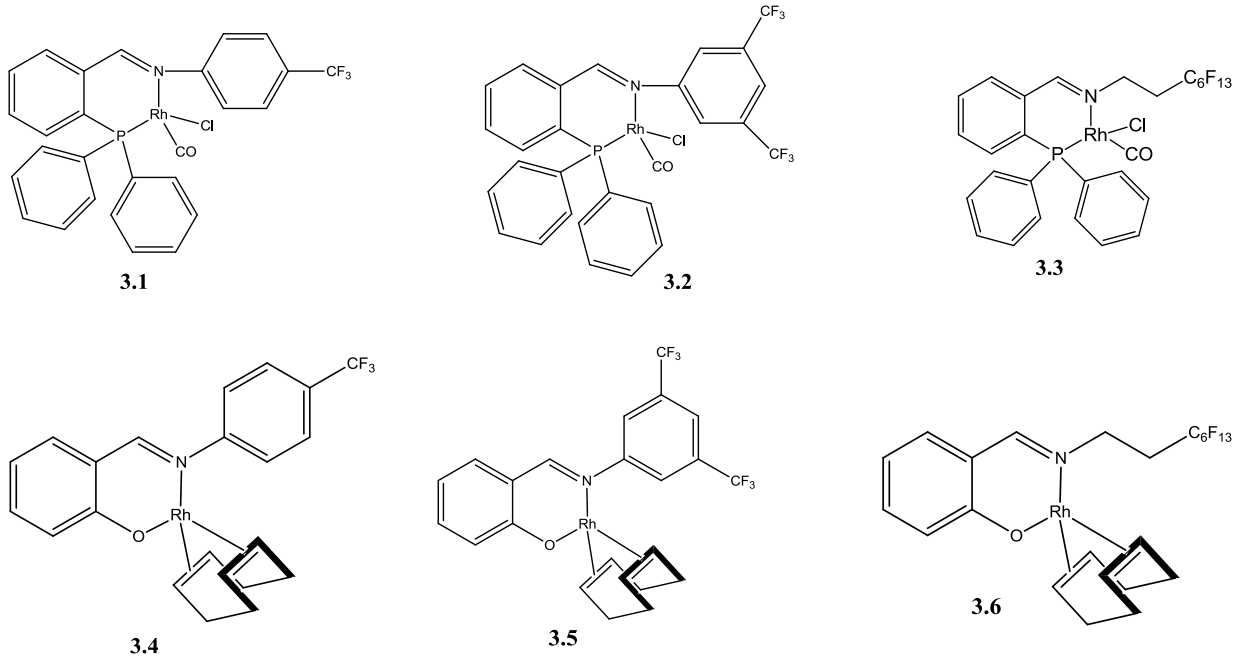

Figure 4.1: Catalyst precursors used in the hydroformylation of 1-octene.

The fluorous biphasic hydroformylation experiments were performed at different times 2 - 8 hours, different pressures 20 – 40 bars of syngas pressure ($CO:H_2$ = 1:1) and at different temperatures 75 - 100 °C. The different pressures 20, 30 and 40 bars and temperatures used were

based on the literature work that has been reported.[15-20] The reactions were performed in toluene and perfluoromethylcyclohexane (PMCH). A low catalyst loading of 0.00249 mmol of each catalyst precursor was used (catalyst:substrate ratio =1:500).

4.2.1 Fluorous biphasic hydroformylation using complex 3.3

4.2.1.1 Effect of syngas pressure on conversion

The effect of pressure was investigated at 75 °C and pressure was varied from 20 to 40 bar syngas pressure at different times. Conversion is defined as the total amount of substrate converted to products (desired and undesired products).[21a] **Figure 4.2** below displays the percentage conversion of 1-octene to products over time at different pressures and constant temperature (75°C) using iminophosphine complex **3.3**.

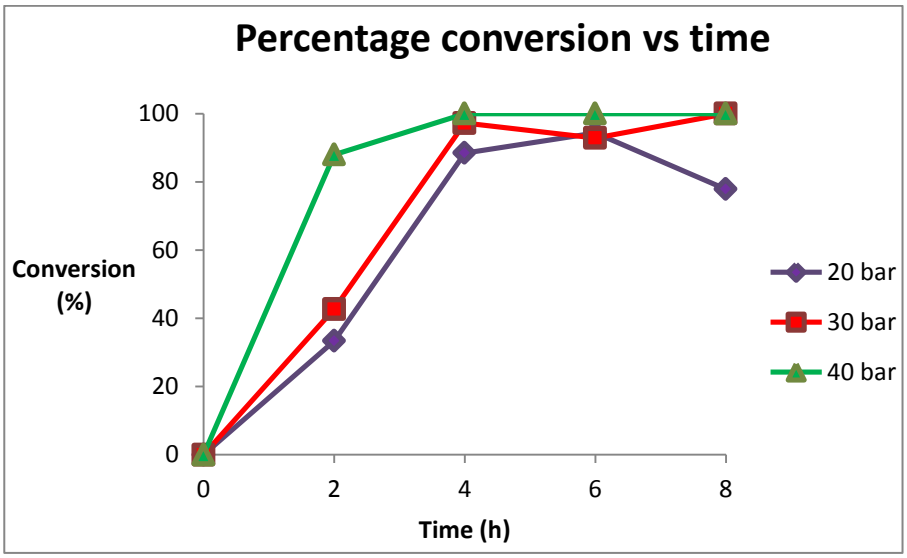

Figure 4.2: Percentage conversions of 1-octene over 8 hours using catalyst precursor **3.3** at 75 °C and 20, 30 and 40 bar syngas pressure. (Average error estimate: ± 2.38, ± 0.45, ± 0.10)

Figure 4.2 illustrates that the percentage conversion of 1-octene increases as time and pressure increases. At lower pressures (20 and 30 bars), low conversions of about 40 % in the first 2 hours are observed whereas at 40 bars the percentage conversions are above 80 %. The low conversions over the first 2 hours at 20 and 30 bars may be indicative of an induction period. At 40 bars high conversions are obtained as compared to 20 and 30 bars. This suggests that at higher pressures the induction period proceeds faster compared to lower pressures. During this period

the pre-catalyst is being converted to the active species hence the low conversion. As the reaction progresses the conversions increase and this is indicated by the high conversions (> 80 %) after 4 hours (**Figure 4.2**) at all the different pressures. At 40 bars the conversions remain constant after 4 hours and at 20 and 30 bars the conversions drop slightly but still above 80 % at 6 – 8 hours. This drop might be due to the catalyst losing its activity after 6 h.

The catalyst activity is measured in terms of either turnover frequency (TOF) or turnover number (TON).[21b] TOF is the number of moles of product produced divided by the number of moles of catalyst per hour (TOF = $Mol_{product}/Mol_{catalyst}$ x h^{-1}). Turnover number refers to how many moles of substrate can a mole of catalyst convert before reaching its inactivity. The catalyst to substrate ratio used was 1: 500 (0.00249: 1.25 mmol). Turnover number results using catalyst **3.3** at different pressures and reaction times are displayed in **Figure 4.3**.

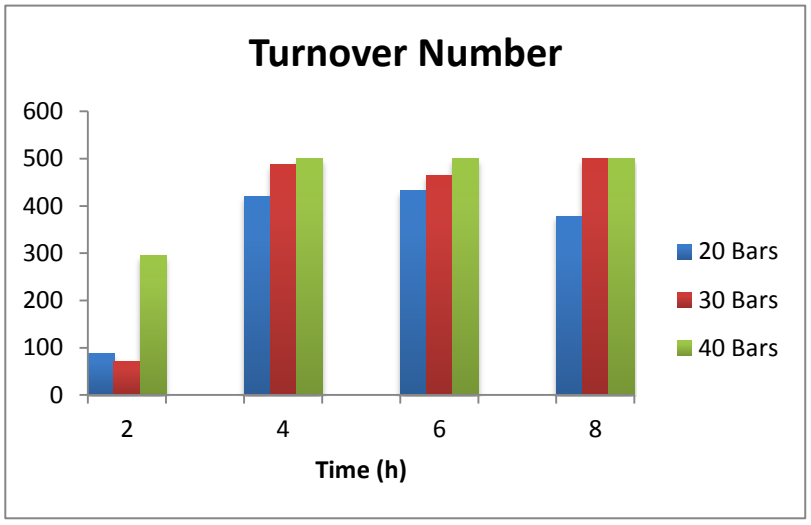

Figure 4.3: Effect of pressure on TON in hydroformylation of 1-octene using catalyst precursor **3.3** at 75 °C and: (a) 20 bars, (b) 30 bars and (c) 40 bars and at different reaction times. (Average error estimate: ± 2.38, ± 0.45, ± 0.10)

Figure 4.3 displays very low turnover numbers for the first 2 hours at 20 and 30 bars (< 100) and moderate at 40 bars. After 4 hours at 20, 30 and 40 bars high turnover numbers were observed. This may be due to catalyst converting more substrate to products at longer reaction time compared to shorter reaction time. **Figure 4.3** also illustrates that turnover numbers increases as pressure increases. The increase in TON as pressure increases might be due to catalyst

converting more substrate at high pressures than at low pressures. This could also mean that the reaction proceeds faster at high pressures than at low pressures.

4.2.1.2 Chemoselectivity

The hydroformylation reaction can yield different products such as alcohols, aldehydes and *iso*-octenes. These products contain different functional groups and a catalyst can favour one functional group over another. This is termed as chemoselectivity.[21b] The chemoselectivity was investigated at different pressures and reaction times at 75 °C. The results are shown in **Table 4.1**. Catalyst precursor **3.3** is generally highly selective towards aldehydes at high pressures and longer reaction times.

Table 4.1: Hydroformylation results of 1-octene using complex **3.3**.

Entry	Time (h)	Pressure (bar)	Temperature (^{o}C)	Conversion (%)	Total aldehydes	Iso-octenes	n:iso
1	2	20	75	33.49	23.23	76.77	4.79
2	4	20	75	88.46	94.96	5.04	0.76
3	4[a]	20	100	84.50	83.30	16.70	0.32
4	6	20	75	94.33	91.62	8.37	0.85
5	8	20	75	77.85	97.02	2.98	0.55
6	2	30	75	42.68	32.69	67.30	1.29
7	4	30	75	97.20	99.99	-	0.47
8	4[a]	30	100	99.99	99.99	-	0.34
9	6	30	75	92.87	99.99	-	0.49
10	8	30	75	99.99	99.99	-	0.092
11	2	40	75	87.92	67.07	32.92	0.74
12	4	40	75	99.99	99.99	-	0.17
13	4[a]	40	100	99.99	99.99	-	0.28
14	4[b]	40	75	75.93	90.72	9.27	1.83
15	6	40	75	99.99	99.99	-	0.54
16	8	40	75	99.99	99.99	-	1.84

Hydroformylation of 1-octene in toluene (2 mL) and perfluoromethylcyclohexane (2 ml), 1:1 CO/H_2, 20, 30 & 40 bar, 75 °C temperature, catalyst loading 0.00249 mmol, 1:500 = catalyst:substrate. GC conversions were obtained using *n*-decane as internal standard, average error estimate: ± 2.38, ± 0.45, ± 0.10. Total aldehydes are composed of a mixture of branched aldehydes and linear aldehydes and % sum of mixture is 100 %.[a]Temperature 100 ^{o}C. [b]Catalyst:Substrate = 1:2500.

Table 4.1 shows that at 20 bars there are aldehydes and *iso*-octenes present throughout the 8 hour period. As the pressure was increased to 30 and 40 bars, *iso*-octenes only appear over the

first 2 hours and no *iso*-octenes observed after longer reaction times (4 – 8 hours). This means that the iso-octenes undergo hydroformylation to branched aldehydes. However, after 4 hours at 40 bars and 75 °C when catalyst to substrate ratio was increased from 1:500 to 1:2500, 9.3 % *iso*-octenes were observed. This means that the catalyst had more substrate to convert and a large amount of substrate was converted to aldehydes while a small amount was converted to *iso*-octenes. This could imply that the isomerization reaction occurs at a slower rate than the hydroformylation reaction.

The percentage aldehydes formed at all pressures are greater than 90 % after 4 hours. It has been reported in literature that isomerization increases with the decrease in syngas pressure and also increases with an increase in temperature.[22, 23] **Table 4.1** shows that at 4 hours, 20 bars and 75 °C, 5.04 % of *iso*-octenes were observed, however when the temperature was increased to 100 °C, the percentage of *iso*-octenes increased to 16.5 %. Isomerization reaction leads to the formation of *iso*-octenes, for example, 2-octene, 3-octene and 4-octenes. The selectivity towards *iso*-octenes at shorter reaction time and low pressures suggests that hydroformylation requires higher syngas pressures thus we observe less hydroformylation and more isomerization products at low pressures and shorter reaction times.

4.2.1.3 Regioselectivity

The aldehydes formed in the hydroformylation reaction of 1-octene can be linear (nonanal) or branched (2-methyl octanal, 2-ethyl heptanal and 2-propyl hexanal) aldehydes (**Figure 4.4**). Regioselectivity can be defined as the selectivity of a reagent towards a certain site within a particular functional group.[21] In case of hydroformylation reaction, the anti-Markovnikov hydride insertion to the terminal olefin gives linear products and the Markovnikov hydride addition to the internal olefin results in the formation of branched products. Studies have shown that electronic[24-27] and steric[28-30] properties of ligands around the active species metal center influence the regioselectivity of the metal center. Casey and co-workers indicated that for catalysts containing bidentate ligands, regioselectivity is usually determined by the hydride migration from the metal center to the coordinated alkene ligand (**Figure 4.4**, reaction **3.8- 3.9a** or **3.9b**).[31a]

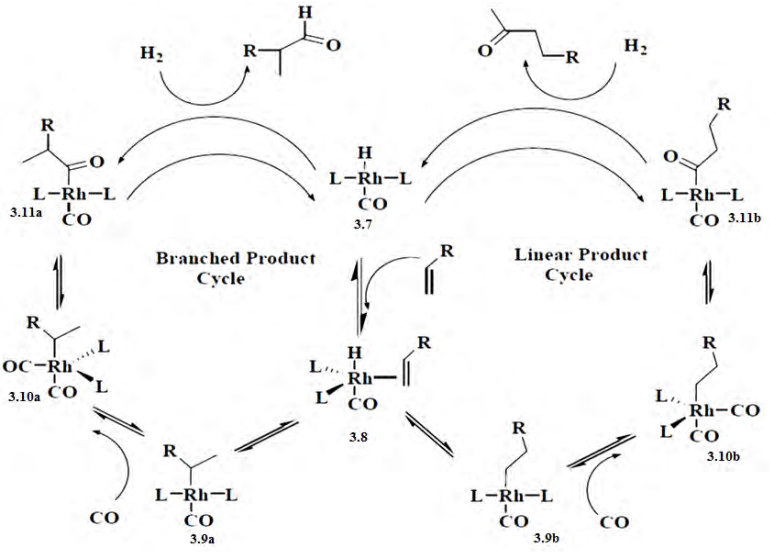

Figure 4.4: Mechanism of Rh-Catalyzed hydroformylation cycle.[31b]

Regioselectivity results of iminophosphine-based catalyst precursor **3.3** at different pressures and at different reaction times are shown in **Figure 4.5**.

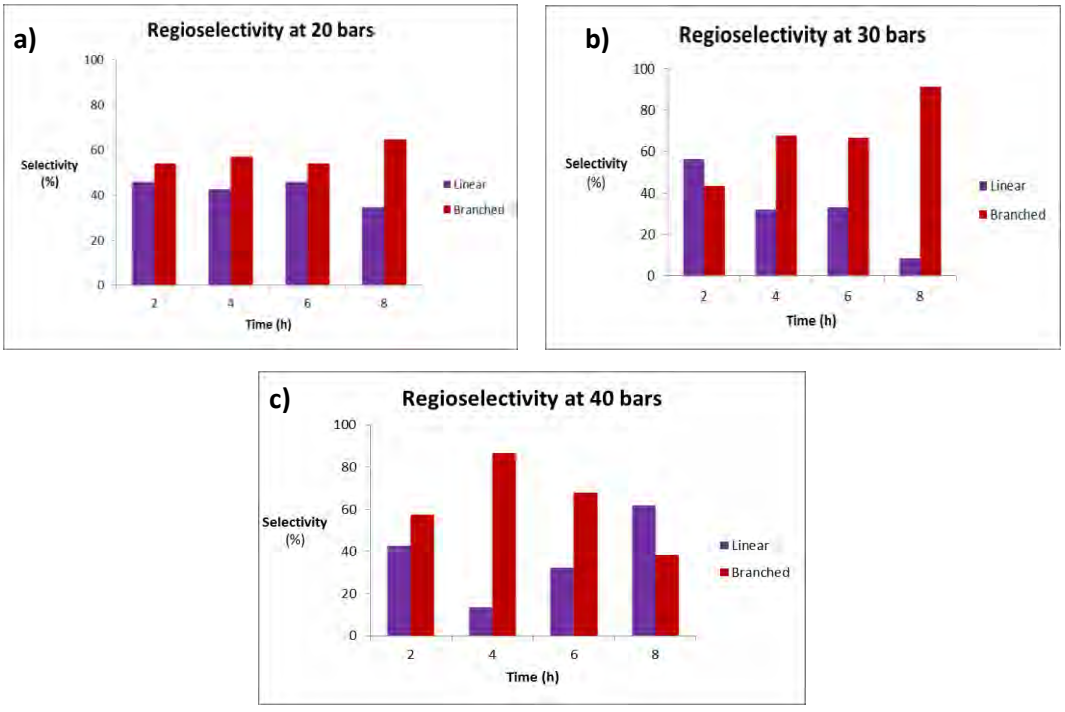

Figure 4.5: Effect of pressure on regioselectivity in hydroformylation of 1-octene using catalyst precursor **3.3** at 75 °C and (a) 20 bars, (b) 30 bars and (c) 40 bars (Average error estimate: ± 2.38, ± 0.45, ± 0.10).

Figure 4.5 shows that catalyst **3.3** moderately favours the formation of branched aldehydes at all different pressures. We observed *iso*-octenes for the first 2 hours at 30 and 40 bars, however after 4 hours no *iso*-octenes were observed. This may suggest that the isomerized alkenes were hydroformylated to branched aldehydes. Alternatively, the formation of branched aldehydes could be by direct hydroformylation at the second olefinic carbon of 1-octene.

Linear aldehyde formation is based on the steric crowding created by the ligand around the metal center. The bulkier the ligand the more the formation of linear aldehydes.[32-34] Catalyst precursor **3.3** exhibits a bulky diphenylphosphino group around the metal center, which can lead to the formation of linear aldehydes. However, the results in **Figure 4.5** shows that linear aldehydes are only favoured at 40 bar 8 hours and 30 bar 2 hours.

Very high selectivities towards branched aldehydes were observed at 30 bars, 8 hours and at 40 bars 4 hours. Interestingly, when higher catalyst to substrate ratio was used (1:2500) at 40 bars and 75 ^{o}C (4 hours), the catalyst showed selectivities towards linear aldehydes (**Table 4.1**). The *n:iso* ratio improved from 0.28 when catalyst to substrate ratio was 1:500 to 1.83 when catalyst to substrate ratio was 1:2500. The reason for this increase in the *n:iso* ratio could be that there is more substrate to catalyst per unit volume, this can create a pseudo-sterically crowded environment around the metal center resulting in the formation of more linear aldehydes.

4.2.2 Fluorous biphasic hydroformylation using complex 3.6

4.2.2.1 Effect of syngas pressure on conversion

The percentage conversion of 1-octene using salicylaldimine complex **3.6** (**Figure 4.1**) was investigated over an 8 hour period. **Figure 4.6** displays the obtained percentage conversion of 1-octene using catalyst precursor **3.6**. The graph in **Figure 4.6** shows a steady increase in 1-octene conversion over the 8 hour period at different pressures. In the first 2 hours catalyst precursor **3.6** displays high conversions (> 75 %) at 20 and 40 bars and moderate conversions at 30 bars (52.37%). The lower conversion in the first 2 hours could indicate the induction period, where the pre-catalyst is being converted to the active species.

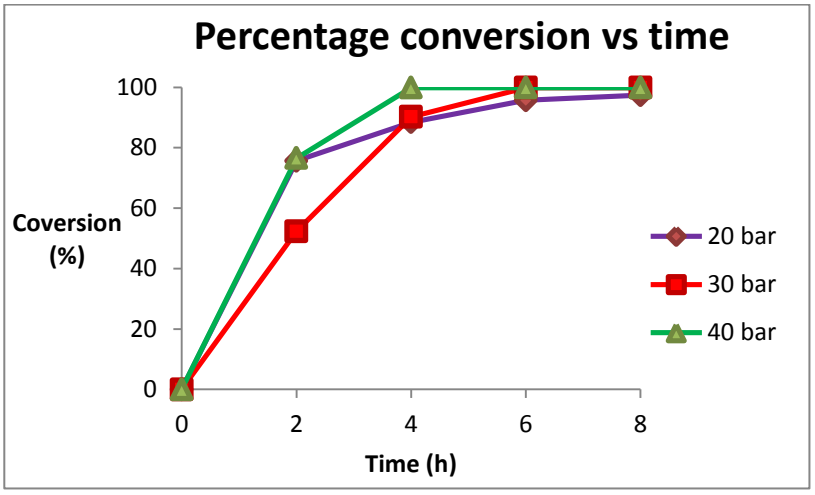

Figure 4.6: Percentage conversions of 1-octene over 8 hours using catalyst precursor **3.6** at 75 °C and 20, 30 and 40 bar syngas pressure. (Average error estimate: ± 0.96, ± 0.11, ± 0.5).

After 4 hours, the percentage conversions at all pressures were above 85 % and 40 bars displaying almost 100 % conversions. At 6 - 8 hours the catalyst displays almost 100 % conversions at 20, 30 and 40 bars.

Figure 4.7 illustrates the turnover numbers at different pressures and reaction times. TON calculations were based on the number of moles of aldehydes formed. The graph below illustrates that TON increases at the pressure and reaction time increases. Similarly, the low turnovers could be due to the induction period. This may possibly also mean that the hydroformylation reaction is slow at lower pressures and shorter reaction times.

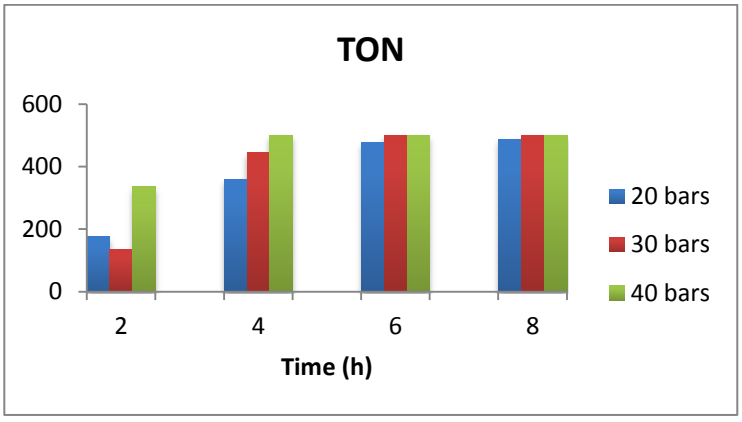

Figure 4.7: Effect of pressure on TON in hydroformylation of 1-octene using catalyst precursor **3.3** at 75°C and: (a) 20 bars (± 0.96), (b) 30 bars (± 0.11) and (c) 40 bars and at different reaction times (± 0.5).

4.2.2.1 Chemoselectivity and Regioselectivity

The chemo- and regioselectivity results are displayed in **Table 4.2**. This shows that chemoselectivity towards aldehydes increases as time and pressure increases. At 20 bars, 2 hours the catalyst displays selectivity towards *iso*-octenes. On increasing the reaction time, the selectivity towards aldehydes increases to 100 % after 8 hours, thus proving as previously reported that branched aldehydes form mainly from internal olefins. At 30 and 40 bars, the catalyst is highly selective towards aldehydes after 6 hours and 4 hours, respectively.

In general, catalyst precursor **3.6** is highly selective for branched aldehydes over linear aldehydes under all the conditions. This is indicated by the very low *n:iso* ratios (< 0.9) in **Table 4.2**. The low *n:iso* ratios can be due to less steric hindrance around metal center, hence the catalyst favours branched aldehydes over linear aldehydes. In the first 2 hours at 20, 30 and 40 bars, selectivity towards branched aldehydes is above 50 % and increased to above 90 % after 4 hours. After 6 - 8 hours at 20, 30 and 40 bars good selectivities towards branched aldehydes were obtained.

Table 4.2: Hydroformylation results of 1-octene using complex **3.6**.

Entry	Time (h)	Pressure (bar)	Temperature (^{o}C)	Conversion (%)	Total aldehydes	Iso-octenes	n:iso
1	2	20	75	75.69	47.49	52.51	0.85
2	4	20	75	88.45	81.16	18.83	0.057
3	6	20	75	95.68	99.80	0.36	0.36
4	8	20	75	97.39	99.99	-	0.18
5	2	30	75	52.37	50.89	49.10	0.096
6	4	30	75	90.22	98.78	2.44	0.066
7	6	30	75	99.99	99.99	-	0.43
8	8	30	75	99.99	99.99	-	0.15
9	2	40	75	76.59	87.2	12.78	0.224
10	4	40	75	99.99	99.99	-	0.027
11	6	40	75	99.99	99.99	-	0.010
12	8	40	75	99.99	99.99	-	0.109

Hydroformylation of 1-octene in toluene (2 mL) and perfluoromethylcyclohexane (2 ml), 1:1 CO/H_2, 20, 30 & 40 bar, 75 °C temperature, catalyst loading 0.00249 mmol, 1:500 = catalyst:substrate. GC conversions were obtained using *n*-decane as internal standard, average error estimate: ± 0.96, ± 0.11, ± 0.5. Total aldehydes are composed of a mixture of branched aldehydes and linear aldehydes and % sum of mixture is 100 %.

4.2.3 Summary

Catalytic evaluation of iminophosphine catalyst precursor **3.3** and salicylaldimine catalyst precursor **3.6** in 1-octene hydroformylation has been studied. Different conditions were used in order to find the optimum catalytic conditions for the fluorous biphasic system. Based on the results obtained in the catalytic evaluations of catalyst **3.3** and **3.6** it was established that, catalyst precursors **3.3** and **3.6** both display the best results at 40 bar, 75 ^{o}C and 4 h being the shortest reaction time possible. This conclusion was based on comparing catalyst selectivity for aldehyde formation and activity at different reaction conditions. The catalytic performance of both precursors (**3.3** and **3.6**) is similar, salicylaldimine based catalyst precursor **3.6** being slightly superior than iminophosphine based catalyst precursor **3.3**. This is based on the higher selectivity (regio- and chemoselectivities) displayed by **3.6** over **3.5** at the chosen optimum conditions (40 bar, 75 ^{o}C). Both precursors display similar TON (500.8) (**Table 4.1** and **4.2**) at the established optimum conditions. The established optimum reaction conditions (4 hours, 40 bars and 75 ^{o}C) were further used in the hydroformylation of 1-octene using the synthesized catalyst precursors **3.1 - 3.2** and **3.4 - 3.5** (**Figure 4.1**).

4.2.4 Fluorous biphasic hydroformylation using complex 3.1 - 3.2 and 3.4 - 3.5

4.2.4.1 1-Octene conversion

Iminophosphine Rh(I) complexes **3.1 - 3.2** and salicylaldimine complexes **3.4 - 3.5** were used as catalyst precursors in the fluorous biphasic hydroformylation of 1-octene. Reactions were carried out for 4 hours in (2 ml) toluene/PMCH (2 ml) (1:1 ratio) using the established optimum reaction conditions (40 bar 1:1 H_2/CO at 75 ^{o}C). Catalyst loading was 0.00249 mmol (1:500 catalyst: substrate ratio). The hydroformylation results are shown in **Table 4.3**. From the results illustrated in **Table 4.3**, catalyst precursors **3.1 - 3.2** and **3.4 - 3.5** generally show excellent percentage conversions (> 90 %) under the established reaction conditions.

Table 4.3: Hydroformylation results of 1-octene using complex **3.1-3.2** and **3.4-3.5**

Catalyst	Conversion (%)	Total aldehydes	Iso-octenes	TON
3.1	99.99	100	-	500.80
3.2	99.99	100	-	500.80
3.4	99.67	99.99	0.016	499.12
3.5	99.80	99.99	0.0099	499.76

Hydroformylation of 1-octene in toluene (2 mL) and perfluoromethylcyclohexane (2 ml), 1:1 CO/H_2, 40 bar, 75 °C temperature, catalyst loading 0.00249 mmol, 1:500 = catalyst:substrate. GC conversions were obtained using *n*-decane as internal standard, average error estimate: ± 0.20, ± 0.14, ± 0.17, ± 0.10. Total aldehydes are composed of a mixture of branched aldehydes and linear aldehydes and % sum of mixture is 100 %

Table 4.3 also illustrates the TON for Rh(I) catalyst precursors (**3.1 - 3.2** and **3.4 - 3.5**). This shows that the Rh(I) iminophosphine based catalyst precursors **3.1** and **3.2** exhibit higher TON compared to the salicylaldimine catalyst precursors (**3.4** and **3.5**). Catalyst precursors **3.1** and **3.2** have similar turnover numbers (500.8), similarly **3.4** and **3.5** have similar TON, pre-catalyst **3.5** showing higher TON (499.76) than **3.4** (499.12). The salicylaldimine and iminophosphine complexes are chelating complexes, meaning they have greater stability. The salicylaldimine complexes display slightly lower turnover numbers; probably because they are less stable than the iminophosphine complexes, hence having lower turnover numbers. Iminophosphine-based Rh(I) catalyst precursors have been shown to display good TON in our research group.[35]

4.2.4.2 Chemoselectivity and Regioselectivity

Using the established optimal reaction conditions (T = 75 °C, syngas pressure = 40 bars), catalyst precursors **3.1 - 3.2** and **3.4 - 3.5** show high chemoselectivity for aldehyde products (> 99 %) (**Table 4.3**). Little amounts of *iso*-octenes were present for the salicylaldimine-based catalyst precursor (**3.4** and **3.5**). **Figure 4.8** shows that catalyst precursors (**3.1**, **3.4** and **3.5**) favour branched aldehydes at the chosen optimal reaction conditions, and the iminophosphine catalyst precursor **3.2** is selective for linear aldehydes. This suggests that hydroformylation of the isomerized 1-octene is favoured or direct hydroformylation at the second olefinic carbon of 1-octene is favoured.

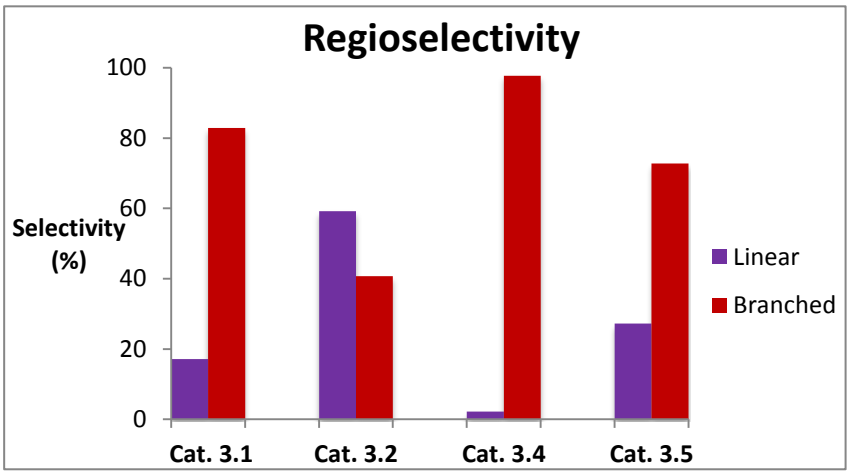

Figure 4.8: Regioselectivity of catalyst precursor **3.1-3.2** and **3.4-3.5** in hydroformylation of 1-octene using at 75 °C and 40 bars. (Average error estimate: ± 0.20, ± 0.14, ± 0.17, ± 0.10)

Figure 4.8 also shows that catalyst precursor **3.4** displays more superior selectivity towards branched aldehydes (98 %) compared to the other catalyst precursors. Catalyst precursors **3.1** and **3.5** display moderate to high selectivity (83 % and 73 %, respectively) for branched aldehydes. The iminophosphine catalyst precursor **3.2** shows moderate selectivity towards linear aldehydes (59 %).

4.2.5 Recyclability studies

Recycling studies were performed using iminophosphine complex **3.3** and salicylaldimine complex **3.6**. The fluorous layer which contains the catalyst and the fluorous solvent was recycled after the first run by decanting the organic layer (contains toluene, products and some unreacted 1-octene), followed by adding fresh substrate of 1-octene dissolved in toluene onto the fluorous layer containing the catalyst. The results illustrating substrate conversions are shown in **Figure 4.9**

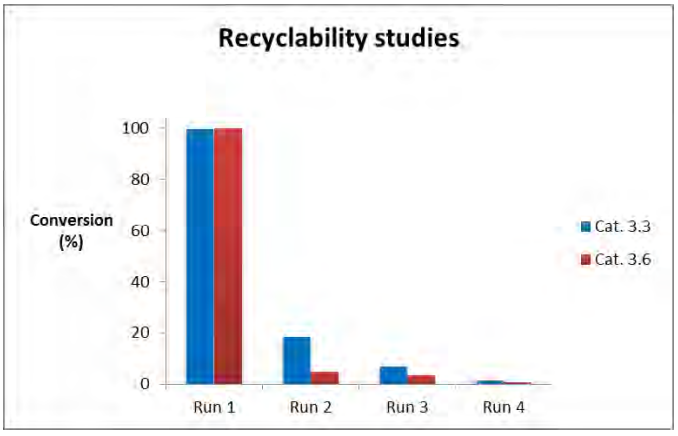

Figure 4.9: Fluorous biphasic hydroformylation of 1-octene using complex **3.3** and **3.6** in recyclability studies, 1:1 CO/H_2 at 40 bars, 4 hours, at 75 ^oC. Initial catalyst loading 0.00249 mmol, 1:500 Catalyst:substrate ratio. (Average error estimate: ± 0.14, ± 1.89, ± 1.51, ± 0.91)

Unfortunately, **Figure 4.9** shows that the conversions decrease drastically after the first run, from conversions greater than 90 % to conversions less than 20 % for both catalysts (**3.3** and **3.6**). The decrease in conversions could be that there is low concentration of the catalyst in the fluorous layer thus resulting in the loss of activity. Moreover, decreasing conversions after each run could be the due to the loss of the catalyst into the organic layer (leaching of the catalyst). Also, solubility tests show that the catalysts show solubility in toluene in addition to PMCH. This can also be the reason for the observed decline in conversion. The separation of the two phases was good, however the organic layer was coloured (light brown), which indicates that there is leaching of the catalyst into the organic layer.

Even though the conversion decreased, both catalyst precursors were selective for aldehydes and no *iso*-octenes were observed after each successive run. Both catalysts were found to favour branched aldehydes over the linear products after each run. Thus, chemo- and regioselectivity is maintained nonetheless. The turnover frequency decreased after each run, meaning that the catalysts were losing their catalytic activity.

4.2.6 Rh Leaching Studies

Catalyst precursor **3.3** was used as a model to prove that there is metal leaching into the organic layer. The organic layer was re-used by adding a fresh substrate and running the reaction. After the reaction, the results products were analyzed by GC, and greater than 90 % 1-octene

conversions were observed. This means that most of the catalyst leached into the organic layer and this is the reason why there is a huge drop of 1-octene conversion after the second run.

Inductively coupled plasma mass spectrometry (ICP-MS) was used to quantify the metal loss of catalyst precursor **3.3** by analyzing the organic layer. The obtained data showed that the metal loss into the toluene is 93 %. This contributes to the drop in the conversion after the first run.

4.2.7 Reactions Omitting Toluene

Foster and co-workers studied the behavior of 1-octene and nonanal with fluorous solvent in the presence and absence of toluene.[36] Interestingly, they established that 1-octene is completely miscible with perfluoromethylcyclohexane at temperatures above 60 ^{o}C under 20 bar (CO: H_2, 1:1). However nonanal phase separated even at temperatures above 80 ^{o}C. This result of omitting the organic solvent might be advantageous. One commercial advantage will be that distillation would be unnecessary for removing toluene from the products after separation of the catalyst.[36, 37] The absence of the organic phase might also reduce the level of leaching of the catalyst into the organic phase.[36]

For this reason, hydroformylation of 1-octene was carried out in perfluoromethylcyclohexane under the same hydroformylation conditions used when using toluene and PMCH (4 hours, 40 bars at 75 ^{o}C) except that the amount of toluene was replaced by the same volume of the PMCH. The reactions were monitored by GC.

4.2.7.1 1-Octene Conversion

The percentage conversions of 1-octene are displayed in the **Figure 4.10**, for comparison reasons the results obtained when using both the organic and fluorous solvent are also included.

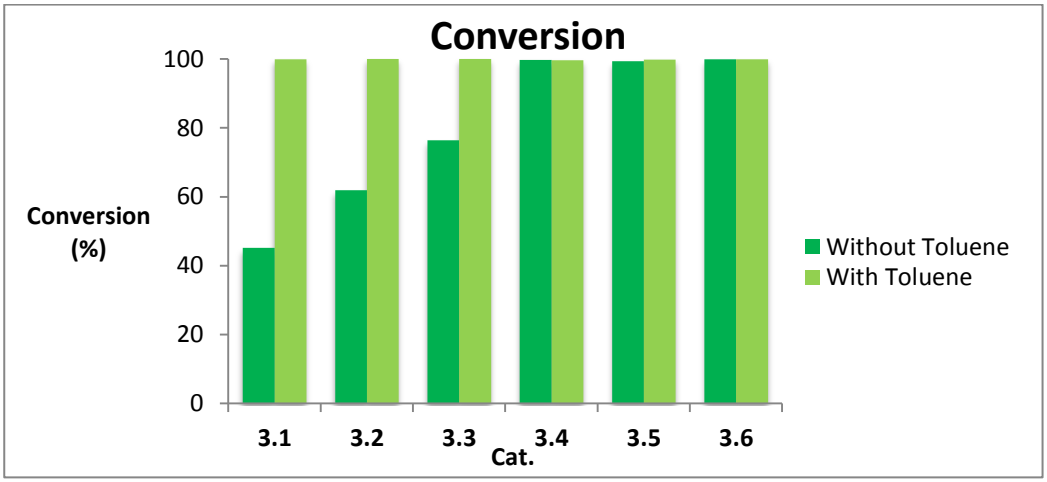

Figure 4.10: Percentage conversions of 1-octene in PMCH or PMCH/Toluene over 4 hours using catalyst precursor **3.1 - 3.6** at 75 ^{o}C and 40 bar syngas pressure. (Average error estimate: ± 1.23, ± 0.51, ± 1.90, ± 1.40, ± 0.21, ± 1.01)

Figure 4.10 generally shows that when using only the fluorous solvent the salicylaldimine complexes **3.4 - 3.6** display better 1-octene conversion than the iminophosphine complexes **3.1 - 3.3**. Complex **3.3** shows better conversions (76 %) compared to **3.2** (62 %) and **3.1** (45 %). All the salicylaldimine complexes **3.4 - 3.6** display conversion greater than 90 %. Comparing the conversions against when toluene was used, **Figure 4.10** illustrates that the conversions did not change when using salicylaldimine complexes **3.4 - 3.6**, however the iminophosphine complexes **3.1 - 3.3** display lower conversions when using only fluorous solvent compared to when toluene was also present. The reasons for the change in conversion when using iminophosphine-based pre-catalysts are unclear.

Changes in turnover numbers were also observed when toluene was omitted from the system. The results are depicted in **Figure 4.11**. For comparison reasons the TON results when toluene was included in the system are also shown in **Figure 4.11**. The changes in TON were only observed in the iminophosphine catalyst precursors **3.1 - 3.3** and there was no change in TON for the salicylaldimine catalyst precursors **3.4 - 3.6** when toluene was omitted. Looking at **Figure 4.11**, it is observed that the turnover numbers of catalyst precursors **3.1 - 3.3** are lower than when toluene was omitted from the system compared to when it was included. The TON for catalyst precursor **3.1** decreases from 500.60 to 226.16, for catalyst **3.2** it decreased from 500.80 to 310.20 and similarly for catalyst **3.3** it decreased from 500.84 to 384.84.

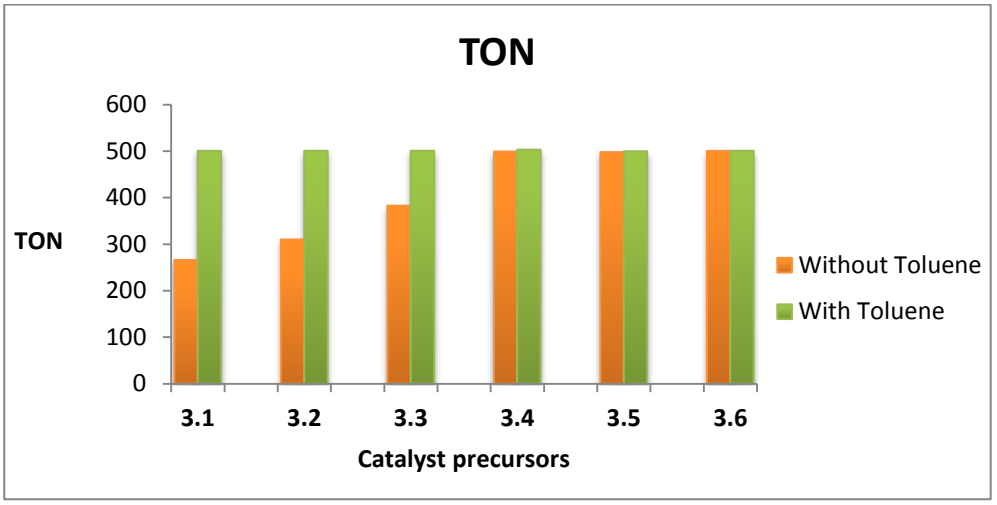

Figure 4.11: Turnover numbers for the Rh(I) catalyst precursor **3.1-3.2** and **3.4-3.5** in hydroformylation of 1-octene using at 75 °C and 40 bars. (Average error estimate: ± 1.23, ± 0.51, ± 1.90, ± 1.40, ± 0.21, ± 1.01)

The difference in the rates may be due to differential solubility of the gases and the order of reaction with respect to the two gases.[36] The rates in this work did not increase as compared to the results obtained in literature.[36]

4.2.7.2 Chemoselectivity and regioselectivity

In terms of chemoselectivity, the catalyst precursors **3.1 - 3.6** were highly selective towards aldehydes. There were no other products observed in reactions carried out in PMCH. There is no significant difference in chemoselectivity when comparing the results when toluene was included.

Regioselectivity results for the catalyst precursors **3.1 - 3.6** were also obtained and the results are shown in **Figure 4.12a**. The iminophosphine complexes **3.1 - 33** and salicylaldimine complex **3.5** favour the formation of linear aldehydes. Catalyst precursors **3.4** and **3.6** display selectivity towards branched aldehydes with catalyst precursor **3.4** being more selective than **3.6**.

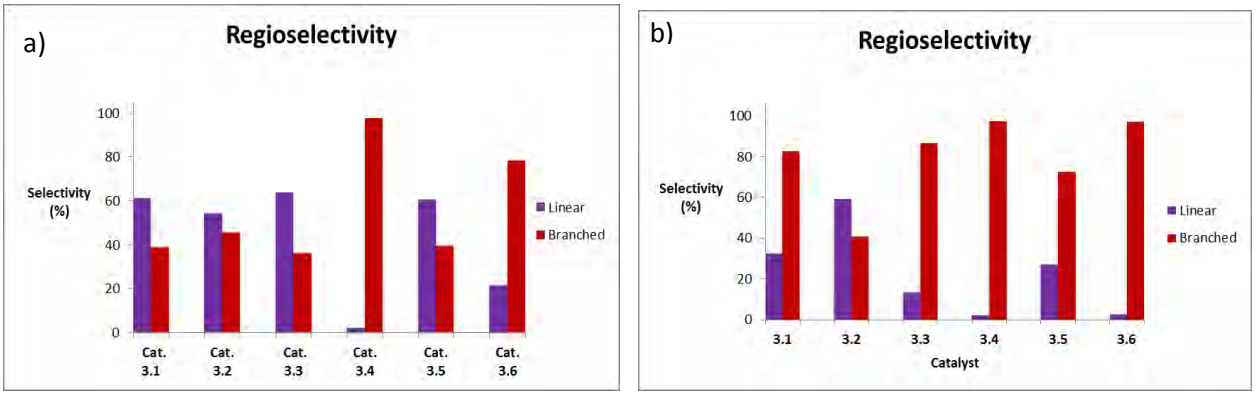

Figure 4.12: Regioselectivity of catalyst precursor **3.1-3.6** when using a) Without toluene or b) In the presence of toluene at 75 ^{o}C and 40 bar syngas pressure after 4 hours. (Average error estimate: ± 1.23, ± 0.51, ± 1.90, ± 1.40, ± 0.21, ± 1.01)

The catalyst precursors **3.1 - 3.3** and **3.5** display moderate selectivity of 55 - 60 % towards linear aldehydes. Interestingly, omitting toluene from the system resulted on increased selectivity for linear aldehydes (**Figure 4.12 a**). Catalyst precursors **3.1**, **3.3**, and **3.5** changed from favouring branched aldehydes when toluene was included to favouring linear aldehydes in the absence of toluene (**Figure 4.12 a** & **b**). The increased *n:iso* ratio is similar to what was observed in the literature when toluene was omitted from the system.[36-38] Foster and co-workers mentioned that the reasons for the increased n:iso ratios are not clear.[36]

4.2.7.4 Recycling the fluorous layer used in the neat reaction

Recycling studies were performed using iminophosphine complex **3.3** at 40 bars and 75 °C for 4 hours. The fluorous layer was recycled after the first run by decanting the products, followed by adding fresh substrate of 1-octene onto the fluorous layer. The results obtained are displayed in **Table 4.4**.

Table 4.4: Hydroformylation results of 1-octene in fluorous solvent using complex **3.3**.

Runs	Conversion (%)	Total aldehydes	Iso-aldehydes (%)	n-aldehydes (%)	n:iso	TOF (h^{-1})	TON
1	76.44	100	36.18	63.88	1.76	95.71	382.83
2	82.74	100	4.60	95.36	20.56	103.59	410.00
3	5.27	100	35.70	64.29	1.80	6.60	26.41

Hydroformylation of 1-octene in perfluoromethylcyclohexane (4 ml), 1:1 CO/H2, 40 bar, 75 °C temperature, catalyst loading 0.00249 mmol, 1:500 = catalyst:substrate. GC conversions were obtained using *n*-decane as internal standard, average error estimate: ± 0.11, ± 1.40, ± 1.71. Total aldehydes are composed of a mixture of branched aldehydes and linear aldehydes and % sum of mixture is 100 %

The catalyst displays good conversions of 76 % in the first run and conversions increased in the second run to 83 %. This could be that the catalyst becomes more active after the first run. However the conversions dropped to 5 % in the third run. Meaning that the catalyst lost its activity or the catalyst is leaching into the products and the 1-octene that is still present. As compared to the recycling results obtained when toluene was included, there is no significant difference in conversions except that here the conversion drops after the third run instead of the second run.

The catalyst **3.3** is still selective towards aldehydes (100 % aldehydes). Catalyst **3.3** favours the formation of linear aldehydes in each run. In the first run 64 % of linear aldehydes were observed, in the second run 95 % of linear aldehydes were detected and in the third run 64 % linear aldehydes were also observed. **Table 4.4** also shows that the TON was high in the second run (410.00) compared to the first (382.83) and the third run shows very low TON (26.41) as expected since the conversion is low.

4.2.8 Comparison of this work with other systems

It is useful to compare the catalysts that we have developed to those available commercially and reported in literature. Catalyst **3.3** showed the best results at the established optimum reaction conditions (40 bars and 75 ^{o}C). These results were compared to those results obtained from hydroformylation of 1-decene under fluorous biphasic conditions by Horvath.[39] The results were also compared to the results obtained from the BASF and UCC process (**Table 4.5**). Both these processes entail the hydroformylation of propene. In Horvath's work, lower concentrations of Rh (0.156 mmol/dm^3) were used compared to this work (0.623 mmol/dm^3), but his phosphorous concentration [P] (42.7 mmol/dm^3) was higher than this work (0.623 mmol/dm^3) (**Table 4.5**).

Table 4.5: Comparison of results obtained from the hydroformylation of 1-octene in PMCH using the rhodium catalyst **3.3**, a literature precedent and with industrial processes.[36]

	This work[a]	**Horvath**[b]	**UCC**[c]	**BASF**[c]
[Rh] (mmol dm^{-3})	0.623	0.156	2.7	1.8
[P] (mmol dm^{-3})	0.623	42.7	286	150
[alkene] (mmol dm^{-3})	311.75	1012	-[d]	-[d]
Pressure (bar)	40	10	15-18	16
Temperature (^{o}C)	75	100	90-95	110
Rate (mol dm^{-3} h^{-1})	0.00016	0.16	2-4	1.0
TOF (h^{-1})	125.21	1020	740	500
l/b	0.2	4.5	8.8	5.3
Isomerization (%)	-	7.8	-[c]	-[c]
Linear aldehyde %	13.36	74.8	89.5	83.0
Rh loss (mg Rh (mol aldehyde^{-1})	-[f]	0.12	-[f]	-[f]
P loss (%)	-[f]	Significant	-[f]	-[f]

[a] 1-Octene as substrate, P(4-$C_6H_4C_6F_{13}$)$_3$ in perfluromethylcyclohexane. [b] 1-decene as a substrate Rh/P($CH_2CH_2C6F_{13}$)$_3$ in 50:50 vol % of toluene and PMCH. [c] Propene used as a substrate, Rh/PPh_3 in condensed aldehydes. UCC process as run by Union Carbide, BASF process run by BASF. [d] Propene introduced in gas phase. [e] Propene cannot isomerize. [f] Data unavailable

The temperature used in this work was lower than in Hovarth's work; however our pressures were higher (40 bars) than the pressures used in his work (10 bars) (**Table 4.5**). Our *n:iso* ratios were lower than their work (0.2 *ca*. 4.5), and also our linear selectivities and reaction rates (TOF h^{-1}) were lower than Hovarth's work. We did not observe any isomerization as we used higher pressures compared to Horvath's work.

Our results were also compared to the obtained results from the BASF and UCC process from the hydroformylation of propene (**Table 4.5**). The results show that our [Rh] and [P] were lower than the concentrations used in the two processes. Also our temperatures were lower (75 ^{o}C) compared to the two processes (90 - 110 ^{o}C); however the pressures used were lower than ours (15 - 18 bars *ca*. 40 bars). The rates, linear selectivity and *n:iso* ratios obtained in the other two processes were higher compared to this work (**Table 4.5**). Also there is no loss of substrate to isomerization in these industrial processes as propene does not isomerize, and also in this work no isomerization of 1-octene was observed.

4.3 Conclusion

Catalyst pre-cursors **3.1 - 3.6** were evaluated in the hydroformylation of 1-octene and they showed good activity. All catalysts except **3.2** were selective for branched aldehydes. However, catalyst **3.3** displayed regioselectivity towards linear products when catalyst to substrate ratio was increased from 1:500 to 1:2500. Reactions without toluene were also carried out using catalyst pre-cursors **3.1 - 3.6**. The results show that catalyst **3.1 - 3.3** and **3.5** are selective for linear aldehydes. All catalyst showed good chemoselectivity towards aldehydes over *iso*-octenes. Catalyst **3.3** and **3.6** were used in recycling studies. Both catalysts showed poor conversions after the second run, therefore they cannot be recycled. Catalyst **3.3** was used when the fluorous layer used in the neat reaction was recycled; the results show good conversions after the first and the second run; however conversions decreased after the third. The best results obtained when using catalyst **3.3** were compared to the available commercially available processes and Horvath's work and the catalyst **3.3** showed poor results compared to the results obtained in Horvath's work and the BASF and UCC process. Overall, the catalysts showed good activity and selectivity.

4.4 Experimental

4.4.1 *General*

All chemicals and GC grade toluene were obtained from Sigma-Aldrich and were used without further purification. Products from the reaction were analyzed on a Perkin Elmer Clarus 580 GC gas chromatography. The rhodium content in toluene layer were analyzed by Inductively coupled plasma mass spectrometry (ICP-MS) using a Perkin Elmer Elan600 quadrupole ICP-MS with a Cetax LSX-200 UV laser module.

4.6.2 *General Procedure for the Biphasic hydroformylation reactions*

The biphasic reactions were performed in a 90 ml stainless steel pipe reactor. The reactor was charged with either toluene 1:1 toluene/PMCH (4 ml), 1-octene (139.95 mg, 1.25 mmol), internal standard *n*-decane (34.92 mg, 0.249 mmol) and either one of catalyst precursors **3.1-3.6** (0.00249 mmol, Rh ratio:substrate = 1:500) in separate reactions. For reactions without toluene 4 ml of PMCH was used, 2 ml of PMCH replaced the 2 ml of toluene so that the total amount of solvent remained constant. The pipe reactor was flushed with nitrogen three times, followed by flushing twice with syngas (1:1 $CO:H_2$). This was then pressurized, stirred and heated to the desired pressure of syngas and temperature. Reactions for optimizing reaction conditions were performed over an 8 hour period and samples were collected at the beginning and at the end of each reaction. All reactions were carried out in duplicates and show good reproducibility. The ICP-MS results were obtained by digesting the samples (5 mg) using MARS-5 Microwave digester. A mixture of 6 ml concentrated HCl solution; 2 ml concentrated HF solution and concentrated HNO_3 solution was used to digest the sample.

4.5 References

1. C.W. Kohlpaintner, R.W. Fischer, B. Cornils, *Appl. Catal. A: General*, **221**, 2001, 212.
2. B. Cornils, W.A. Herrmann, *Aqueous-Phase Organometallic Catalysis, 2nd Ed.* Chapter 4, Wiley-VCH, Verlag GmbH and Co., Weinheim, 2004, pp 244.
3. F. P. Pruchnik, *Organometallic Chemistry of Transition Metal*, Plenum Press, New York, 1990, 691.
4. L. H. Slaugh and R. D. Mullineaux, *US Patent, US3239569*, 1966.
5. M. G. Humphrey, C. E. Powell, M. P. Cifentes, J. P. Morall and M. Samoc, *Pol. Preprints*, **45**, 2004, 367.
6. J. K. MacDougall, M. C. Simpson, M. J. Green and D. J. Cole-Hamilton, *J. Chem. Soc. Dalton Trans.*, 1996, 1161.
7. A. M. Trzeciak and J. J. Ziolkowski, *Coord. Chem. Rev*., **190-192**, 1999, 883.
8. G. T Whiteker and C. Cobley, *Top. Organomet. Chem*., **42**, 2012, 35.
9. G. D. Frey, *J. Organomet. Chem*., **754**, 2014, 5.
10. B. Cornils, C.D. Frohning and C.W. Kohlpaintner*, J. Mol. Catal. A,* **104**, 1995, 17.
11. D. U. Parmar, H. C. Bajaj, S. D. Bhatt and R. V. Jasra, *Bull. Chem. Soc. India*, **2**, 2003, 34.
12. B. Cornils, W.A. Herrmann, M. Rasch and M. Beller*, Angew. Chem. Int. Ed. Engl.,* **33**, 1994, 2144.
13. P. Eibracht, L. Barfacker, C. Buss, C. Hollmann, B. E. Kistsos-Rzychon, C. L. Kranemann, T. Rische, R. Roggenbuck and A. Schmidt, *Chem. Rev.,* **99**, 1999, 3329.
14. I. T. Horvath and J. Ràbài, *Science*, **266**, 1994, 72.
15. I. T. Horvath, G. Kiss, R. A. Cook, J. E. Bond, P. A. Stevens, J. Rabai and E. J. Mozeleski, *J. Am. Chem. Soc.,* **120**, 1998, 3133.
16. A. Aghmiz, C. Claver, A. M. Masdeu-Bulto, D. Maillard and D. Sinou, *J. Mol. Catal. A: Chem*., **208**, 2004, 97.
17. T. Mathivet, E. Monflier, Y. Castanet, A. Mortreux and J. Couturier, *Tetrahedron*, **58**, 2002, 3877.
18. T. Mathivet, E. Monflier, Y. Castanet, A. Mortreux and J. Couturier, *R. C. Chimie*, **5**, 2002, 417.

19. E. Perperi, Y. Huang, P. Angeli, G. Manos and D. J. Cole-Hamilton, *J. Mol. Catal. A: Chem*., **221**, 2004, 19.

20. a) E. Perperi, Y. Huang, P. Angeli, G. Manos, C. R. Mathison, D. J. Cole-Hamilton, D. A. Adams and E. G. Hope, *Chem. Eng. Sci*., **59**, 2004, 4983. b) K. V. Raghavan and B. M Reddy, *Industrial Catalysis and Separations: Innovations for Process Intensification*, CRC press, 2014, pp 332.

21. W. Thybaut and G. B. Marin, *Testing of Catalytic Properties*, Ghent University, Laboratory of Chemical Technology, Krijg Slaan 281-S5, 900, Ghent Belgium.

22. R. Lazzaroni, G. Ucello-Barretta and M. Benetti, *Organometallics*, **8**, 1989, 2323.

23. R. Lazzaroni, A. Rafaelli, R. Settambolo, S. Bertozzi and G. Vitulli, *J. Mol. Catal.*, **50**, 1989, 1.

24. J. D. Unruh and J. R. Christenson, *J. Mol. Catal.*, **14**, 1982, 19.

25. L. A. Van der Veen, M. D. K. Boele, F. R. Bergman, P. C. J. Kamer, P. W. N. M Van Leeuwen, K. Goubitz, J. Fraanje and H. Schenk, *J. Am. Chem. Soc*., **120**, 1998, 11616.

26. C. P. Casey, E. L. Paulsen, E. W. Beuttenmueller, B. R. Proft, L. M. Petrovich, B. A. Matter and D. R. Powel, *J. Am. Chem. Soc*., **119**, 1997, 11817.

27. C. P. Casey, E. L. Paulsen, E. W. Beuttenmueller, B. R. Proft, B. A. Matter and D. R. Powel, *J. Am. Chem. Soc*., **121**, 1999, 63.

28. Z. Freixa, P. W. N. M.Van Leeuwen,. *Dalton Trans*., **10**, 2003, 1890.

29. a) H. K. Reinius, P. Suomalainen, H. Riihimaki, E. Karvinen, J. Pursiainen and A. O. I. Krause, *J. Catal*., **199**, 2001, 302. b) E. Zuidema, E. Daura-Oller, J. J. Carbo´, C. Bo and P. W. N. M. van Leeuwen, *Organometallics*, **26**, 2007, 2234.

30. H. Riihimaki, P. Suomalainen, H. K.Reinius, J. Suutari J, S. Jaaske-lainen, A. O. I. Krause, T. A. Pakkanen and J. T. Pursiainen, J. *Mol. Catal*., **200**, 2003, 69.

31. a) C. P. Casey, L. M. Petrovich, *J. Am. Chem. Soc*., **117**, 1995, 6007. b) C. Claver, M. Dieguez, O. Pamies and S. Castillon, *Top Organomet. Chem.*, **18**, 2006, 35.

32. V. K. Srivastava, R. S. Shukla, H. C. Bajaj and R. V. Jasra, *Applied Catalysis A : General*, 2005, **282**, 31.

33. C. A. Tolman, *Chem. Rev.*, **77**, 1977, 313.

34. J. T. Desanto, J. A. Mosbo, B. N. Storhoff, P. L. Bock and R. E. Bloss, *Inorg. Chem.*, **19**, 1980, 3086.

35. N.C. Antonels, J.R. Moss and G.S. Smith, *J. Organomet. Chem*., **696**, 2011, 2003.

36. D. F. Foster, D. Gudmunsen, D. J. Adams, A. M. Stuart, E. G. Hope, D. J. Cole-Hamilton, G. P. Schwarz and P. J. Pogorzelec, *Tetrahedron*, **58**, 2002, 3901.

37. D. J. Adams, D. J. Cole-Hamilton, E. G. Hope, P. J. Pogorzelec and A. M. Stuart, *J. Organomet. Chem*., **689**, 2004, 1413.

38. D. F. Foster, D. J. Adams, D. Gudmunsen, A. M. Stuart, E. G. Hope and D. J. Cole-Hamilton, *Chem. Commun*., 2002, 722.

39. I. T. Horvath, G. Kiss, R. A. Cook, J. E. Bond, P. A. Stevens, J. Rabai and E. J. Mozeleski, *J. Am. Chem. Soc*., **120**, 1998, 3133.

Overall summary and future outlook

5.1 Overall summary

A number of fluorocarbon-containing iminophosphine (**L1**, **L2** and **L5**) and salicylaldimine (**L6 - L8**) based ligands were synthesized. These were synthesized by reacting various amines with 2-diphenylphoshinobenzaldehyde or salicylaldehyde *via* a Schiff base condensation reaction. The fluorocarbon-containing iminophosphine and salicylaldimine ligands were reacted with rhodium chloro carbonyl dimer or rhodium COD chloride dimer respectively to form new rhodium(I) based fluorocarbon-containing iminophosphine (**3.1** – **3.3**) and salicylaldimine (**3.4** – **3.6**) complexes. The synthesized ligands and complexes were characterized using various spectroscopic and analytical techniques. All complexes were isolated as solids and are stable at room temperature.

The synthesized complexes (**3.1** – **3.6**) were used as catalyst precursors in the hydroformylation of 1-octene. The catalyst precursors showed good 1-octene conversion to products at the established optimum reaction conditions (4 h, 75 °C and 40 bars). All the catalyst precursors showed high chemoselectivities towards aldehydes over *iso*-octenes. There were no other products detected. Generally, all the catalysts showed good regioselectivities towards branched aldehydes, however when toluene was omitted from the system, the catalyst favour the formation of linear aldehydes in general. Thus these systems show versatility and can be used in different solvent systems in order to obtain linear aldehydes.

The fluorous layer was recycled after it was separated by simple decanting the product containing organic layer. Catalyst **3.3** and **3.6** were used in recycling studies, both catalysts showed poor conversions after the second run, therefore they cannot be recycled. Catalyst **3.3** was used when the fluorous layer was recycled; the results show good conversions after the first and the second run however conversions decreased after the third.

5.2 Future outlook

From the hydroformylation of 1-octene results, the fluorocarbon-containing rhodium(I) based complexes showed good activity and selectivities in the fluorous biphasic system. Despite the good facile separation of the two solvents at room temperature, the results obtained from

recycling the fluorous layer were not encouraging. The low solubility of the catalyst in the fluorous solvent is the main reason for these poor results. Future studies may involve adding more fluorous chains or increasing the fluorous chain length in the catalyst; this will increase the affinity of the catalyst to fluorous solvents.